ANALYZING SPATIAL LOCALIZATION OF PROTEINS OF THE ENDOPLASMIC RETICULUM IN BUDDING YEAST, *S. CEREVISIAE*, DURING CELL DIVISION

by

Lindsay C. Schmiedel

A thesis submitted to the Faculty of the University of Delaware in partial fulfillment of the requirements for the degree of Honors Bachelor of Chemical Engineering with Distinction.

Spring 2009

ANALYZING SPATIAL LOCALIZATION

OF PROTEINS OF THE ENDOPLASMIC

RETICULUM IN BUDDING YEAST,

***S. CEREVISIAE*, DURING CELL DIVISION**

by

Lindsay C. Schmiedel

Approved: _____

Anne Skaja Robinson, Ph.D.
Professor in charge of thesis on behalf of the Advisory Committee

Approved: _____

Abraham Lenhoff, Ph.D.
Committee member from the Department of Chemical Engineering

Approved: _____

Michael Keefe, Ph.D.
Committee member from the Board of Senior Thesis Readers

Approved: _____

Alan Fox, Ph.D.
Director, University Honors Program

ACKNOWLEDGMENTS

This work would not have been possible without the support and encouragement of Carissa Young, Ph.D. candidate at University of Delaware, under whose advisement and supervision I began my research. The countless hours she has spent guiding me through experiments, assisting me with data collection and analysis, and completing late night revisions are much appreciated. I would also like to thank my research advisor, Dr. Anne Skaja Robinson, for regularly meeting with me to discuss the progress of my research and to brainstorm ideas for future experiments. I greatly admire her dedication to her students as a professor, a research advisor, and a friend. Also, I thank the rest of the Robinson research group, for welcoming me into the lab and showing me the ropes throughout the past two years.

I thank Dr. Kirk Czymmeck and the Bioimaging Center at Delaware Biotechnology Institute for offering their resources to help me complete my senior thesis. The collection of data for this project would not have been possible without Kirk's supervision, guidance, and patience when sharing his knowledge of confocal microscopy. I would like to thank Dr. Randall Duncan professor at University of Delaware. Although just appointed chairperson of the Biological Sciences Department, Dr. Duncan managed to meet with me to discuss my research and future experiments. Also, thanks to the following organizations for funding for this research: the Undergraduate Research Program, NIH GM 075297, and P20 RR16472, Core Facilities at DBI.

I cannot end without thanking my family and friends, specifically fellow classmate and friend, Rebecca Pagels, and fiancé, Alexander Morse. I am so blessed to have them in my life, continuously encouraging and supporting me. Finally, thanks be to God for showing me how to peacefully and joyfully complete my thesis. I thank Him every day for the love and blessings he has poured over me.

TABLE OF CONTENTS

LIST OF TABLES

LIST OF FIGURES

ABSTRACT

The first organelle of the secretory pathway, the endoplasmic reticulum (ER), is an essential organelle responsible for multiple critical processes of the cell. BiP, the molecular chaperone residing in the ER lumen of yeast, is involved in many of these intracellular processes including karyogamy (nuclear fusion during the mating of diploid cells), ER translocation of nascent protein, protein folding and maturation, and ERAD (ER associated degradation) of misfolded proteins. Due to BiP's involvement in karyogamy and ER biogenesis, we have examined BiP's role in the division of budding yeast, *S. cerevisiae*. The ER is a complex structure consisting of three subdomains including: (i) the peripheral ER found directly beneath the plasma membrane of the cell; (ii) the perinuclear ER, a structure that is continuous with the nuclear envelope; and (iii) a network of ER tubules connecting the former two domains. Using a combination of confocal light microscopy techniques and fluorescent protein variants, we have monitored dividing yeast cells expressing ER luminal proteins BiP and GFP retained in the ER (KGFP), ER membrane protein Sec61, and nuclear pore complex (NPC) protein Nup49, which spans both the perinuclear ER and nuclear membranes.

Observation of ER inheritance during cellular division was classified as a three-step process identified by the segregation of ER subdomains. Phase 1 included the spatial localization of proteins to distinct areas of the peripheral ER as a bud emerges and continues to grow. The timescale of Phase 1 was approximately 55 minutes. Phase 2 consisted of nuclear division and was identified as the segregation of

the perinuclear ER between the mother and daughter cell, which lasted for approximately 35 minutes. Phase 3 included complete separation of the mother and daughter cells. The time period of Phase 3 was approximately 18 minutes, during which ER luminal and membrane proteins returned to a homogeneous spatial distribution in all ER subdomains.

We have confirmed our hypothesis that spatial heterogeneity exists among ER resident and NPC proteins during cellular division and is a consequence of protein function during ER biogenesis. Our experiments continuously monitored ER fusion proteins throughout different time points of cell division. Results include comparison of the ER luminal protein, BiP, and ER membrane protein, Sec61, which indicate that spatial heterogeneity exists in the perinuclear ER during different stages of cell division. KGFP, a construct that is not involved in any ER process, has been used as a control in order to confirm that spatial localization of ER resident proteins is dictated by the protein's function. In addition, we have evaluated the localization of a luminal protein, BiP-mCherry, compared to the NPC identified by Nup49-Venus. Colocalization of these two proteins decreased throughout the progression of cell division, suggesting that BiP is required to leave the perinuclear ER of the mother cell during organelle biogenesis.

In order to determine the mechanism which controls ER inheritance, disruption of yeast microtubules and actin cytoskeleton was performed. Actin depolymerization disrupted ER morphology and altered ER protein spatial localization in budding yeast cells, suggesting a pivotal role for actin in mother-daughter budding. Our research has offered a better understanding of how various ER resident proteins maintain distinct spatial localization patterns as a consequence of their unique

functions during ER inheritance. Furthermore, we have identified specific classifications of spatial localization effects of protein in multiple subdomains of the ER and provided timescales of these specific phases based upon population studies.

Chapter 1

INTRODUCTION

In the secretory pathway, ~30% of proteins are transported from the endoplasmic reticulum (ER) through the Golgi apparatus destined for the cell surface or desired intracellular location. Traffic along the secretory pathway requires translocation across the ER membrane, which makes the ER a unique organelle in this pathway. Perhaps the most complex, multifunctional organelle in eukaryotic cells, the ER is often referred to as the "protein gatekeeper" as it is the first organelle of the secretory pathway (Du *et al*., 2004; Scharder *et al*., 2008). It is responsible for the folding and maturation of newly synthesized proteins, allows properly folded proteins to be secreted, and initiates the degradation and disposal of misfolded proteins (Fewell *et al.*, 2001).

1.1 Introduction to ER Structure

The eukaryotic ER is a complex membrane-bound organelle with continuous luminal regions throughout the cell (Lippincott-Schwart *et al.,* 2001). In yeast cells, specifically *Saccharomyces cerevisiae*, it has been proposed that the ER is composed of three unique structures illustrated in the following schematic in Figure 1.1: the perinuclear ER, the peripheral ER, and a network of tubules (Lowe and Barr, 2007).

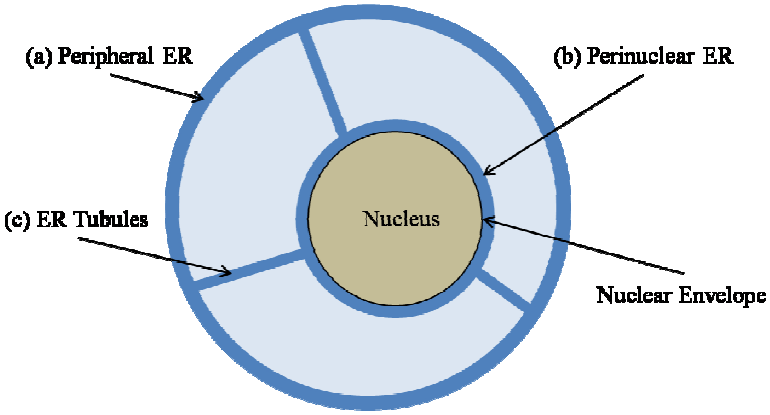

Figure 1.1 Schematic of a yeast cell indicating the three compartments of the ER: (a) peripheral ER, (b) ER tubules, and (c) perinuclear ER. The nucleus and nuclear membrane are labeled for reference.

The peripheral ER (a) is a network which lies under the plasma membrane around the periphery of the yeast cell (Du *et al.*, 2004).The perinuclear ER (b) is a single membrane which is continuous with the nuclear envelope (NE) (Voeltz and Prinz, 2007). The cytosolic network of ER tubules (c) connects the perinuclear ER and the peripheral ER, comprising the entire continuous structure. In general, there is very little known about the maintenance and inheritance of these different domains (Voeltz and Prinz, 2007). Yeast cells, like all eukaryotes, contain cytoskeleton in order to maintain cell shape and cell motility. The yeast cytoskeleton contains both microtubules and two types of actin, both which have been proposed to have roles in cell division of budding yeast (Du *et al.*, 2004).

1.2 ER Resident Proteins

Molecular chaperones and co-chaperones reside in all compartments of the cell, including the ER, where secretory proteins are folded and covalently modified (Vitale and Denecke, 1999). Chaperones exist in a variety of cellular processes including translocation across the ER membrane, binding to unfolded proteins, and preventing protein aggregation (Corsi and Schekman, 1997). The chaperone, Kar2 or BiP (Binding Protein, GRP78) has been identified as a member of the HSP70 family that is found in the ER lumen of yeast, *S. cerevisiae* (Rose *et al.,* 1989). The distal C-terminal domain of BiP contains an HDEL (Histidine-Aspartate-Glutamate-Leucine) sequence to maintain retention in the ER lumen (Pelham *et al.,* 1988). Not only has BiP been identified in the process of binding to hydrophobic regions of unfolded proteins, but has also been observed in numerous other critical intracellular processes, including karyogamy (nuclear fusion during mating), protein folding, and misfolded protein degradation (Rose *et al.,* 1989). BiP is regulated by co-chaperones of the HSP40 family in these intracellular processes (Hennessy *et al*., 2005). The selective ER co-chaperones are known to induce a conformational change in BiP to increase affinity for nascent or unfolded proteins. This family of proteins is characterized by the highly conserved region, the J domain, which is comprised of four α-helices and a HPD loop motif (Corsi and Schekman, 1997). Studies have shown that this domain is the minimal region essential for chaperone/co-chaperone interactions (Hennessy *et al*., 2005). Three main intracellular roles of BiP focused on for this research include translocation, protein folding, and ER quality control through ER associated degradation (ERAD), which are summarized in Figure 1.2.

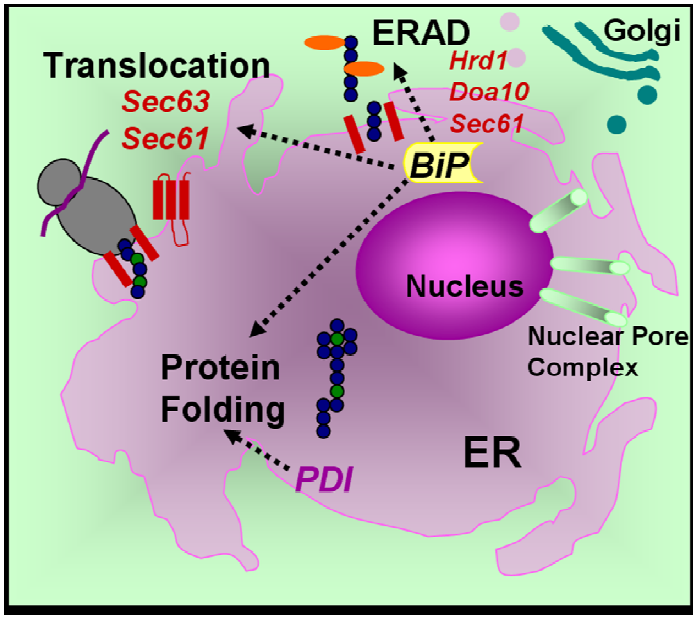

Figure 1.2 Schematic of the endoplasmic reticulum in yeast, *S. cerevisiae*. The various roles of the molecular chaperone, BiP are depicted with arrows pointing different intracellular processes involving other ER resident proteins. BiP is involved in: (a) translocation along with Sec61 and Sec63, (b) protein folding along with PDI, and (c) ERAD involving Hrd1, Doa10, and Sec61. (Figure courtesy of C. L. Young).

1.2.1 Translocation

BiP's role in translocation is the focus of interest for this research. Translocation of soluble and membrane proteins involves a multiprotein translocon pore consisting of the core heterotrimeric Sec61 complex (Sec61αβγ) (Alder *et al.,* 2005). The complex has an aqueous channel that expands from a diameter of 9 to 15 Å to a larger diameter of 40 to 60 Å when a nascent protein is translocated (Vitale and Denecke, 1999). This membrane is sealed either directly or indirectly with the chaperone BiP on the luminal side of the ER (Alder *et al.,* 2005). During translocation

of a nascent protein into the ER, BiP activates the opening of the luminal translocon seal once the nascent protein chains reach a threshold length of approximately 70 amino acids (Alder *et al.,* 2005). The mechanism by which BiP mediates the gating of the Sec61 translocon is controlled by the ATPase cycle. BiP-mediated gating of the translocon requires interaction with an ER membrane-bound J domain co-chaperone protein, Sec63 (Alder *et al.,* 2005).

1.2.2 Protein Folding and Maturation

In addition to acting as the protein gatekeeper, the ER is also a location for protein folding to ensure the structural integrity of each protein prior to secretion (Fewell *et al.,* 2001; Hammond and Helenius, 1995). BiP is known to have preferential binding capabilities to hydrophobic regions of proteins (Brodsky *et al*., 1999). In addition, protein folding defects have been observed in cells that have reduced levels of BiP (Simons *et al*., 1995). This suggests that this molecular chaperone plays a role in folding secretory proteins (Brodsky *et al*., 1999). Similarly, protein disulfide isomerase (PDI) is a 57kDa protein that also resides in the lumen of the ER of eukaryotes and has a role in protein folding (Kersteen *et al.,* 2003). The main intracellular role of PDI is the catalyzed formation of disulfide pairings in the tertiary structure of newly synthesized secretory proteins (Kersteen *et al.,* 2003; Laboissiere *et al.,* 1995). PDI is comprised of five structural domains, an active sequence CGHC (Cys-Gly-His-Cys), and the HDEL yeast ER retention signal (Kersteen *et al.,* 2003). Initially, PDI was also thought to have chaperone activity by reducing the amount of aggregation of unfolded proteins within the cell; however, recently this chaperone role has been attributed to the protein Scj1 (Schlenstedt *et al*., 1995).

1.2.3 ER Associated Degradation

The ER is referred to as a quality control machine, as it is responsible for controlling the selective degradation versus the selective secretion of proteins in the ER (Kabani *et al*., 2003; Brodsky *et al*., 1999). Defective and misfolded proteins from the secretory pathway are removed from the ER through ER-associated protein degradation (ERAD) (Kabani *et al*., 2003). ERAD is also activated to regulate and control levels of correctly folded proteins that are associated with certain intracellular processes (Hampton, 2002). Because the initiation of ERAD can be a result of inefficient protein folding, it is to be expected that the chaperone BiP is involved in this process (Kabani *et al*., 2003). BiP preferential binding to hydrophobic regions of proteins suggests it has the capability to recognize unfolded proteins (Brodsky *et al*., 1999). Studies have used mutations in the ER luminal BiP (*kar2*) to analyze the effect on ERAD efficiency in yeast (Kabani *et al*., 2003; Brodsky *et al*., 1999). These studies have strongly suggested that BiP plays an important role in activating ERAD.

Three ERAD pathways have been proposed for protein degradation. Retro-translocation of targeted proteins mediated by the Sec61 translocon complex is one proposed mechanism of ERAD (Kabani *et al*., 2003; Brodsky *et al*., 1999). Another method of protein degradation is through ubiquitin ligases (E3s). This leads to the second proposed mechanism of ERAD, a process involving Doa10, a ubiquitin ligase located in the yeast ER membrane (Deng and Hochstrasser, 2006; Swanson *et al*., 2001). This transmembrane protein attaches ubiquitin to other ER membrane proteins, soluble nuclear proteins, and soluble cytoplasmic proteins to target for degradation (Deng and Hochstrasser, 2006; Swanson *et al*., 2001; Ravid *et al*, 2006). Through immunofluorescent staining, Doa10 was found to be localized in both the ER and in the inner nuclear membrane (INM) of the yeast cell (Swanson *et al*., 2001). A

third proposed pathway is through the E3 ligase Hrd1 working in conjunction with other degradation ER proteins (Hampton, 2002). Studies of this pathway have revealed its use for degradation of naturally arising misfolded proteins (Hampton, 2002). Like Doa10, Hrd1 is also a transmembrane ER protein; however, due to its smaller size Hrd1 is not localized to the INM (Deng and Hochstrasser, 2006). Although these two pathways are mechanistically independent of one another, Doa10 and Hrd1 appear to work together to maintain acceptable levels of misfolded ER proteins (Hampton, 2002). Localization of these two ERAD proteins occur through the passage into nuclear pore complexes (Deng and Hochstrasser, 2006). Of the three ERAD pathways, only degradation through the protein Sec61 was analyzed and discussed for this research. Our work pertaining to the ERAD proteins, Hrd1 and Doa10, is discussed further in Appendix A2.

1.3 Nuclear Membrane Proteins

Nuclear pore complexes (NPCs) span both the ER and the nuclear envelope (NE) and allow for bidirectional exchange of molecules between the nucleus and the cytoplasm (Belgareh and Doye, 1997). NPCs have a general structure which displays a characteristic eightfold symmetry, containing approximately 30 different proteins (nucleoporins) organized into subcomplexes, which result in a molecular mass of 40 to 60 MDa in yeast (Belgareh and Doye, 1997; Schrader *et al*., 2008). The first complex to be identified in yeast is Nsp1, illustrated in Figure 1.3.

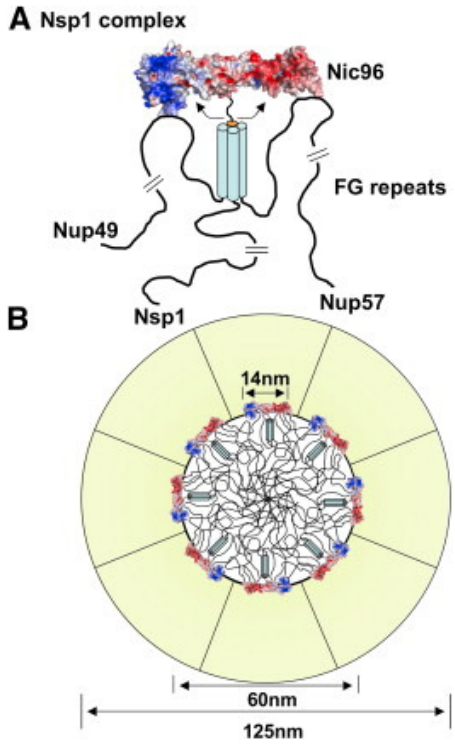

Figure 1.3 Model of the topological arrangement of the Nsp1 complex within the central channel of the NPC. (A) Nsp1-Nup49-Nup57 heterotrimer to Nic96. (B) Model of how Nic96 bridges between the structural core of the NPC scaffold and has access to the central channel. This figure was obtained from Schrader *et al*., 2008.

The Nsp1 complex is comprised of four subunits, Nsp1, Nup49, Nup57 and Nic96, which are held together with coiled-coil interactions (Schrader *et al*., 2008). The localization of these complexes has been shown to be quite dynamic, as they will migrate into dense clusters in particular regions of the NE as they are redistributed among dividing cells (Belgareh and Doye, 1997). In a study comparing Nup49, depicted in Figure 1.3, with other NPC proteins, Nup49 proved to be more abundant in

yeast and resulted in higher expression and fluorescence level when imaged with the confocal microscope (Belgareh and Doye, 1997). Therefore, Nup49 was the main protein studied in this research and was used to track the localization of the NPCs and NE morphology in budding yeast cells.

1.4 Cell Division in Budding *Saccharomyces Cerevisiae*

As previously mentioned, BiP has been found to be involved in karyogamy, the nuclear fusion that occurs in the formation of a diploid nucleus during yeast mating. Research has demonstrated that mutations of BiP in diploid yeast cells prevent karyogamy from occurring during reproduction (Rose *et al.,* 1989). Because of BiP's proposed role in the reproduction of diploid cells, this research seeks to determine if BiP also plays an important role in the budding of haploid yeast cells, *Saccharomyces cerevisiae*. This eukaryote has many intracellular processes similar to that of other more complex eukaryotes; however, there are many more advantages to using this organism for biological studies. Budding yeast cells are easily cultured and grow rapidly, with a doubling time on the order of 90-120 minutes (Herskowitz, 1988). The entire genome of *S. cerevisiae* is known, which allows for extensive genetic studies (Cherry *et al*., 1997; Herskowitz, 1988). *S. cerevisiae* proliferation occurs by the mitotic cell cycle, which is summarized by the diagram in Figure 1.4.

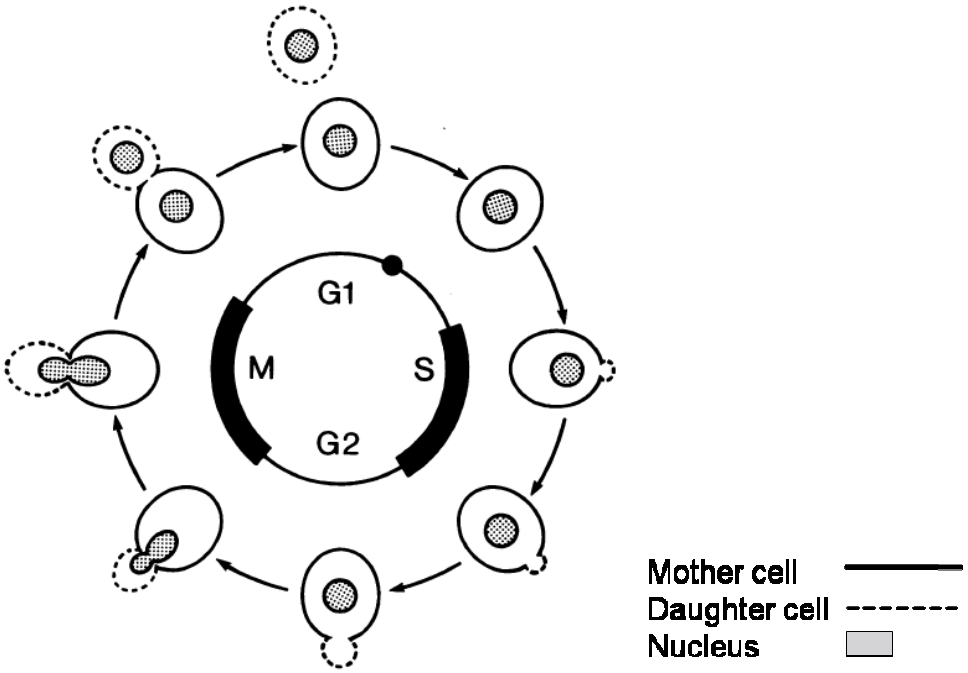

Figure 1.4 ***S. cerevisiae*** **mitotic cell cycle. The phases of the cell cycle are drawn in approximate proportions to their length. S phase is DNA synthesis, M phase is mitosis (nuclear division), and G1 and G2 phases are gaps where cell growth occurs. Figure adopted from Herskowitz, 1988.**

Mitotic cell growth occurs by the mother cell budding, or giving rise to an ellipsoidal daughter cell (Herskowitz, 1988). Once the mother cell (shown in solid black lines) reaches an optimal size, the cell shifts from G1 phase to S phase as a bud (shown in dotted black lines) begins to form and DNA duplication occurs during S phase. The cell then enters the gap G2 phase as the bud grows larger. M phase, mitosis, is marked by the nuclear division occurring between the mother and daughter cell. Finally, the daughter cell pinches off during the final step of mitosis, a step called cytokinesis, as

the cells separate. The daughter cell produced by *S. cerevisiae* is smaller in size than the mother cell and must increase during G1 phase before it can initiate budding of its own (Herskowitz, 1988).

1.5 Goals of Thesis Research

With a more complete understanding of the significance of both the ER and its resident proteins, it is apparent that a mechanism must exist which ensures consistent and faithful organelle inheritance through each cell cycle. The aforementioned proteins, BiP (ER luminal), Sec61 (ER membrane), Sec63 (ER membrane), PDI (ER luminal), Doa10 (ERAD), Hrd1 (ERAD), and Nup49 (NPC), were used to analyze ER morphology and biogenesis in budding yeast, *S. cerevisiae*. To ultimately determine the spatial heterogeneity of these proteins in yeast, this research continuously monitored proteins of interest during cell division under physiological conditions. This objective was accomplished through the combined use of live cell imaging with confocal light microscopy and fluorescent proteins tags to track proteins of interest *in vivo*. Fluorescently tagged proteins of interest were expressed in yeast cells by integrating the fusion proteins into the chromosome of *S. cerevisiae* via homologous recombination. When fluorescent proteins are excited with the laser of the confocal light microscope, fusion proteins emit their individual fluorescence of visible spectra, allowing for multiple proteins to be monitored simultaneously within live yeast cells. We hypothesize that spatial heterogeneity exists between the proteins of the ER membrane, lumen, and nuclear pore complex during cellular division in *Saccharomyces cerevisiae* as a consequence of functionality and organelle biogenesis.

Chapter 2

MATERIALS AND METHODS

This chapter describes the materials and methods used in molecular engineering the constructs for this research. Descriptions of the yeast and bacterial strains, plasmids, and media used are included, along with protocols for DNA preparation and the creation of fusion proteins of interest through homologous recombination.

2.1 Yeast and Bacterial Strains

The yeast strain of *Saccharomyces cerevisiae*, BJ5464 (*MATα ura3-52 trp1 leu2Δ1his3Δ200 pep4::HIS3 prb1Δ1.6R can1 GAL*), was obtained from American Type Culture Collection. BJ5464 is a haploid yeast strain which undergoes budding during the mitotic cell cycle. The *Escherichia coli* bacterial strain DH5α was used as a host for plasmid DNA.

2.2 Media and Agar Plate Protocols

The following protocols were used to make the selective media to grow cell cultures for experiments pertaining to this research. Selective media was used in the molecular engineering of fusion proteins, while the synthetic complete media (SC) was found to be the optimal media for growing and synchronizing cells for confocal microscope experiments.

2.2.1 Yeast Media

2.2.1.1 SC media

Synthetic complete (SC) media was mostly used for growing cells prior to and during live cell imaging experiments. SC media contains 20 g/L of dextrose, 14.7 g/L of sodium citrate, 6.7 g/L yeast N_2 base (YNB), 4.2 g/L of citric acid monohydrate, 3.82 g/L β dropout powder 2xSCAA (an amino acid supplement that does not contain leucine, uracil, or tryptophan) This protocol is from Dr. Anne Skaja Robinson's Lab. To make this SC media complete, 40 mg/L of tryptophan, 40 mg/L of uracil, and 400 mg/L of leucine must be added to the media. The water and salts are autoclaved in 80% of the total volume. The dextrose, YNB, and dropout powder are dissolved in 20% of the total volume and filter sterilized into the water and salt solution.

This choice of media was based on its minimal autofluorescence and ability to provide sufficient nutrients for time series experiments. In time series experiments, SC media was used to synchronize the budding yeast cells, a method derived from the Stationary Phase Cell Synchrony Protocol (Methods in Yeast Genetics, 2005). Several colonies of yeast cells were inoculated into synthetic complete (SC) media and grown in a water bath shaker at 275 rpm and 30°C for one hour prior to use for cell division time series experiments.

2.2.1.2 YPD media and agar plates

YPD media was used to grow yeast cultures during the homologous recombination of fusion proteins as well as for any re-streaking from frozen (-80°C) glycerol stocks. YPD media is comprised of 10 g/L of yeast extract, 20 g/L of peptone,

and 20 g/L of dextrose. To make YPD agar plates, 15 g/L of bacto-agar is added to the mixture. The media is autoclaved before use.

2.2.2 *E. coli* Media

2.2.2.1 LB media

During *E. coli* transformations, DH5α cells were inoculated in LB media and grown in a water bath shaker at 250 rpm and 37°C. LB media contains 10 g/L tryptone, 5 g/L yeast extract, and 5 g/L NaCl. LB+ampicillin plates include an additional 15 g/L of agar and 100 ug/mL ampicillin for selection of the plasmid.

2.3 DNA Preparation

To ultimately create fusion proteins of interest to conduct live cell imaging experiments, DNA must be prepared in *E. coli* cells prior to homologous recombination in yeast. This section for DNA Preparation includes information of the plasmids used and protocols for *E. coli* transformations, DNA miniprep, quantification of DNA, and restriction digests.

2.3.1 Plasmids

Plasmids obtained from the Yeast Resource Center (YRC) were used to construct the fusion proteins of interest (University of Washington). These plasmids include pBS7 (Venus), pBS10 (Cerulean), pBS35 (mCherry). The selective regions, including both the fluorescent protein markers and selective markers, of plasmids were amplified through polymerase chain reaction (PCR) (section 2.5.1) and inserted into the chromosome of yeast through homologous recombination (section 2.5.3). Figure 2.1 illustrates the basic plasmid pBS10 and associated selective regions.

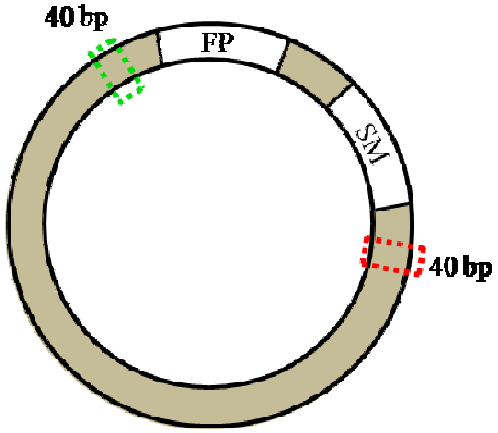

Figure 2.1 DNA plasmid obtained from the YRC. This plasmid contains the fluorescent protein marker labeled FP and the selective marker labeled SM. The F and R indicate the forward and reverse regions of homology on either side of the fluorescent and selective markers.

A unique characteristic shared by all YRC plasmids used in this research is the forward and reverse homology on either side of the selective regions. This similarity was useful when constructing fusion proteins because the same primers could be used for PCR reactions (see section 2.5.1 for more details and Appendix A.1 for table of primers).

The KGFP plasmid was constructed for use as a positive control in experiments described in subsequent chapters. Figure 2.2 illustrates the KGFP plasmid which was expressed in yeast cells (Courtesy of Davis Ng, Temaskek Life SciLab, Singapore).

A

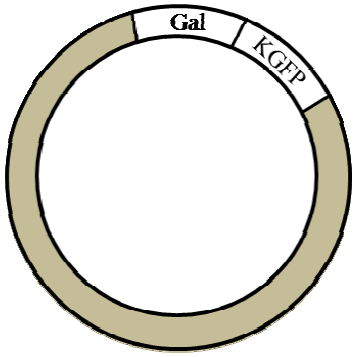

B

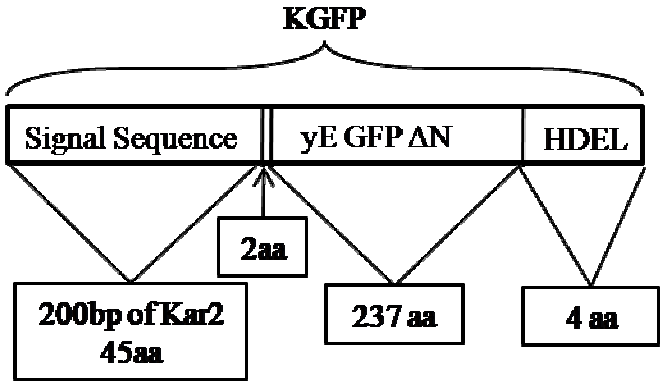

Figure 2.2 (A) KGFP plasmid with a Gal promoter followed by a KGFP sequence. This plasmid was transformed into yeast BJ5464 cells. (B) Sequence of the KGFP section of the plasmid. The first 200bp are dervived from the Kar2 sequence, followed by a 2aa linker, a 237 aa yeast enhanced (yE) green fluorescent protein (GFP), with a 4aa HDEL signal sequence at the end to ensure ER retention.

This KGFP plasmid was inserted into yeast BJ5464 cells. The sequence contains a yeast enhanced green fluorescent protein. This plasmid contains a GAL promoter, which is used to selectively grow yeast cells expressing this plasmid.

2.3.2 *E. coli* transformation

E. coli transformations were completed in order to express DNA plasmids in *E. coli* cells, which later served as a cassette for PCR reactions in the creation of fusion proteins. Immediately after thawing at room temperature, 50µL of DH5α *E. coli* competent cells were mixed with at least 10 ng of DNA. The sample was left on ice for 10 minutes and then placed in a 42°C water bath to be heat shocked for 2 minutes. The *E. coli* cells were directly and immediately placed in 1 mL of LB media to be grown in the water bath shaker for one hour at 37°C and 250 rpm. The LB culture was then centrifuged for four minutes at 2,000 rcf. A portion of the supernatant media was removed, leaving 150 µL of the LB media behind for resuspension. The concentrated *E. coli* transformed cell culture was transferred onto LB + ampicillin plates and grown in an incubator at 37°C for approximately 24 hours. The DNA contained the gene for ampicillin resistance; therefore only transformed DH5α cells containing plasmid were capable of growth on LB+ampicillin plates.

2.3.3 DNA extraction from *E. coli* cells

Following *E. coli* transformations, the DNA expressed in DH5α cells was extracted via the Zyppy^{TM} Plasmid Miniprep Kit as follows. After restreaking *E. coli* cells on selective media, the cells were inoculated in 5 mL of LB media and grown overnight in a 37°C water bath shaker rotating at 250 rpm. 3mL of the cell culture was centrifuged at maximum speed (16000 rcf) for 30 seconds; the supernatant was removed and discarded. The pellet was resuspended in 100 µL of 7x lysis buffer and mixed by inverting the microcentrifuge tube 4-6 times, as the solution changes from opaque to blue. 350 µL of cold neutralization buffer was added to the lysed cells and mixed thoroughly, as the solution's physical appearance changes from blue to yellow,

ensuring complete lysis. The mixed solution was centrifuged for four minutes at 16,000 rcf. The supernatant was transferred into the provided Zymo-Spin™ IIN column. The column was placed into the Collection Tube and spun for 15 seconds at 16,000 rcf. Flow through was discarded and 200 µL of Endo-wash Buffer was added to the column. The solution was centrifuged for 15 seconds at 16,000 rcf. Then 400 µL of Zyppy™ Wash Buffer was added to the column followed by centrifugation for 30 seconds at 16,000rcf. The column was then transferred to a clean 1.5 mL microcentrifuge tube and 30 µL of Zyppy™ Elution Buffer was added directly to the column. The sample was allowed to let stand for one minute at room temperature before centrifugation for 15 seconds at 16,000 rcf eluted the DNA into the clean microcentrifuge tube. 3 µL of the DNA was used to then quantify the concentration and purity by absorbance readings at 280, 260, and 230 nm (DU 640 Spectrophotometer; Beckman, Coulter). An example of the concentration and purity readings is shown in Table 2.1.

Table 2.1 DNA Extraction Absorbance Readings

Sample	Sample Volume Ratio	280nm	260nm	230nm	260/280	[DNA] (ng/µL)
pBS10_1	3µL/250µL	.0501	.0908	.0219	1.82	378.3

The concentration of DNA in the last column was found using the equation:

$$[DNA] = \frac{[260nm]}{(Volume\ Ratio)}\left(\frac{50ng}{\mu L}\right) = \frac{[0.0908]}{\left({}^{3\mu L}/_{250\mu L}\right)}\left(\frac{50ng}{\mu L}\right) = \frac{378.3ng}{\mu L}$$

The calculated concentration of DNA was used for further experiments including restriction digests and PCR. The ratio of the 260nm absorbance reading to the 280nm reading represents the quality of DNA extracted from the *E. coli* cells (Promega Corporation). A 260/280 absorbance ratio that is between 1.7 and 2.0 indicates a very high purity (Promega Corporation).

2.3.4 Restriction Enzyme Digestion

In order to molecular engineer fusion proteins, YRC plasmids need to be linearized by restriction enzymes. Restriction enzymes are unique in that they cut at specific base pairs in the DNA plasmid sequence. Typically, 1µL of enzyme is added to 1µg of purified DNA in a final volume of 50 µL, which includes buffers specific for each enzyme (New England Biolabs NEB) and distilled water. The solution is allowed to incubate for one hour at the recommended temperature. Before digestion, appropriate enzymes must be chosen based on restriction sites and optimal activity. If multiple digestions must occur, it is imperative to ensure that both enzymes are active in the required buffers and suggested incubation temperatures. An illustration of the restriction sites used in plasmids is shown in Figure 2.3.

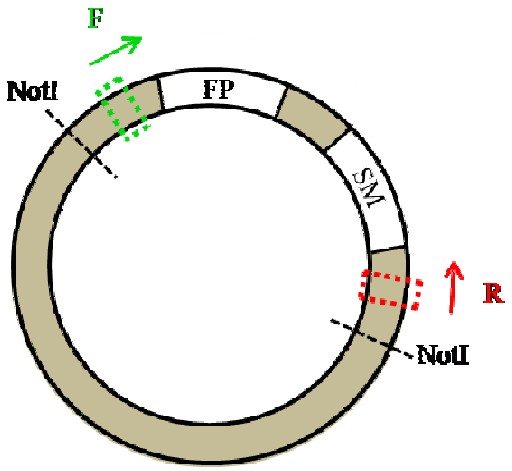

Figure 2.3 Schematic of DNA plasmid showing selective and fluorescent markers (FP and SM), regions of homology to other YRC plasmids (F and R arrows), and restriction sites for restriction enzyme, NotI.

In this example plasmid, restriction sites for the restriction enzyme, NotI, are located on either side of the regions of homology. NotI was used to linearize YRC plasmids to make a smaller DNA template cassette for the PCR experiments described in section 2.5.1.

2.4 Creation of HDEL Plasmids

In order to retain created fusion proteins in the endoplasmic reticulum when expressed in yeast cells, an HDEL retention sequence was inserted into the plasmids illustrated in section 2.3.1. The insertion of this sequence was accomplished by polymerase chain reaction with the use of appropriate primers, which are displayed in Appendix A.1. The sequence of the reconstructed plasmids was verified by the

DNA Sequencing Facility (University of Pennsylvania). The YRC reconstructed HDEL plasmids for each protein of interest were then integrated into the yeast chromosome via homologous recombination, which is explained further in section 2.5.3.

2.5 Creation of Fusion Protein

After DNA preparation of the plasmids containing fluorescent protein markers and selective markers of interest with appropriate ER retention sequence, fusion proteins were created. Polymerase chain reaction (PCR) was used to amplify linearized DNA templates, which were verified through DNA Electrophoresis to ensure the PCR products were the correct length. These experiments were followed by homologous recombination through yeast transformation to insert PCR products into the chromosome of yeast.

2.5.1 Polymerase chain reaction (PCR)

Polymerase chain reaction was used to amplify linearized DNA templates to be used in yeast transformations. The Expand Long Template PCR System (Roche) was used to conduct this experiment. Barrier pipette tips were used throughout the experiment to avoid contamination. Two different solutions (labeled MixI and MixII) are prepared on ice. The 25µL solution in MixI is comprised of 12 µL of dH_2O, 150 ng of linearized DNA, 5 µL of 10µM forward primer, 5 µL of 10µM reverse primer, and 1 µL dNTPs (added in this order). The dNTPs solution added was at a total concentration of 100mM and consisted of dATP, dCTP,dGTP, and dTTP (each ingredient at 25mM concentration). MixII consisted of 19.25µL of dH_2O, 5 µL of Buffer3 (Roche), and 0.75 µL of Expand Polymerase Mix in the specified order to a

final volume of 25µL. The two vials containing MixI and MixII solutions were combined on ice and immediately loaded into the Alpha Unit™ Block Assembly for PTC DNA Engine™ Systems, which was set to amplification for homologous recombination, setting 'HR57' which has an associated annealing temperature of 57°C. The parameters used for the PCR machine are described in Appendix A.1. Protocol used for this experiment was obtained by the Roche, *Expand Long Template PCR System*. The primers used for this research are shown in Appendix A.1.

2.5.2 DNA Agarose Gel Electrophoresis

Agarose gel electrophoresis is a highly effective method for identifying DNA fragments between the lengths of 0.5-25 kb (Current Protocols Molecular Biology, 2000). This experiment was used to verify correct digestions by restriction enzymes, to quantify DNA concentrations to be used in yeast transformations, and to ensure the correct PCR products. A DNA agarose gel at a final concentration of 0.8% is made by adding 0.24g of agarose to 30mL of TAE solution. The agarose mixture is heated in a microwave at high power for 35 seconds. The DNA electrophoresis gel box is filled with TAE buffer and the gel is poured into the DNA electrophoresis gel tray. A comb is placed into the polymerizing agarose gel to yield wells for samples to be loaded. The DNA Electrophoresis (Bio-Rad Laboratories) apparatus is run for 60 minutes at 100 volts to allow for complete electrophoresis. The DNA samples in the agarose gel are stained with ethidium bromide for approximately 10 minutes so that the samples can be compared to a 1kb ladder (Biolabs) using UV light.

2.5.3 Homologous Recombination via Yeast Transformation

Fusion proteins were created using a unique method, homologous recombination, where linearized DNA from the amplified PCR product was first purified (method described in Appendix A.1) and then directly inserted into the chromosome of yeast. Figure 2.4 illustrates the methods used to create a fusion protein for any of the proteins of interest.

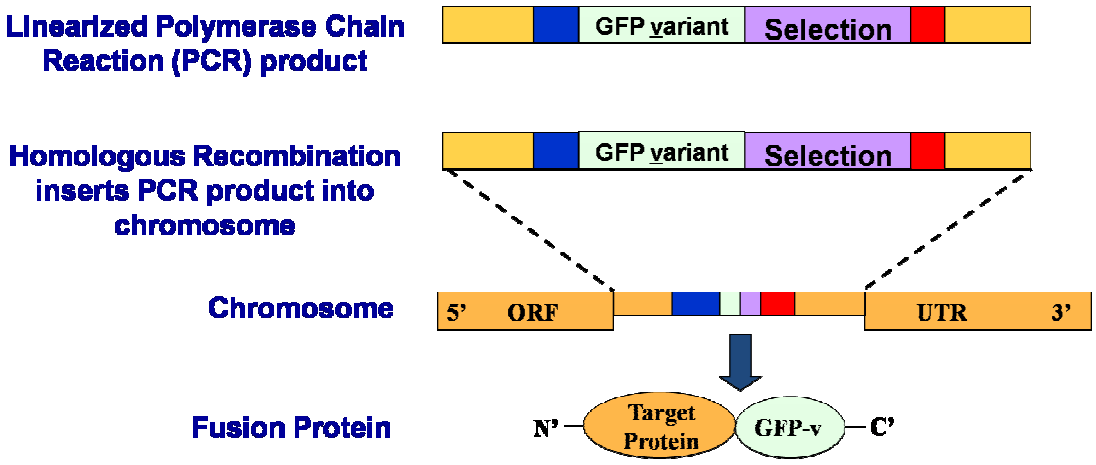

Figure 2.4 **Schematic of homologous recombination for the creation of fusion proteins. The linearized PCR product in the top line includes the the fluorescent protein (FP) and selective markers (SM) with forward and reverse regions of homology to the respective primers. Through homologous recombination, the DNA was placed into the chromosome of yeast through primers which have 40 base pairs homology to both the PCR DNA and the chromosome. This results in cells expressing the target protein with the GFP-v tag. (Figure courtesy of C. L. Young).**

The protocol for homologous recombination was derived from the protocol found in Methods of Enzymology (Gietz and Woods, 2002). Yeast cells were grown in 10 mL of YPD media at 30°C overnight. Before experiment, yeast cells must be in midlog phase. The yeast cell culture is spun down via centrifugation for seven minutes at 4°C and at 2,500 rcf. The resulting pellet is washed with 5mL of distilled water, followed by centrifugation. The wash with distilled water and centrifugation was repeated. The pellet of yeast cells were then resuspended in 100 µL of 100 mM LiAc and transferred into a microcentrifuge tube. The LiAc solution was removed, spun down by centrifugation for 15 seconds and supernatant was removed by pipetting. The following substances were added to the cell pellet in this order: 240 µL of 50% PEG, 36µL of 1M LiAc, 125 µL of 2mg/mL sperm carrier DNA (ssDNA). Prior to addition, the ssDNA was heated at 95°C for 5 minutes and then placed on ice. Lastly, the suggested ratios of PCR insert and plasmid vector were added to the cell solution. The sample was allowed to grow for 45 minutes in a yeast incubator at 30°C. The sample was then heat shocked for 25 minutes in a 42°C water bath. Immediately, the transformed yeast cells were recovered by centrifugation for 60 seconds at 6,000 rcf. Depending on the selective marker of the plasmid of interest, either 300 µg/ml of hygromycin B (hphB) or 200 mg/l of G418 was added to the YPD media (Goldstein and McCusker, 1999; Wach, 1999). The cells were resuspended in 2-3mL of YPD media and grown for 3-4 hours in the 30°C shaker. Cells were spun down by centrifugation for four minutes at 2,000rcf. A portion of the supernatant was removed, leaving behind 150µL to resuspend the cells. This concentrated sample was plated on YPD plates with appropriate selective marker and incubated at 30°C for approximately two days.

Chapter 3

LIVE CELL IMAGING

In order to analyze and ultimately model living cells under physiological conditions, it is imperative to study live cells and their expression of proteins under those same physiological conditions. The study of organelle dynamics and intracellular mechanisms has been revolutionized with the introduction of fluorescent protein (FP) technology, which allows individual proteins to be tagged with FP variants and monitored through live cell imaging (Lippincott-Schwartz, 2004). Using a combination of confocal light microscopy and FP variants, we show that spatial heterogeneity exists between various ER resident proteins during cell division. This chapter explains the methods of FP technology, the specifics of confocal light microscopy, the limitations on this experimental system, and the techniques used to analyze ER dynamics and heterogeneous localization of ER proteins within live yeast cells. An example of how live cell imaging and associated troubleshooting was used in initial experiments is also presented in this chapter.

3.1 Fluorescent Proteins

A promising tool for biological imaging is the use of fluorescent proteins (FPs), specifically the green fluorescent protein (GFP) and the red fluorescent protein (DsRed). Several studies have shown this pair of red and green fluorescence probes is optimal when viewing multiple fusion proteins simultaneously in a cell, a characteristic true of this research (Albertazzi *et al.,* 2009). This is because the red and

green spectral emission peaks are separated by a sufficient gap of approximately 70 nm, whereas yellow and green undergo crosstalk, as their emission peaks are only separated by 25 nm (Rizzo and Piston, 2005). GFP is a 27 kD protein derived from the jellyfish *Aequorea victoria* (Lippincott-Schwartz, 2004). Although the entire structure is essential to the development and maintenance of the protein's fluorescence, the actual fluorophore is derived from an amino-acid triplet (Ser65-Try66-Gly67) (Lippincott-Schwartz, 2004; Rizzo and Piston, 2005). In 2008, Martin Chalfie, Osamu Shimomura, and Roger Y. Tsien were awarded the Nobel Prize in Chemistry for their discovery and development of GFP. In contrast, DsRed is derived from a protein from the sea coral of the genus *Discosoma* (Davis, 2004). DsRed is not used as readily as GFP due to likelihood of aggregation and slow maturation of the protein (Jakobs *et al.* 2000; Rizzo and Piston, 2005). However, DsRed is 2.2 fold brighter than GFP (Davis, 2004). Engineered DsRed contains nine amino acid substitutions to enhance its solubility, reduce an undesirable green emission during maturation, and accelerate its maturation (Rizzo and Piston, 2005). The ultimate goal is to tag the eukaryotic proteins of interest with FPs, which results in fluorescence in the cell when these proteins are excited with the confocal microscope laser. This signal can be correlated to the number of corresponding molecules present in cells, which ultimately can lead to determination of relative protein concentrations within a given intracellular compartment. Protein and organelle dynamics can be determined by tracking these fusion proteins through time series analysis.

Both GFP and DsRed have been modified through site-directed mutagenesis to yield proteins which have greatly improved spectral characteristics, including increased fluorescence, greater photostability, and a shift in the emission

peaks resulting in numerous colors across the visible and IR spectrum (Shaner *et al.,*2004; 2005; 2007). The following table and figure include mutations that were made to both the wildtype GFP and the wildtype DsRed to create different FP variants.

Table 3.1 Mutations relative to wtGFP (Shaner *et al.,*2005)

GFP variant	**Mutations relative to wtGFP**
EGFP	F64L, S65T
EYFP	S65G, V68L, S72A, T203Y
Venus	F46L, F64L, S65G, V68L, S72A, M153T, V163A, S175G, T203Y
Cerulean	F64L, S65T, Y66W, S72A, H148D, N149I, M153T, V163A

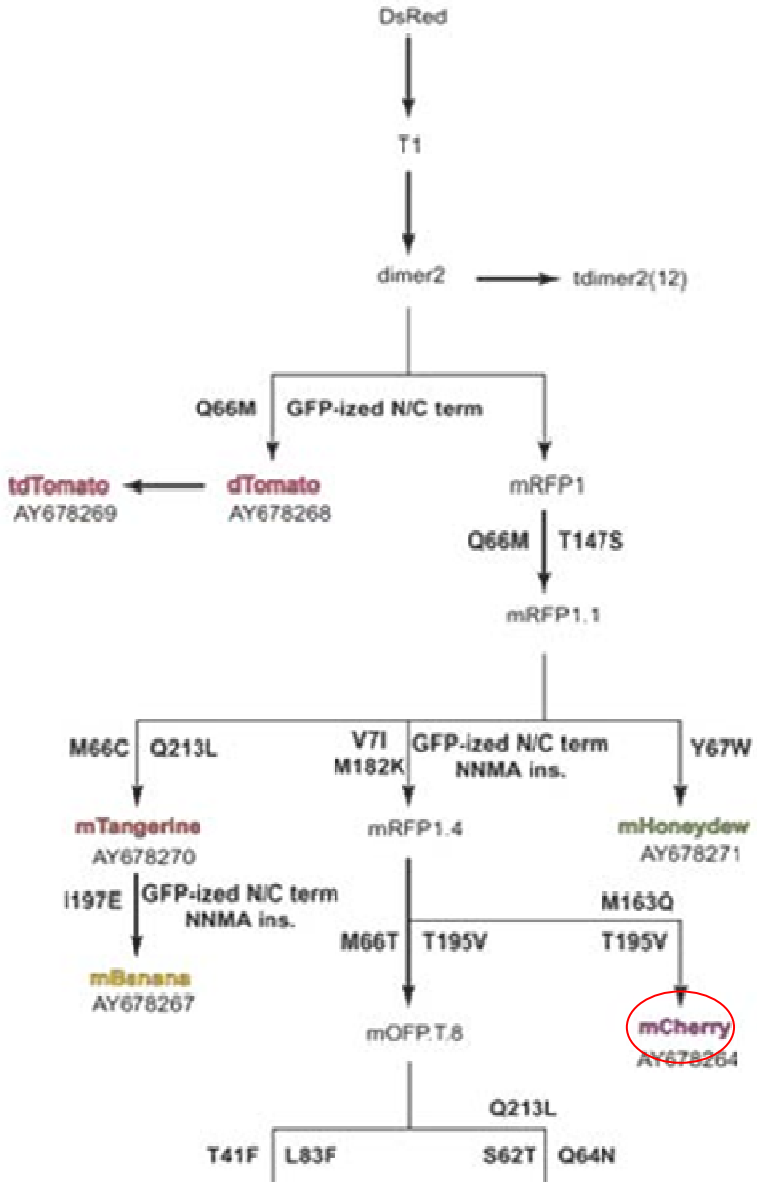

Figure 3.1 Schematic of a genealogy of DsRed-derived variants with mutations critical to the phenotype of each variant (Shaner *et al.*, 2004).

The site-directed mutagenesis of GFP and DsRed referenced in Table 3.1 and in Figure 3.1 were implemented to shift emission peaks and improve protein expression properties (Shaner *et al.,* 2004; 2005). The main DsRed variant studied for this research application is mCherry, circled in red Figure 3.1. The properties of the fluorescent proteins used in this research are summarized in Table 3.2.

Table 3.2 Properties of the best FP variants (Shaner 2005).

Class	Protein	Excitation (nm)	Emission (nm)	Brightness	Photostability
Red	mCherry	587	610	16	96
Yellow	Venus	515	528	53	15
Yellow	EYFP	514	527	51	60
Green	EGFP	488	507	34	174
Blue	Cerulean	433	475	27	36

The brightness of each FP variant was found by taking the product of extinction coefficient and quantum yield at pH 7.4 under ideal maturation conditions. The photostability parameters presented in Table 3 represent the time for photobleaching from an initial emission rate of 1,000 photons/s down to 500 photons/s. One of the most attractive aspects of the discovery of GFP variants is their use in labeling of multiple fusion proteins in single cells (Shaner *et al.,* 2005). The research presented in this thesis includes the use of multiple fusion proteins expressed simultaneously in yeast cells. This allows for concurrent live cell monitoring of several types of proteins within the ER, which naturally provides a more complete picture of organelle biogenesis and spatial localization of numerous proteins in various organelles.

When selecting FPs to use for *in vivo* biological applications, there are a few important characteristics to consider. A successful FP to be used for live cell imaging must have efficient fluorescent expression relating to the inherent concentrations of the proteins of interest. For example, when considering the number of molecules per cell of proteins BiP and Nup49, their concentrations greatly differ (337,000 for BiP versus 4,760 for Nup49) (Ghaemmaghami *et al.,* 2003). Therefore, when selecting fluorescent tags for creation of fusion proteins, a lower intensity FP should be chosen for BiP, while a higher intensity FP should be chosen for Nup49. Another characteristic is choosing an FP that yields minimal toxicity to the cells, which is indicated by cell viability, expected and consistent cell growth rates, and natural intracellular protein trafficking (Fehrenbacher *et al.,* 2002). FPs have been found to rarely demonstrate toxic effects to most cells. In fact, numerous biological applications using the FPs shown in Table 3.2 have been previously used involving the yeast *S. cerevisiae* with minimal toxic effects. In addition to non-toxic effects, tagging a protein with an FP must also not alter the native protein function or transport. Generally, the fusion of an FP tag does not alter the protein's native function or transport (Lippincott-Schwartz, 2004). The FP signal must also be brighter than the inherent autofluorescence of the cell, an attribute of the FPs in Table 3.2 that has also been proven in previous research applications.

An additional quality of FPs is adequate photostability to withstand repetitive imaging during the course of the experiment. The eventual photobleaching upon extended excitation is inevitable for FPs; however, their rate of photobleaching is significantly lower than that of many other small-molecule dyes. For this research, where multiple images are taken over a time period of approximately two hours to

capture cell division, using photostable proteins is very important. Finally, when tagging multiple proteins of interest with FPs in a single cell, a technique frequently used in this research, it is imperative to minimize crosstalk between excitation and emission channels (Shaner *et al.,* 2005). Crosstalk is an undesirable phenomenon which occurs when two or more signals overlap and are indistinguishable, which is an obvious problem when differentiating between two or more fusion proteins of interest. As previously explained, red and green FPs are the optimal pair when monitoring multiple fusion proteins simultaneously (Rizzo and Piston, 2005; Albertazzi *et al.,*2009). Because this research includes tracking the localization of multiple fusion proteins within the same yeast cells, there was an aim to have a red and green combination of fluorescent proteins within the system. The DsRed variant mCherry was chosen due to its optimized signal and increased photostability (Shaner *et al.,* 2007). The FP Venus, an optimized variant in the yellow spectrum, was used in combination with mCherry for this research.

3.2 Confocal Light Microscopy

Confocal light microscopy is an optical imaging technique that is often used in biological applications. Confocal microscopes are unique when compared to conventional wide-field microscopes because they eliminate out-of-focus objects resulting in increased contrast and detail of images (Murray, 2005). An inverted Zeiss AxioObserver light microscope, equipped with the Zeiss LSM5 DUO laser scanning confocal scanhead, and an inverted AxioExciter light microscope, equipped with LSM 710 laser scanning confocal scanhead, were used for this research. The advantage of confocal light microscopy over other techniques is that it captures in focus light emitted only by a single plane of a specimen, which is called an optical slice. With the

use of pinhole technology, the microscope is able to eliminate light from objects outside of the focal plane from reaching the detector. A laser beam is used to scan the sample of interest pixel-by-pixel in a scanning pattern to create the final image. The resulting image has very high resolution in all three dimensional directions: x, y, and z (theoretical resolution in x and y directions: ~200nm and in the z direction: ~500 nm). Confocal microscopy allows for three-dimensional image reconstruction by combining a through focus stack of many optical slices through a specimen, which then can be further processed by various imaging techniques, such as deconvolution. It is necessary to choose objectives that yield the best combination of resolving power, (determined by numerical aperture), working distance, and any additional optical corrections pertaining to the system being analyzed (Zeiss). Figure 3.2 shows the beam path through the LSM confocal microscope.

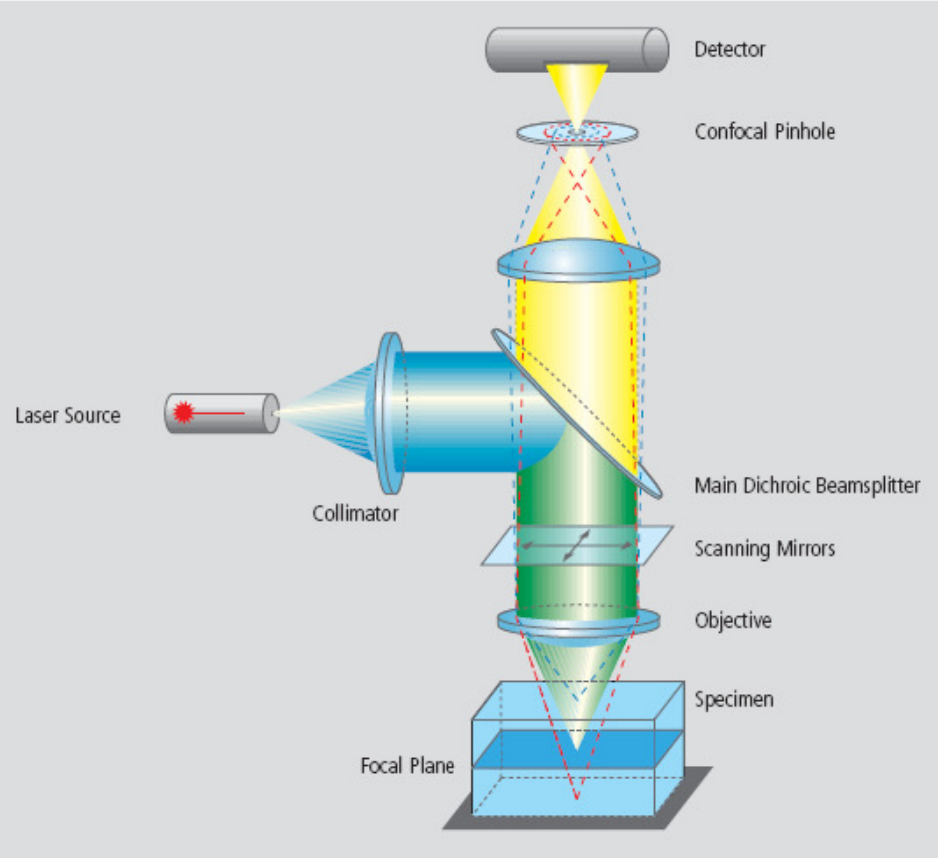

Figure 3.2 **The laser source creates a beam of light, which travels through a collimator lens, and directed towards the sample by the dichroic beamsplitter. The beam is then focused through the objective lens to the focal plane of the specimen. The in-focus fluorescence that is collected by the objective lens is refocused to the confocal pinhole to the photo-multiplier tube detector, where the photons are collected to result in a final fluorescent image. Out-of-focus light is blocked by the pinhole aperture and the emission wavelength of the specific fluorescent probe can be collected by using band pass or emission filters in front of the detector (not shown in diagram). It is in this way that the laser beam is raster scanned, point-by-point across the objective focal plane that an in-focus digital image is created.**

Fluorescence is defined as spontaneous emission of light after excitation. First the molecule is excited by radiation from light, which causes electrons to absorb energy and move to a higher energy level. This higher energy level is an unstable state, which leads to the electrons returning to their native state while emitting the absorbed energy in the form of light. Molecules that have these light absorbing and emitting properties are referred to as fluorophores. The emitted light is in the form of less energy, which ultimately creates emission in a different region of the visible spectra, which is equivalent to a different color (Foster, 1997). An example of the excitation and emission peaks is shown below in Figure 3.3.

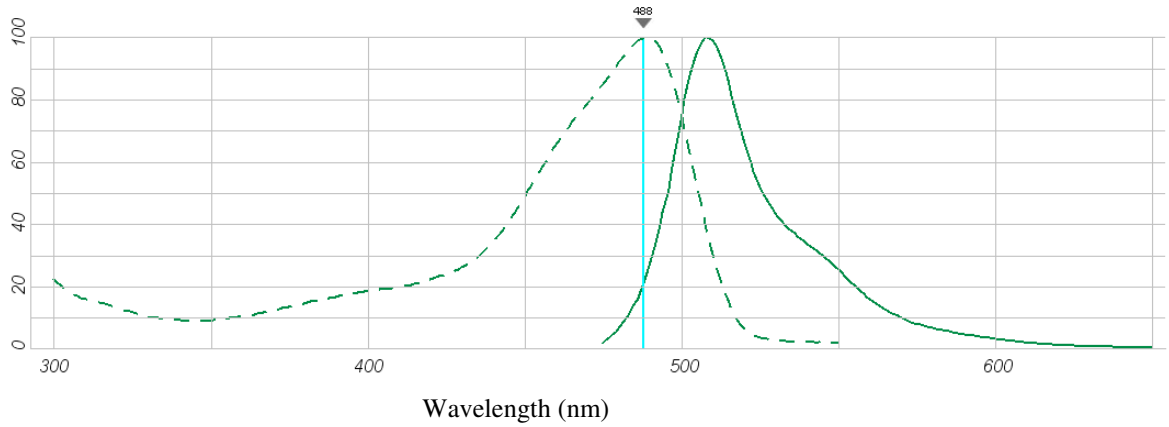

Figure 3.3 Representative excitation and emission curves for a blue exciting fluorophore. The x-axis is the wavelength of light nanometers. The y-axis represents the relative intensity of light. The solid blue vertical line represents the laser light wavelength at 488nm. The dashed line is the excitation curve and the solid line is the emission curve for EGFP when excited with the 488nm laser light. This image was obtained using the Spectra Viewer (Invitrogen).

From Figure 3.3, it is apparent that when the fluorophore represented by the curve (dashed green line) is excited with a 488 nm laser beam (blue vertical line), the energy

is emitted from a skewed emission curve (solid green line) with the peak at approximately 510nm.

One of the most useful features of the LSM5 DUO system for this research project is the ability to obtain simultaneous multifluorescence images and differential interference contrast (DIC) transmitted light images without compromising resolution or efficiency. Each fluorescent image is displayed as its own channel, which allows for independent adjustment of channel parameters to optimize conditions for each fluorescent probe. This feature was very valuable to this research, because it allowed for simultaneous tracking of the multiple fusion proteins of interest in a single cell. The main differences between the LSM 510, used for earlier experiments, and the LSM 710, used in several latter experiments, is the enhanced sensitivity and reduced background noise of the 710 system (Zeiss). These superior qualities allow for better live cell imaging results that indicate the system is greater, approximately five times more sensitive than the LSM 510 (personal communication with Dr. Kirk Czymmek). Due to time constraints and limited access to the LSM 710, only a few of the experiments were performed on this highly advanced system.

3.3 Confocal Materials and Methods

This section includes protocols and methods used in live cell imaging experiments. All confocal microscopy parameters were identified and varied to obtain optimized final live cell imaging techniques and settings. Zeiss software macros were implemented for further analysis and favorable environment settings, such as heating stage and nutritious media, were included to stabilize the system. The protocols for preparing cells for each FP variant imaged and other techniques for immobilizing the cells during experiments are also included in this section.

3.3.1 Confocal Light Microscope Parameters and Configurations

3.3.1.1 LSM Parameters

The LSM5 DUO and LSM 710 depends on similar parameters that may be varied to achieve the optimal configuration for each fusion protein and their respective image channels. The first parameter to be specified is the objective lens and its associated numeric aperture (NA). The observed brightness of a fluorescent image is explained by (Rines *et al.,*2005).

$$b \approx B\left(\frac{NA^4}{M^2}\right)E$$

In this equation *b* is the observed brightness of the fluorescent image, *B* is the fluorescent brightness of the object, *M* is the magnification of the lens, *NA* is the objective numeric aperture, and *E* is the transmission efficiency of the optics (Rines *et al*., 2005). When comparing the observed brightness of the 63x/NA 1.4 lens to that of the 100x/NA1.45 lens, the 63x lens is ~2.2 times brighter than its counterpart. For this research application, observed brightness is an important aspect when choosing an objective lens due to repetitive imaging over time course studies. A greater observed brightness results in less photobleaching effects over time.

When scanning images on the LSM systems, different parameters associated with the mode included: frame size in pixels, the scan speed of the laser, the pixel depth of the collected data, the direction and method of scanning, and the zoom of the frame. Typical frame sizes for snapshots and population studies in this research were 1024x1024 for the LSM5 DUO and 2048x2048 for the LSM 710. The images collected had a pixel depth of 12 bits which resulted in a theoretical resolution of 71.36µm in the x-direction and 71.36µm in the y-direction for the LSM5 DUO. 12 bit

images collected on the LSM 710 resulted in a theoretical resolution of 89.92µm in the x-direction and 89.92µm in the y-direction. However, for time series experiments, where total scan time for each image and photobleaching were an issue, the frame size was typically 1024x512 or 1024x256 for LSM5 DUO and 2048x300 for the LSM 710. The smaller y-direction frame size was selected because the laser scans faster in the x-direction than in the y-direction. Choosing a smaller frame size in the y-direction resulted in reduced total scan times and reduced photobleaching of cells nearby the cells of interest that were not being analyzed. In addition to the frame size, the zoom of the scanned image can be adjusted. By increasing the pixel resolution or zoom factor, the magnification can be increased for the given theoretical resolution of the objective lens.

For images collected in this research, the mode of the system was set to the 'line' setting, which collects images from each channel line-by-line simultaneously. The scan speed of the laser beam was able to be adjusted, which resulted in different image acquisition times depending on frame size and resolution of the image. A measured pixel time is on the order of microseconds and represents the total time the laser is located on each pixel. As the microscope is collecting emission wavelength the method of either 'mean' or 'sum' is specified. The 'mean' setting averages the signals collected from a specified number of pixel scans and reduces background noise. The 'sum' setting finds the summation of the signals collected from the specified number of pixel scans. For purposes of both the time series experiments and the single snap shots of budding yeast cells, the 'mean' setting was used.

Different channels are set up for the different images being scanned. For instance, when scanning cells which express only one fluorescent protein, there will be

three images: one for the fluorescence channel and the second for the DIC transmitted light channel and a third for the merged image (merges channels 1 and 2). If multiple fusion proteins are being expressed simultaneously in the cell, there will be a DIC transmitted light channel, channels for each of the fluorescence images, and a merged image of all fluorescent and transmitted light channels. The parameters associated with each channel are able to be varied and analyzed separately. The parameters associated with each channel include: pinhole, detector gain, the amplifier gain, amplifier offset, and laser power. In contrast to the LSM5 DUO, which allows for independent channel pinhole adjustments, the LSM 710 has a single pinhole, so they cannot be changed independently. Any pinhole adjustments directly affect the contrast, lateral resolution and the optical section thickness of the specimen. Ultimately for both systems, a pinhole of 1 Airy Unit (AU) is desired to receive the maximum amount of signal while excluding out-of-focus light. The detector gain parameter controls the intensity of the signals, while the amplifier offset adjusts the background level present in the image. Each fluorescent channel is excited with a specific and sample dependent percentage of the associated laser. The laser power can be adjusted for different experiments. If only single snapshots of yeast cells are being taken, the experiment can afford increased laser power to collect greater intensity signals. However, for long time series experiments, a reduced laser power must be used to minimize the amount of photobleaching of the fluorescence.

Each of the aforementioned parameters and settings were adjusted to yield the optimal configuration for each channel. The example shown in Table 3.3 includes the optimized settings for the LSM5 DUO when imaging BiP-mCherry.

Table 3.3 Optimized configuration for Venus Channel

Mode

Objective lens	Plan-Apochromat 63x/1.40 Oil DIC M27				
Frame Size	1024x1024	X	65.86µm	Y	65.86µm
Scan Speed	8	Pixel Time	1.28µs	Scan Time	
Pixel Depth	12 bit	Mode	Line		
Scan Direction	→	Method	Mean	Number	4
Zoom	2.2	Rotation	-		
Offset X	-	Offset Y	-		

Channel 1	Ch1 Red				
Pinhole	1.21AU	Pinhole	132 µm	Optical Slice	~1 µm
Detector gain	714				
Amplifier gain	2.24				
Amplifier Offset	-0.21				

Excitation	
Ch1	560nm 2.0%

This setting was used for both snapshots and time series analysis of BiP-mCherry fusion protein in budding yeast cells.

3.3.1.2 Channel Configurations

Another important aspect of using GFP variants is to choose correct filter configuration settings during microscopy, to ensure photostability and correct emission intensities (Shaner *et al.,* 2005). The configuration used for mCherry strains is shown in Figure 3.4.

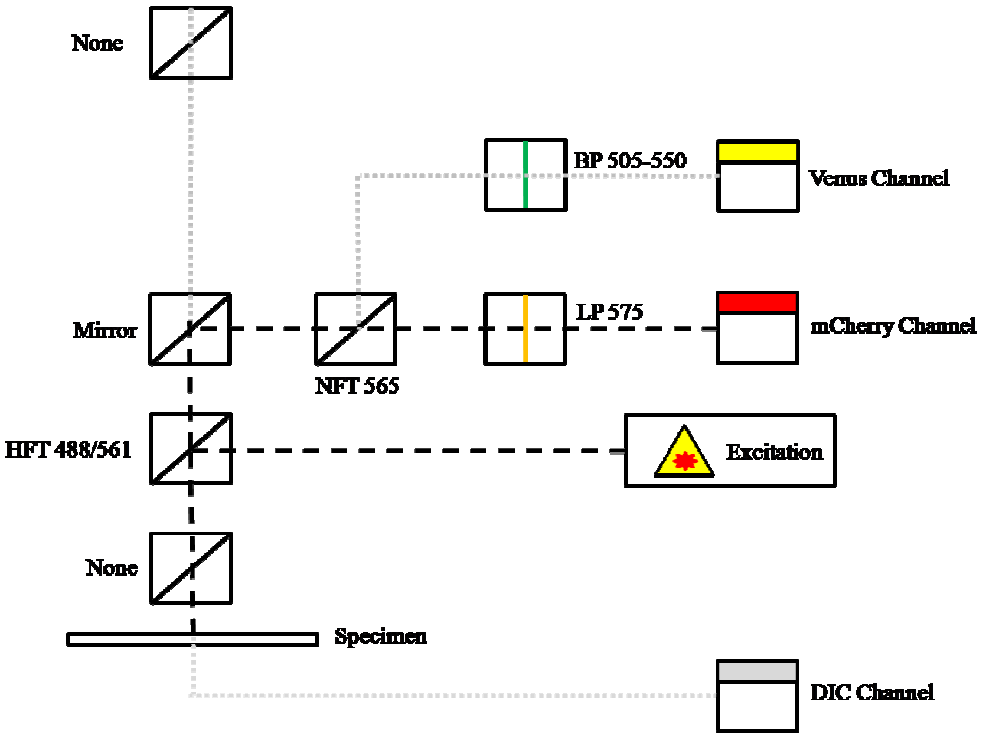

Figure 3.4 Configuration used in LSM5 DUO for mCherry strains. The excitation beam which is emitted from the fluorescent sample is sent through a HFT 488/561 filter. It is then directed through a NFT 565 filter, which splits the signal above and below 565nm. The signal that falls above 565nm is then sent through a long pass (LP) 575 filter which collects signals above 575nm (the mCherry signal).

This configuration only detects the fluorescence from the sample in the range of the mCherry fluorescence emission wavelength, which is around 610nm. In order to collect the Venus signal, the following configuration illustrated in Figure 3.5 is used.

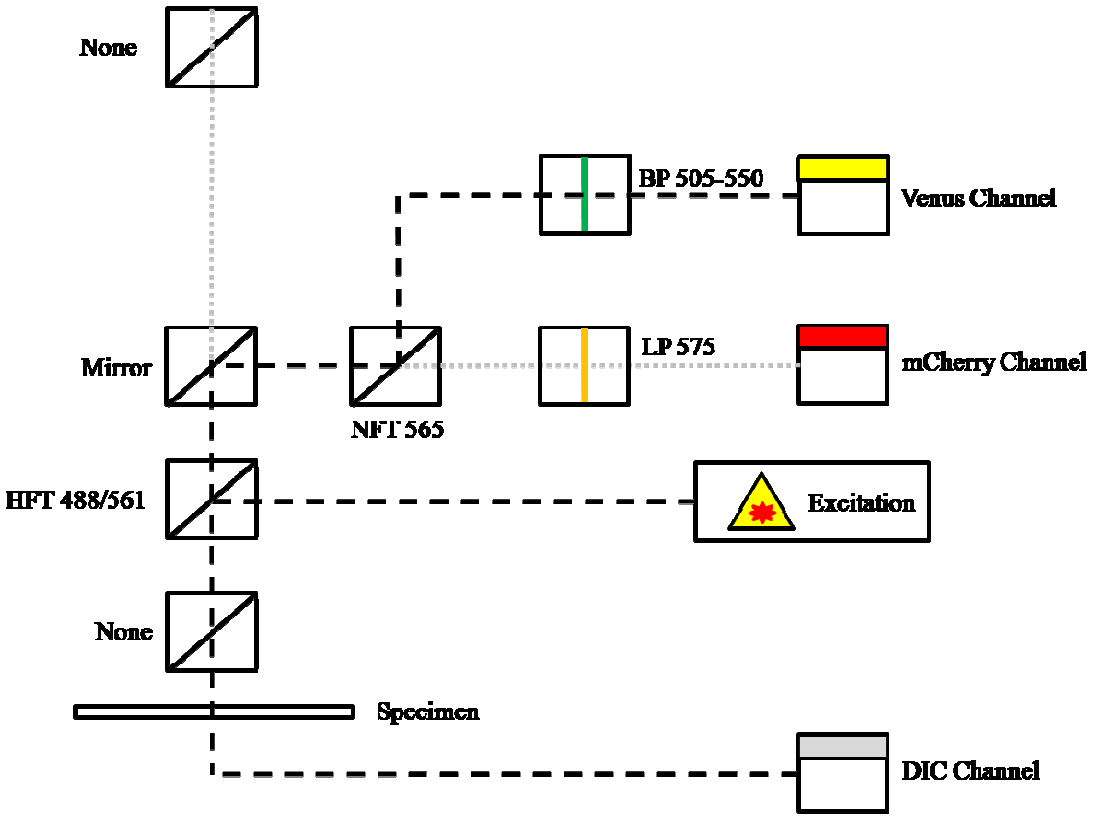

Figure 3.5 Configuration used in LSM5 DUO for Venus. The excitation beam which is emitted from the fluorescent sample is sent through a HFT 488/561 filter. This signal is directed by a mirror through a NFT 565 filter, which splits the signal above and below 565nm. The signal that falls below 565nm is then sent through a band pass (BP) 575 filter which collects signals between 505 and 550 nm.

This configuration only collects the emission photons from the Venus fluorescence, which emits light at around 528 nm. The signal is also passed through the specimen and collected for the DIC transmitted light image. The confocal microscope allowed

for multiple fluorescent images to be taken simultaneously through the use of these two configurations.

3.3.1.3 Photobleaching

For some experiments, which are noted as they are referenced in subsequent chapters, Anti Slow Fade Gold™ (Invitrogen) was used to minimize photobleaching and signal quenching during repetitive scans in time series experiments. There were many other parameters that were used to reduce the photobleaching of the cells. For other experiments, the confocal laser power was reduced to minimize photobleaching throughout the duration of time series experiments.

3.3.2 Time Course Study Preparation

3.3.2.1 Media Selection

Before time series images were obtained for live yeast cells, it was necessary to determine the appropriate media to use for imaging. The two determining factors in this assay include minimal autofluorescence, which leads to decreased signal to noise ratio (SNR) for observed fusion proteins, and the ability to provide essential nutrients to maintain cell growth over a period of several hours. Tested media in this experiment included: YPD media (10 g/L of yeast extract, 20 g/L of peptone, and 20 g/L of dextrose), synthetic complete (SC) media (20 g/L of dextrose, 14.7g/L of sodium citrate, 6.7 g/L yeast N2 base (YNB), 4.2 g/L of citric acid monohydrate, 3.82 g/L amino acid supplement), and phosphate buffer saline (PBS) media. Samples were prepared for *S. cerevisiae* BJ5464 cells expressing BiP-Venus fusion protein in each of the three medias YPD, SC, and PBS. Images were captured with the Zeiss LSM5

DUO confocal microscope and analyzed using histograms constructed by Zeiss software and ImageJ. PBS resulted in images with the most clarity, the greatest SNR, and the overall least amount of autofluorescence. However, PBS does not provide sufficient nutrients for cells and therefore arrests cell growth and cannot be used for time series analysis of yeast cells. YPD media yields a cell growth rate of approximately 2 hours. It provides an abundance of nutrients to support time series experiments. However, the resulting images indicate an extremely low SNR for the fusion proteins of interest. Even if the YPD media was filter sterilized, instead of autoclaved, the media will still autofluoresce due to the yeast extract and peptone present in the solution. SC media provided both the nutrients required to support cell division time series experiments and the low SNR needed for high quality, clear scans to be analyzed. Time series studies of cell division used in this research imaged cells in either SC media or SD-ura media, based on selectivity of the strain. SC media was used for strains with FP integrated into the chromosome and SD-ura media was used for the KGFP plasmid retained by ura selection.

3.3.2.2 Cell preparation for imaging

All BJ5464 strains expressing fusion proteins that have been integrated into the chromosome of the yeast cells are prepared for imaging experiments by placing in 1-3mL of SC media. BJ5464 yeast cells expressing the KGFP plasmid were taken from selective plates and grown in 3mL of SD-ura media for ~10 hours and then placed in SG-ura media for another 8 hours to ensure expression (Protocol optimized by C. L. Young). All cultures were then allowed to grow for one hour at 30°C and 275 rpm in mid-log phase to reach a final concentration of 1-2 OD_{600}/mL. In order to analyze yeast cells under normal physiological conditions, the cells need to be grown

to mid-log phase to ensure healthy growth. This protocol was derived from the Stationary Phase Cell Synchrony protocol (Methods in Yeast Genetics, 2005). The protocol suggested that allowing for initial cell growth for a period of time shifted the cells into a stationary phase (G_0 arrest). Resuspending the cells in fresh media allows the cells to reenter the cell cycle synchronously. After 1 hour of midlog phase growth, the culture was centrifuged for 4 minutes at 2,000rcf, followed by the removal of the supernatant. Cells were resuspended in 250µL of fresh SC media. Either 15µL of the cell suspension was plated in the 1% poly-D-lysine coated NUNC chamber wells (Lab-Tek #1.5) or 3µL was plated on a 2% agarose immobilization plate. A growth time of one hour in SC media was found to be the optimal timescale to evaluate cellular division.

3.3.2.3 Environmental Settings

The imaging of a population of cells over long time periods was limited due to the translational movement of the cells. Experiments were originally performed on 1% poly-D-lysine coated wells, a treatment which partially immobilized cells and only allowed for slight movement of the population of cells. However, for time series experiments of tracking specific cells through division, this slight translational movement was unacceptable. The solution for these time series experiments was to plate the cells on a 2% agarose plate, which is known to have no limitations on cell division (personal communication with Erik Snapp, Albert Einstein College). In addition to adjusting the immobilization techniques, it appeared that temperature gradients also seemed to limit optimal cell growth. Yeast cells prefer to grow at 30°C, whereas the original experiments were performed at an varying 23°C. Therefore, an environmental chamber was used during experiments to ensure that the stage of the

confocal microscope was maintained at a relatively constant temperature of 35°C. Due to temperature gradients between the environmental chamber, the stage, and the microslides containing the sample of interest, the temperature set point of 35°C was sufficient to ensure the actual sample was at the desired 30°C. This environmental chamber made it possible to view cell division of *S. cerevisiae* over several hours.

Although agarose plates and the environmental chamber led to appropriate environmental conditions for cell division, an occasional drift in the experimental set-up caused translational movement of cells in the x-y direction. Therefore, the manual stage control was synchronized between the microscope and the Zeiss software, thereby adjusting the stage location to track the same cells throughout division. A macro titled 'MultiTime' was used for several time series experiments. This macro allowed the imaging of multiple populations of yeast cells in different locations to be viewed simultaneously. Various fixed locations were defined while using this macro, and the LSM5 DUO was able to autofocus each of these locations sequentially, allowing multiple time series images to be taken virtually simultaneously.

3.3.3 Cell Immobilization Techniques

Two different previously mentioned cell immobilization techniques used for live cell imaging experiments are 1% poly-D-lysine treatment and 2% agarose plating. It takes between 30 seconds and several minutes for the LSM systems to take a high quality image representing one time point in a cell division. For these experiments, the poly-D-lysine protocol (section 3.3.3.1) was sufficient for immobilizing cells. However, when time series images were taken over the course of 1 to 2 hours, the immobilization with agarose protocol (section 3.3.3.2) was more

appropriate, as this technique immobilized the cells more effectively for the duration of these longer experiments.

3.3.3.1 Poly-D-Lysine protocol

Cells were immobilized by coating the wells of NUNC #1.5 chambers (Fisher Scientific, Lab-Tek™) with poly-D lysine (Sigma). Approximately 250 to 300µL of 1% poly-D-lysine, stored in aliquots at -20°C, was used to coat the inner four wells of the chambers. The reagent was incubated at room temperature for at least three hours, followed by 3-5 rinses with dH_2O. Chambers were placed inverted to dry overnight before use.

3.3.3.2 Immobilization with Agarose Protocol

This protocol was modified from the Guide to Yeast Genetics and Molecular and Cell Biology, Pt C (Tatchell and Robinson, 2002). 20mg of Sea Plaque Agarose (Cambrex Lot No. AG3979) was added to 1mL of PBS (or selective media) and was heated at 65°C for 6 minutes. The 2% agarose media was allowed to cool at room temperature for 30 seconds. 700µL of the agarose mixture was plated on a microslide (Corning 75x25mm plain thickness: 0.96-1.06mm ½ Gross; No. 2947) in a smooth line across the length of the slide. A second microslide was immediately placed over the agarose media to evenly spread across the entire length of the slide. After the plates were allowed to sit for 5 minutes, a razor blade was used to pry the two microslides apart, resulting in an intact smooth gel with minimal bubbles attached to only one of the slides. At this point, the cell sample was plated on the agarose layer. The cell sample was then covered with a coverslip (VWR International Microcover Glass 22x22 No 1 ½ Cat No. 48366227). The razor blade was used to trim away the

remaining agarose that was not covered by the coverslip. After discarding this excess agarose, a coat of clear nail polish (Sally Hansen) was applied around the perimeter of the coverslip to create a seal and secure the sample. The nail polish was allowed to dry before viewing under the microscope.

3.4 Results of Live Cell Imaging of BiP-Cerulean and Sec63-Venus

The hypothesis of this research is that spatial heterogeneity exists among ER resident proteins in budding yeast cells. Initially, to prove this hypothesis, live cell imaging was used to track localization of ER luminal fusion protein BiP-Cerulean and ER membrane fusion protein Sec63-Venus expressed in *S. cerevisiae* BJ5464 yeast cells. The BiP concentration within the cell is approximately 337,000 molecules/cell, which vastly exceeds the concentration of Sec63, which is approximately 17,700 molecules/cell (Ghaemmaghami *et al.,* 2003). These concentration differences were taken into consideration when choosing which FP marker to tag the ER resident proteins of interest. Cerulean, which has a relatively low brightness of 27 (Table 3.2), was chosen for the high concentration BiP, while Venus, which has an extremely high relative brightness of 53, was chosen for the low concentration of Sec63. The fusion proteins BiP-Cerulean and Sec63-Venus were created using homologous recombination, a technique described in section 2.5.3.

Two types of experiments were performed with the two fusion proteins. The first experiment was taking images at different time points in cell divison of yeast cells expressing BiP-Cerulean and Sec63-Venus simultaneously. Two images that were taken at different time points in cell division are shown in Figure 3.5.

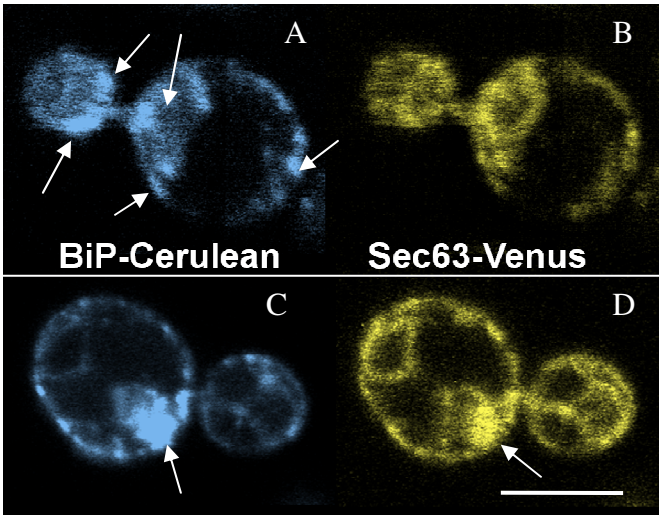

Figure 3.5 **Yeast cells expressing fusion proteins BiP-Cerulean (blue) and Sec63-Venus (yellow) simultaneously. Top two images (A and B) are at earlier time points in cell division and bottom images (C and D) are at later time points. Zeiss5 DUO confocal microscope, Plan-Apochromat 63x/1.40 Oil DIC M27 objective lens. Scale bar is ~5µm.**

Figure 3.5 shows yeast cells at two different time points in cell division. (A) and (B) show the localization patterns of BiP-Cerulean (blue) and Sec63-Venus (yellow) at early time points in cell division. It appears that there are high concentrations of BiP-Cerulean localized in different compartments of the dividing cell (indicated with white arrows), that are not seen in the Sec63-Venus budding cell (B). At later time points in cell division, illustrated by figures (C) and (D), the concentrations at the neck of the mother and daughter cells appear to have different localization patterns for BiP and Sec63. These results suggested that there was possible spatial heterogeneity existing

between ER resident proteins. However, in order to capture the entire cell cycle, time series experiments were needed to track both fusion proteins throughout cell division.

Time course experiments were performed with poly-D-lysine treated NUNC #1.5 chambers at around 23°C using the LSM5 DUO confocal microscope. Cells were grown in SC media for 1 hour prior to imaging. One set of time series results for BiP-Cerulean and Sec63-Venus is shown in Figure 3.6.

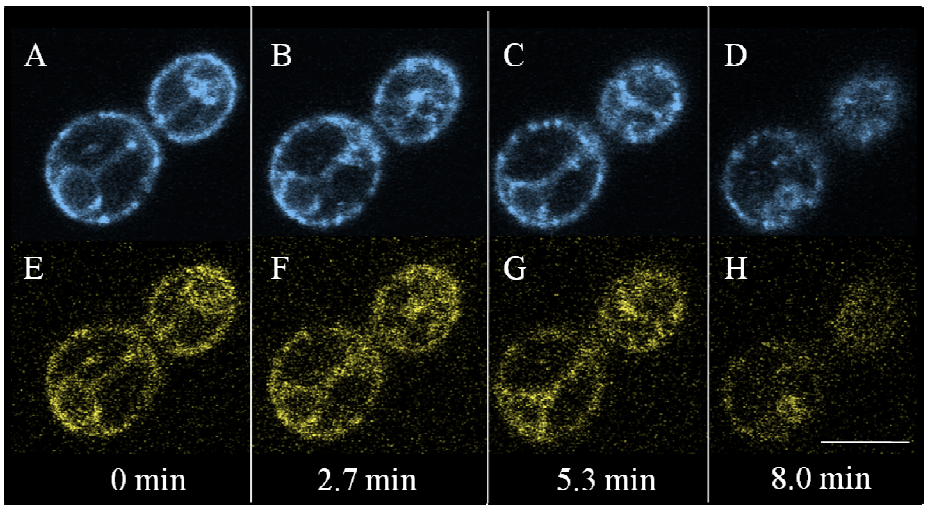

Figure 3.6 Time series of yeast cells expressing fusion proteins BiP-Cerulean (blue) and Sec63-Venus (yellow) simultaneously through cell division. Time between images and scale bar (~5µm) are shown at the bottom of the figure. Zeiss5 DUO confocal microscope, Plan-Apochromat 63x/1.40 Oil DIC M27 objective lens.

Figure 3.6 shows four points in the time series of a yeast cell dividing. The top images labeled (A) through (D) are the BiP-Cerulean (blue) images and the bottom images labeled (E) through (H) are the Sec63-Venus (yellow) images at the same time points in cell division. One apparent issue with this data is the brevity of the time series,

lasting a total of 480 seconds. As previously stated, the doubling time for yeast cells is between 90 and 120 minutes (Herskowitz, 1988). It is evident that an eight minute time series is far from capturing the entire yeast cell cycle. The main reasons for this short time series include photobleaching (loss of FP signal) and movement of the cells in all three directions. Even after adjustment of LSM parameters such as laser power, scan speed, pinhole, and detector gains, the Venus FP still displayed rapid photobleaching even after just a few scans. It is also apparent in both the BiP-Cerulean images and the Sec63-Venus images that by the fourth time point (at eight minutes), the budding cell is completely out of focus. This is a perfect example of how the poly-D-lysine is insufficient for immobilizing cells during time series experiments.

After examining all of the limitations of the BiP-Cerulean and Sec63-Venus experimental system, it was clear that a new direction needed to be taken in order to prove our hypothesis. Previous studies have shown that imaging YFP (Venus) and CFP (Cerulean) as a fluorescent protein pair in far from ideal (Albertazzi *et al.,* 2009). There is significant crosstalk between the two emission and excitation curves and they are highly sensitive to the local chemical environment (Albertazzi *et al.,* 2009). Therefore, it was decided that new strains of BiP-mCherry and Sec61-Venus were to be used for analysis of ER resident proteins. The fusion proteins mCherry appeared to be more stable and a higher intensity than the Cerulean. In addition to adjusting the FP used to track the ER resident proteins, the ER membrane protein was changed from Sec63 to Sec61. Although both proteins are located in the ER membrane and are involved in translocation, Sec61 has a higher concentration of almost 25,000 molecules/cell, whereas Sec63 has a lower concentration of 17,700 molecules/cell (Ghaemmaghami *et al.,* 2003). The lower concentration of Sec63

expressed in the cell caused the photobleaching in time series experiments to be a recurring issue.

After making adjustments to using BiP-mCherry and Sec61-Venus as the proteins of interest, time course studies were performed successfully, resulting in images with higher photostability and higher resolution. Another adjustment was using agarose to immobilize the cells during time series (see protocol in section 3.3.3.2). Each of these adjustments combined to allow for complete analysis of the ER resident protein localization in budding yeast cells. A time series of yeast cells expressing these two fusion proteins is shown in Figure 3.7.

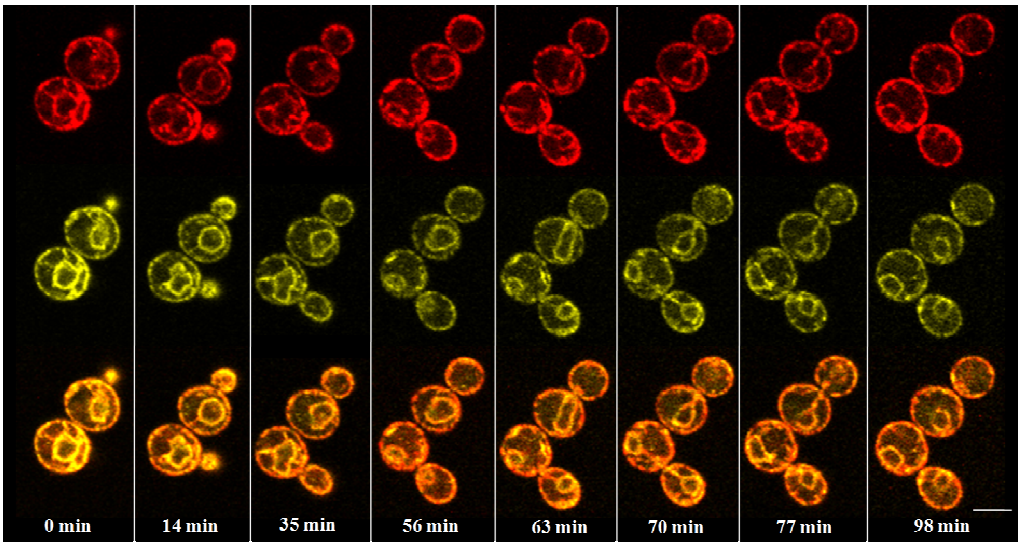

Figure 3.7 Time series analysis of S. cerevisiae yeast cells expressing BiP-mCherry and Sec61-Venus simultaneously though cell division. Time between images and scale bar (~5µm) are shown at the bottom of the figure. Zeiss5 DUO confocal microscope, Plan-Apochromat 63x/1.40 Oil DIC M27 objective lens.

It is apparent that the 98 minute time series summarized in Figure 3.7 provides far superior results when compared to the images of the 8 minute time series in Figure 3.6. There is minimal photobleaching occurring with the BiP-mCherry and Sec61-Venus, the images are clearer with a higher SNR. There is less translational movement of the cells. With the experimental setup designed and optimized, it was then possible to analyze and attempt to prove that spatial heterogeneity exists among ER resident proteins in budding yeast cells during cell division.

Chapter 4

ER STRUCTURE AND MORPHOLOGY

The ER is a complex organelle and the site of many intracellular processes. It has been proposed that the ER comprises three main compartments: the peripheral ER, the perinuclear ER, and a network of ER tubules. The structure and morphology of this essential organelle are discussed in this chapter. In order to track its structure and morphology, the ER luminal KGFP, a green fluorescent protein with an ER retention sequence, is imaged in live yeast, *S. cerevisiae*. Results include images of KGFP localized in the three compartments of the ER in live yeast cells. The primary focus of our research is to evaluate the localization of ER luminal, ER membrane, and NPC proteins in budding yeast cells. Confocal microscopy results show localization differences between BiP (luminal), Sec61 (membrane) and Nup49 (NPC) in live yeast cells. In addition, an in-gel fluorescence assay illustrates the relative concentration differences of ER resident proteins in yeast. Furthermore, the dynamics and continuity of the ER are confirmed. Fluorescence Loss in Photobleaching (FLiP) experiments have been performed on yeast cells expressing KGFP in order to verify the continuous structure of the ER during cellular division.

4.1 ER structure

4.1.1 Three Subdomains of the ER

Many organelles in eukaryotic cells are not only complex, but also maintain several domains in the organelle, each with a unique shape (Voeltz and Prinz,

2007). The endoplasmic reticulum is no exception. It has been proposed that the ER comprises three main structures or subdomains: the perinuclear ER, the peripheral ER, and a network of tubules (Lowe and Barr, 2007; Loewen *et al.,* 2007; Du *et al.,* 2004; Voeltz and Prinz, 2007). Each structure has its own unique shape and is segregated between the mother and daughter cells differently. A schematic of these three domains is shown in Figure 4.1.

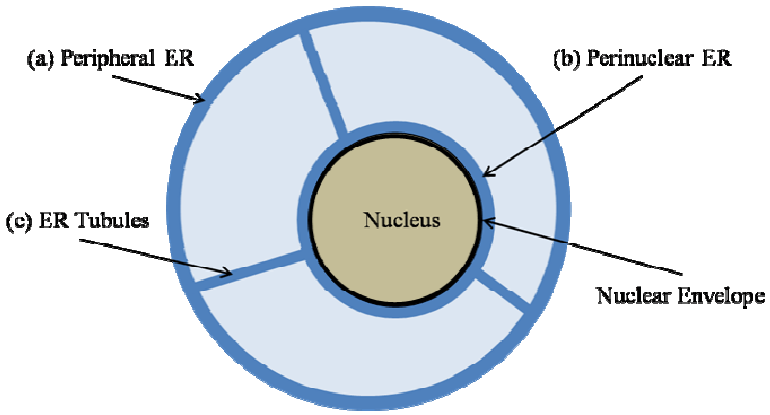

Figure 4.1 Schematic of a yeast cell indicating the three compartments of the ER: (a) peripheral ER, (b) ER tubules, and (c) perinuclear ER. The nucleus and nuclear membrane are labeled for reference.

The peripheral ER, labeled (a) in Figure 4.1, is a cortical network which lies under the plasma membrane and is a similar structure to that of higher eukaryotic cells (Du *et al.,* 2004).The perinuclear ER, labeled (b) in Figure 4.1, is a single membrane which is continuous with the nuclear envelope (NE) (Voeltz and Prinz, 2007). The network of ER tubules, labeled (c) in Figure 4.1, connect the perinuclear ER and the peripheral ER. Although there is very little known about the maintenance and inheritance of

these different domains, subcompartmentalization appears to be a common theme among other organisms (Voeltz and Prinz, 2007).

To verify the three domains shown in Figure 4.1, live cell images of yeast cells expressing KGFP were captured by confocal microscopy, using the Zeiss LSM 710. As previously mentioned, KGFP is the green fluorescent protein with a HDEL ER retention sequence that retains the fluorescent protein in the lumen of the ER. This protein has no functionality and simply marks the structure of the ER lumen. This protein was used as a positive control throughout all live cell imaging experiments to verify the luminal ER morphology. Figure 4.2 is an image of a single yeast cell expressing KGFP.

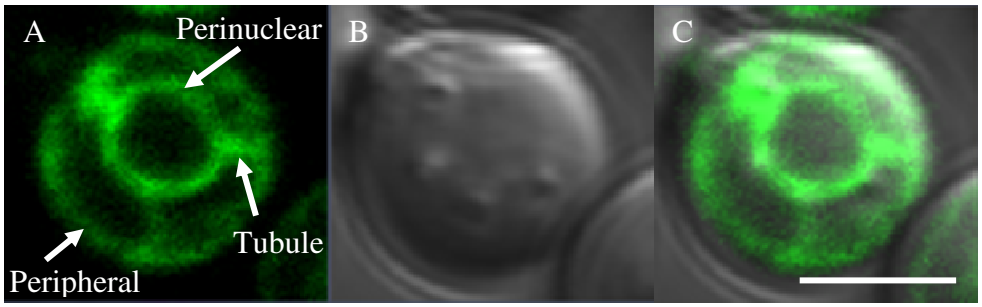

Figure 4.2 **Image of a single yeast cell, *S. cerevisiae*, expressing KGFP. Image (A) is the fluorescent image of KGFP in the lumen of the ER. Image (B) is the DIC transmitted light image of the yeast cell. Image (C) is the merged image of (A) and (B). Zeiss5 DUO , Plan-Apochromat 63x/1.40 Oil DIC M27 objective lens. Scale bar is ~5µm**

Figure 4.2 shows the localization of KGFP in the three subdivisions of the ER. In image (A) each compartment is labeled: peripheral ER, perinuclear ER, and the ER tubules. The consistency of this result with the literature suggests that yeast cells

expressing KGFP can in fact be used as a positive control for ER identification in live cell imaging assays. The spatial localization of other ER resident proteins, which inherently possess functionality, were compared to KGFP in order to determine if functionality plays a role in ER protein localization.

4.1.2 Localization of ER resident proteins and NPC proteins in yeast

Previous research has verified that functional ER resident proteins are localized in the aforementioned subdomains of the ER of budding yeast cells (Fehrenbacher *et al*., 2004). Freeze-substitution experiments have revealed that ER membrane proteins are localized near the plasma membrane (peripheral ER) of yeast cells (Fehrenbacher *et al*., 2004). Immuno-EM experiments indicated that similar ER resident proteins were found in both the peripheral ER and the perinuclear ER (Fehrenbacher *et al*., 2004). When analyzing the ER resident proteins for this research, one would expect to see similar localization that was depicted in the results of these two experiments and by KGFP in section 4.2.1.

BiP is a luminal ER protein involved in numerous intracellular processes such as protein translocation, protein folding and maturation, and protein degradation. Just as KGFP is localized to the three domains of the ER, the molecular chaperone BiP should have similar spatial localization patterns. To monitor BiP in live cells, the fusion protein BiP-mCherry was expressed in yeast, *S. cerevisiae*, and images were captured by confocal microscopy, using the Zeiss LSM 710. Figure 4.3 presents the results for BiP-mCherry localization.

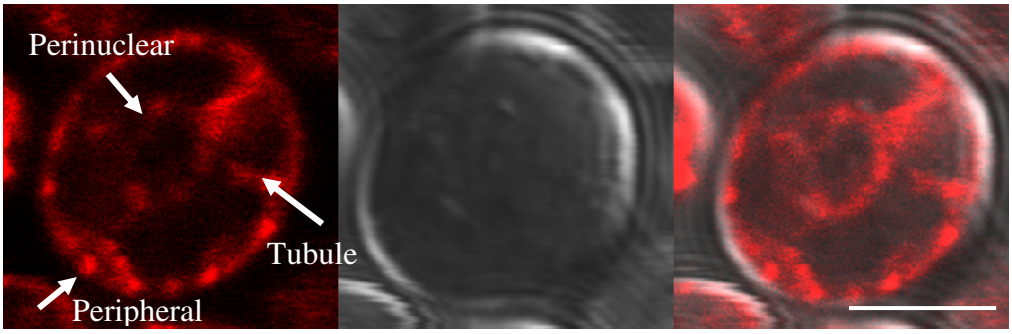

Figure 4.3 Image of a single yeast cell expressing BiP-mCherry. The three domains are indicated and labeled on this image. Zeiss 710 confocal microscope, Plan-Apochromat 63x/1.40 Oil DIC M27 objective lens. Scale bar is ~5µm.

Comparing the BiP-mCherry expression in Figure 4.3 to that of KGFP in Figure 4.2, both appear to be similarly distributed in all three domains of the ER. This experiment was repeated for PDI-mCherry, another luminal ER protein involved in protein folding and maturation, and Sec61-Venus, a membrane ER protein involved in protein translocation and degradation (e.g. ERAD). Results for single yeast cells individually expressing PDI-mCherry and Sec61-Venus are shown in Figure 4.4.

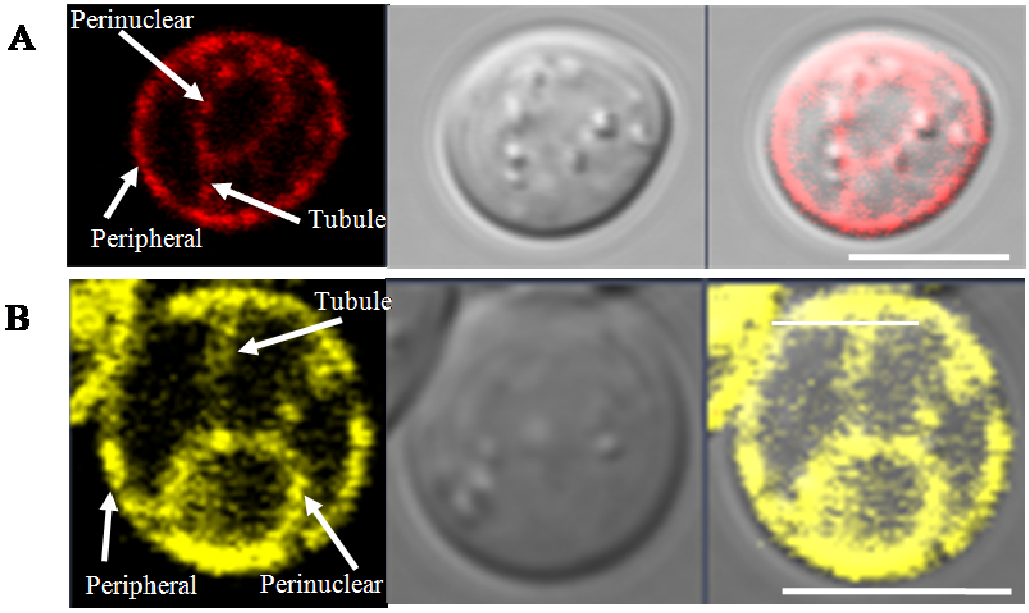

Figure 4.4 **(A) Yeast cell, *S. cerevisiae*, expressing PDI-mCherry (red) luminal ER protein. (B) Yeast cell, *S. cerevisiae*, expressing Sec61-Venus (yellow) membrane ER protein. Zeiss5 DUO confocal microscope, Plan-Apochromat 63x/1.40 Oil DIC M27 objective lens. Scale bars each represent ~5µm.**

Both PDI-mCherry and Sec61-Venus appear to also localize similarly to KGFP, as they, too, completely fill the three domains of the ER. The last protein that is examined in this research is Nup49, a protein within the nuclear pore complex (NPC).

As previously mentioned in Chapter 1, NPCs span the continuous membranes of the perinuclear ER and the NE to allow for bidirectional exchange of molecules between the nucleus and the cytoplasm (Belgareh and Doye, 1997). The location of NPCs is illustrated in Figure 4.5.

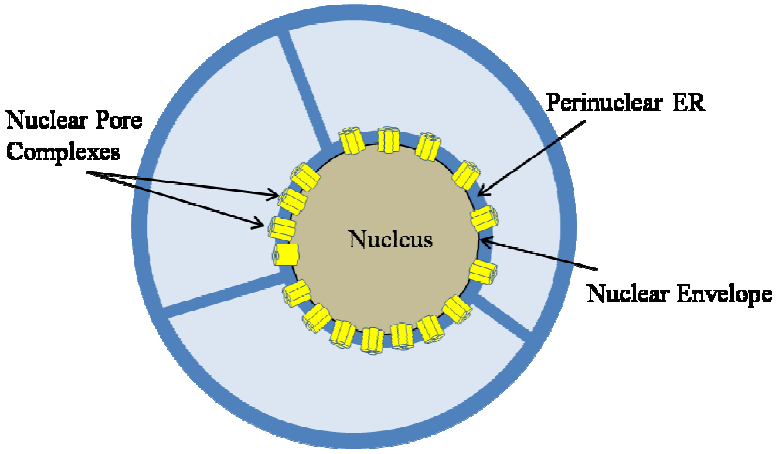

Figure 4.5 Schematic of the ER of the yeast cell and the localization of NPCs spanning the NE and the perinuclear ER.

To verify the localization of the NPC at the perinuclear ER and NE sites, a fusion protein for a nucleoporin in the NPC was expressed and analyzed in live yeast cells, *S. cerevisiae*. In a previous study comparing various nucleoporins, Nup49p proved to be more abundant in yeast and results in a higher expression and fluorescence level when tagged with GFP (Belgareh and Doye, 1997). Nup49-GFP has also been shown to localize correctly to the NPC and used in confocal microscopy time series analysis to show successive changes in NE morphology during cell division (Belgareh and Doye, 1997). Therefore, Nup49 was selected to track the NE and perinuclear morphology in yeast cells. Figure 4.6 shows the Nup49-Venus fusion protein localization in *S. cerevisiae.*

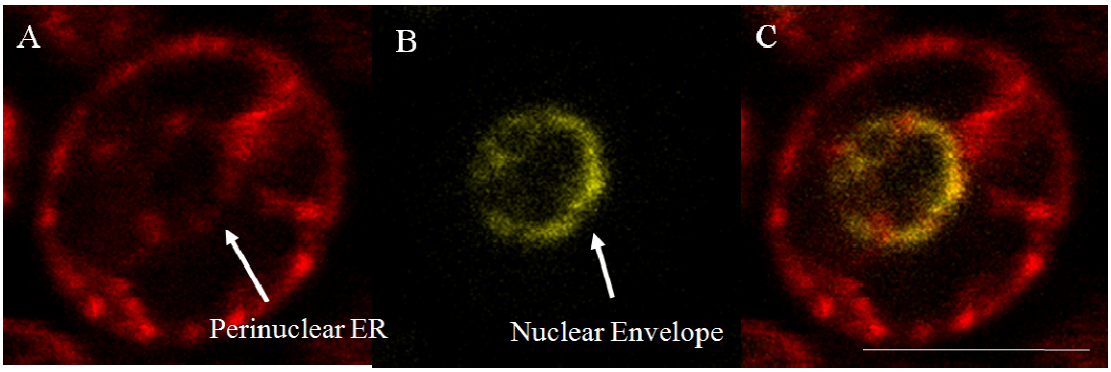

Figure 4.6 Images of a single yeast cell expressing BiP-mCherry and Nup49-Venus. (A) Fluorescence image of BiP-mCherry (red) localized in the ER. (B) Fluorescence image of Nup49-Venus (yellow) localized to the nuclear envelope. (C) Merged fluorescence images of BiP and Nup49 Zeiss 710 confocal microscope, Plan-Apochromat 63x/1.40 Oil DIC M27 objective lens. Scale bar is ~5µm.

In Figure 4.6, it is apparent that the Nup49-Venus is only localized to the continuous NE and perinuclear ER membranes, indicated by the arrows in the merged image (C). This protein serves an important role in subsequent experiments because it can be used to mark the exact perinuclear ER localization and dynamics throughout cell division. Although the location of the three domains is apparent in a cell that is not undergoing division, the compartment localization differences are more complex during ER inheritance. This is discussed further in Chapter 5.

4.2. Relative concentrations of ER resident and NPC proteins

Although it appears that functionality of the ER resident proteins does not have an effect on their distributions in the ER subdomains, their functionalities do play a role in determining relative concentrations of the proteins in the cell. Table 4.1

summarizes the approximate number of molecules present per cell of selective proteins.

Table 4.1 ER resident and NPC protein approximate concentrations (number of molecules per cell) in yeast, *S. cerevisiae*. This table was obtained from Ghaemmaghami *et al.,* 2003.

Protein	Family	Concentration (molecules/cell)	Protein Size (Da)	Cellular Function
BiP	ER Chaperone	337,000	74,467	Translocation/ Protein Folding/ ERAD
Sec61	ER Co-chaperone	24,800	52,936	Translocation/ERAD
Sec63	ER Co-chaperone	17,000	75,344	Translocation
PDI	ER Chaperone	-	58,227	Protein Folding
Nup49	Nuclear Pore Complex Protein	4,760	49,142	NE channel

As previously discussed, these concentration differences pose an issue when analyzing multiple fusion proteins of interest with fluorescent tags of varying intensities. Relative concentrations must be considered with selecting appropriate FP variants so that selective proteins are paired with adequate fluorescent probes. An in-gel fluorescence assay was performed to further understand how the concentration differences in Table 4.1 result in varying fluorescence expression of fusion proteins *in vivo*. To perform this experiment, fusion proteins were created for each protein in Table 4.1 using the same FP Venus. After growing the cells to mid-log phase, cells were lysed and fluorescence was measured (protocol in section 4.2.4). The result of the in-gel fluorescence experiment is displayed in Figure 4.7.

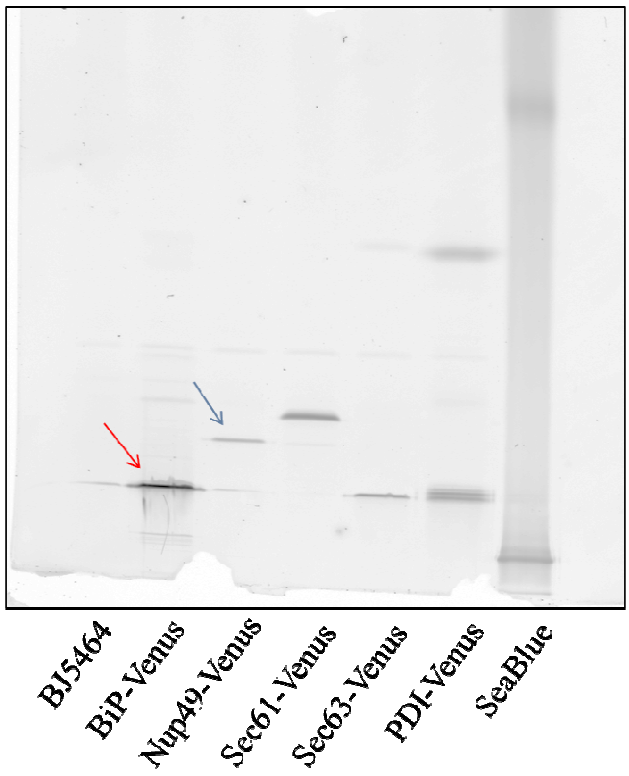

Figure 4.7 In gel fluorescence results. Each well is labeled with the respective protein. The red arrow indicates the BiP-Venus concentration compared to the blue arrow indicating the Nup49-Venus concentration.

After normalizing the fluorescence intensity by correcting for autofluorescence of the parental strain, BJ5464, the relative integrated densities were quantified for each protein in the assay. The results are shown in Figure 4.8.

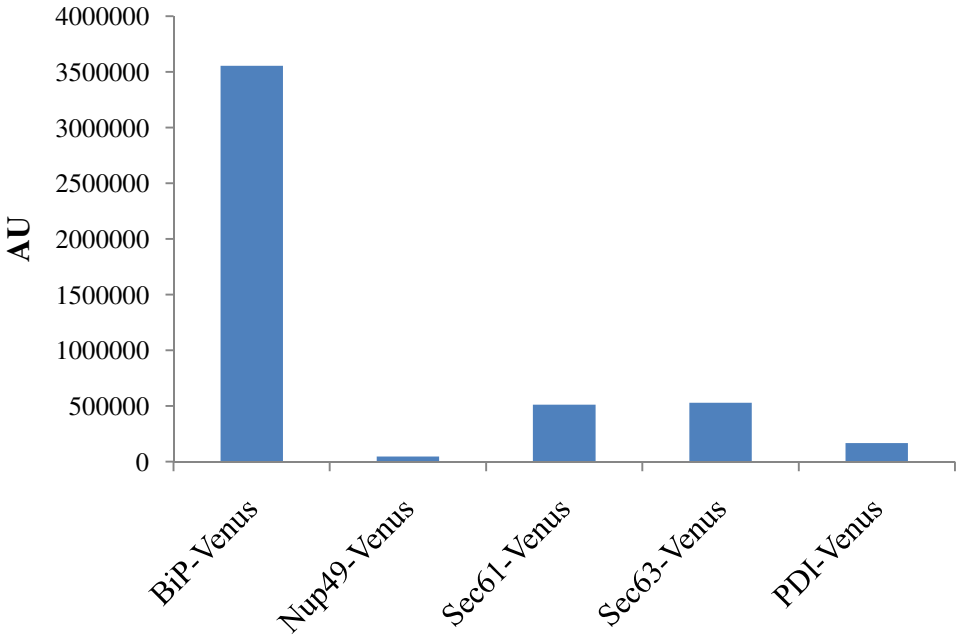

Figure 4.8 Relative integrated density for each protein concentration band of the in-gel fluorescence experiment (Figure 4.7).

Similar trends are depicted by the in gel fluorescence results in Figure 4.8 to the relative concentrations reported by Ghaemmaghami *et al.,* 2003. The results indicate that a lower intensity fluorescent protein variant should be chosen for the BiP fusion protein (such as mCherry), while it is necessary to use a high intensity FP (such as Venus) for the low concentrated Nup49. The concentrations found for Sec61 and Sec63 are relatively similar, which is also consistent with literature. Although the relative concentration of PDI was not reported above in Table 4.1, literature indicates the PDI has a higher concentration in yeast cells (Mizunaga, *et al*., 1990). However, PDI in Figure 4.8 appears to be less concentrated within the cell when compared to

BiP. Due to the doublet band in the gel displayed in Figure 4.7 and its low concentration shown in Figure 4.8, PDI is not discussed further. Further details concerning the progress of research on PDI are included in Appendix A.2.

4.2.1 In gel Fluorescence with SDS PAGE Protocol

To find the relative fluorescence expressed by different fusion proteins, in-gel fluorescence in conjunction with a SDS PAGE experiment was performed. Five different yeast strains were examined: BJ5464 (negative control), BJ5464 BiP-Venus, BJ5464 Sec61-Venus, BJ5464 Sec63-Venus, BJ5464 PDI-Venus, and BJ5464 Nup49-Venus. Each of the strains were grown in YPD media for three hours at mid-log phase in a water bath shaker at 30°C and 275 rpm. The samples were normalized to 0.5 OD and centrifuged at 8000 rcf for one minute. The supernatant was discarded and the pellet was resuspended in 200 µL of lysis buffer (250 µL 1M TrisHC pH=7, 250 µL 20% SDS, 4.5 mL dH2O). Zirconium silica beads were added to each sample. To completely lyse cells, each sample was vortexed for 30 seconds followed by incubation on ice for 30 seconds, and repeated. Supernatant was removed with gel-loading tips and placed in clean microcentrifuge tubes. The samples were then centrifuged for 1 minute at 8,000 rcf. The supernatant was transferred to new microcentrifuge tubes. 66µL of each sample was combined with 33µL of 3xSDS buffer dye (addition of 100mM DTT). 40µL of each sample was loaded into a 12% polyacrylimide cassette gel (1.5mm). The SDS PAGE was run for two hours at 150 V with SDS buffer. The fluorescence of each sample was viewed by using the typhoon scanner (Vendor) with a 488nm laser (filter settings).

4.3 Continuous Structure of the ER

Previous research has shown that membrane and luminal regions of the ER are continuous throughout the yeast cell (Lippincott-Schwartz *et al.,* 2001). Continuity of membrane-bound organelles, such as the ER, can be determined with the use of Fluorescent Loss in Photobleaching (FLiP) experiments. FLiP is a photobleaching technique where the loss of a protein's fluorescence is monitored through a time series. A collection of images of the entire cell are captured as a specific region of the cell is repeatedly bleached (Lippincott-Schwartz *et al.,* 2001). Through the duration of this repetitive bleaching, if the fluorescent proteins from other regions of the cell can diffuse into the bleached area, a total loss of fluorescence will result. This experiment directly indicates whether the subcompartments of the ER are continuous and proteins can freely diffuse between them. FLiP experiments are often used to determine the extent of continuity between intracellular membranes. The results of FLiP experiments include either the confirmation of a continuous membrane allowing protein diffusion or the determination that diffusion is restricted (Lippincott-Schwartz *et al.,* 2001).

Recent FLiP experiments involving both soluble and membrane-bound GFP fusion proteins localized in the ER showed complete loss in fluorescence upon repetitive bleaching of a small area in the ER. This proves that both membranes and luminal regions of the ER are continuous throughout both yeast and mammalian cell (Lippincott-Schwartz *et al.,* 2001; Terasaki *et al.,* 1996). A schematic of this result is shown in Figure 4.9.

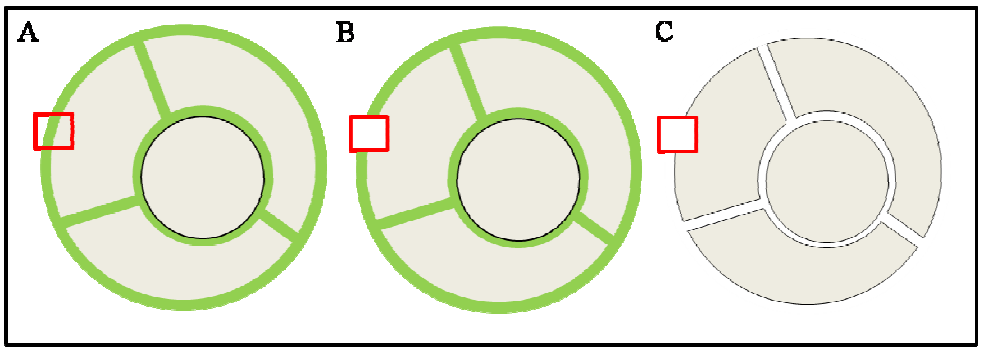

Figure 4.9 **Schematic of a FLiP experiment performed on the ER of yeast cells. The red box in all three images represents the small region being repeatedly bleached. (A) shows the ER fluorescence prior to being bleached. (B) shows the fluorescence loss in the peripheral ER in the location it is being bleached. (C) Shows the complete loss of fluorescence in the continuous ER of the yeast cell at later time points.**

We have attempted to prove that this continuous structure of the ER remains continuous as it is partitioned into the daughter cell throughout cell division. A FLiP experiment was conducted to prove this hypothesis. KGFP, a green fluorescent protein localized to the lumen of the ER, was expressed in budding yeast (courtesy of C. Young). A FLiP experiment was performed by repetitively bleaching a small portion of the mother ER with the Zeiss5 DUO confocal microscope while images were collected of the entire budding cell throughout the duration of the experiment. A population of other cells was also included in the images as a control. Results of the time series experiment are shown in Figure 4.10.

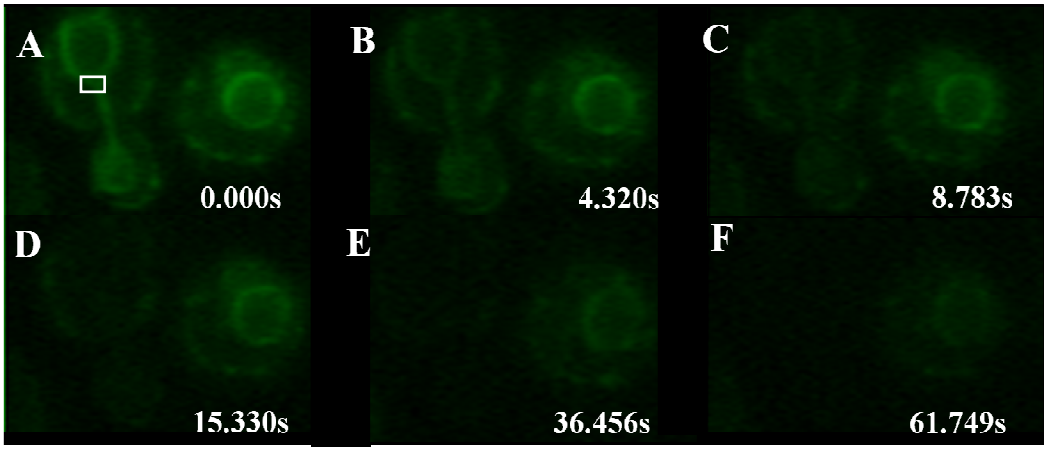

Figure 4.10 ***S. cerevisiae*** **haploid cells expressing soluble GFP retained in the ER at 30^0C. Plan-Neofluar 63x magnification/NA 1.4 oil LSM5LIVE. Continuous photobleaching of the daughter cell, scan rate of 80 frames per second. The white region of interest in Figure A represents the area being repetitively photobleached.**

It is apparent from Figure 4.10 that as the mother ER is being repetitively photobleached, the fluorescence of the ER luminal GFP throughout the entire ER of the budding cell is decreased. This indicates that the ER is a continuous structure extending from the mother to the daughter cell. Future work includes performing FLiP experiments on other strains of yeast cells expressing functional ER proteins of interest such as BiP, Sec61, and PDI. These experiments would provide more information about how functionality of the proteins results in different spatial localization within the ER.

Chapter 5

PROTEIN LOCALIZATION DURING CELL DIVISION

Although much has been discovered about the ER structure and morphology of eukaryotes, it remains unclear how this complex structure is inherited during cell division (Voeltz and Prinz, 2007). Very limited knowledge exists regarding the exact mechanism for ER biogenesis and how ER functional resident proteins are involved in this process. The hypothesis of this research is that spatial heterogeneity between ER luminal, ER membrane, and NPC proteins exists during cell division. Using confocal microscopy and proteins of interest fused with FP variants, multiple ER resident and NPC proteins are analyzed simultaneously in dividing yeast cells. We believe that spatial heterogeneity of these proteins is important during ER inheritance of budding yeast cells. This chapter introduces the cell cycle of budding yeast cells, provides details concerning previous ER inheritance research, and presents our live cell imaging results of ER fusion proteins during cell division.

5.1 Introduction to the Yeast Cell Cycle

In live cell imaging experiments, a complete yeast cell cycle, which is illustrated in more detail in Figure 1.2 of Chapter 1, was determined through visual examination of DIC transmitted light images collected with the confocal microscope. Figure 5.1 displays the DIC transmitted light images of a yeast cell initiating bud emergence and continuing bud growth throughout a time series experiment.

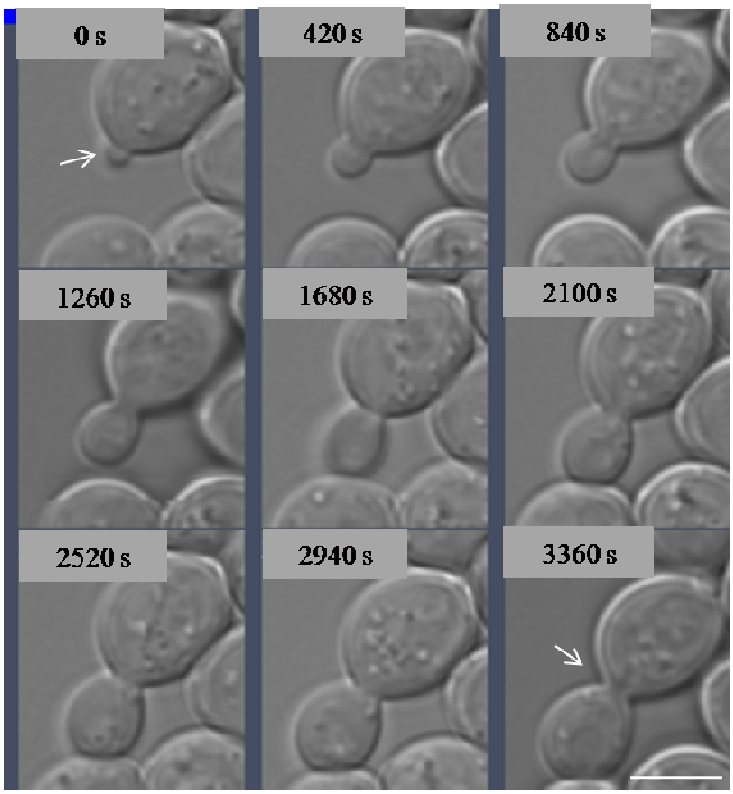

Figure 5.1 DIC transmitted light images of a yeast cell dividing. Zeiss5 DUO confocal microscope, Plan-Apochromat 63x/1.40 Oil DIC M27 objective lens. Timestamps in the upper left corner of images indicate multiple time points of the series. The scale bar at the bottom right of the figure is ~5µm.

The arrow in the first image (time point 0 s) indicates a bud emerging from the mother cell. Over time, the bud increases in size while remaining connected to the mother cell, indicated by the arrow in the last image (time point 3360 s). DIC transmitted light images were also used to indicate the completion of the cell cycle, referred to as

cytokinesis. Figure 5.2 shows yeast cells completing the cell cycle, as the mother and daughter cells separate during G1 phase.

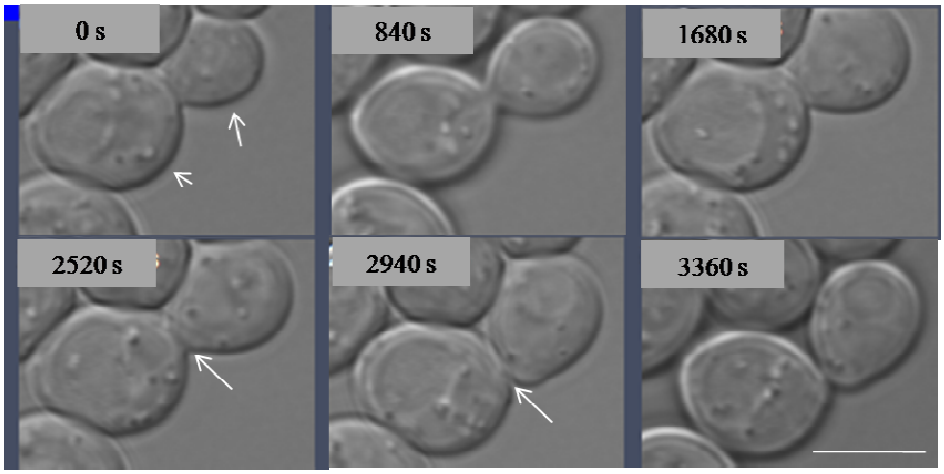

Figure 5.2 DIC transmitted light images of a yeast cell completing cell division. Zeiss5 DUO confocal microscope, Plan-Apochromat 63x/1.40 Oil DIC M27 objective lens. Timestamps in upper right corner of images indicate multiple time points of the series. The scale bar at the bottom left of the figure is ~5µm.

The time series in Figure 5.2 shows the progression of the yeast cells through the end of the cell cycle. The mother and daughter cell dividing are marked with white arrows in the first image (0 s). The mother and daughter cells are still connected at time point 2520 s, indicated by the white arrow. The arrow in the next time point (2940 s) shows how the cells separate and begin to move away from one another, indicative of cytokinesis.

In order to verify mitosis occurrence in live yeast cells, the NPC fusion protein was used as an indicator of the nuclear envelope (NE) in order to monitor

nuclear division. Figure 5.3 shows an example of how Nup49-Venus marks the NE and perinuclear ER during mitosis.

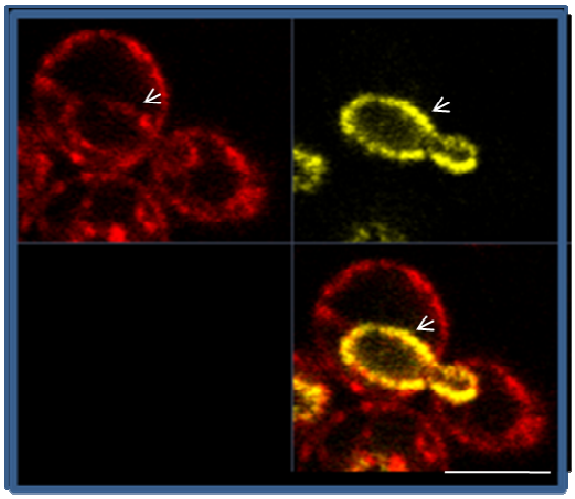

Figure 5.3 Mitosis occurring in yeast cells expressing BiP-mCherry (red) and Nup49-Venus (yellow). Arrows indicate the perinuclear ER and the NE are localized similarly during division. Zeiss5 DUO confocal microscope, Plan-Apochromat 63x/1.40 Oil DIC M27 objective lens. Scale bar is ~5µm.

Figure 5.3 indicates that the Nup49-Venus, which is localized at the NE, can be used to mark the perinuclear ER during the division of the nucleus..

5.2 Introduction to ER Inheritance

As previously discussed, the ER is an essential organelle in eukaryotic cells. It is the first organelle in the secretory pathway and is the site for many intracellular processes such as protein translocation, protein folding and maturation,

and protein degradation. As cells divide, there must be a quality control process in place to ensure faithful ER inheritance for every cell cycle (Du *et al*., 2004). This essential, large, single-copy organelle cannot be synthesized *de novo* and therefore must be actively partitioned during cell division (Du *et al*., 2004). In *S. cerevisiae* cells, the ER must be segregated into the daughter cell prior to complete cell division. Previous electron microscopy work has shown that the ER is the first organelle to be inherited during S phase of the mitotic cell cycle, explained in Section 5.1 (Fehrenbacher *et* al., 2002). Irrespective of this knowledge, there are many aspects of ER inheritance and biogenesis that have yet to be determined. Therefore, the results obtained by monitoring ER resident proteins during cell division provide more insight into the mechanism of ER inheritance during cellular division of budding yeast cells.

5.3 Segregation of Three ER Domains

The ER of *S. cerevisiae* is comprised of three subdomains: peripheral ER located directly beneath the plasma membrane, a network of cytosolic ER tubules, and the perinuclear ER, which is continuous with the NE, and has been previously described in section 4.2.2. Although the continuous structure of the ER has been confirmed, with ER tubules connecting the perinuclear and peripheral domains, the partitioning of these compartments is different (Du *et al*., 2004). Morphological studies have revealed the dynamics of the peripheral ER to be drastically different to the dynamics of the perinuclear ER during cell division (Lowe and Bar, 2007). A mechanism in which these three domains are partitioned into the daughter cell has been described as a step-wise progressive process (Lowe and Bar, 2007; Belgareh and Doye, 1997; Loewen *et* al., 2007), which is summarized in Figure 5.4.

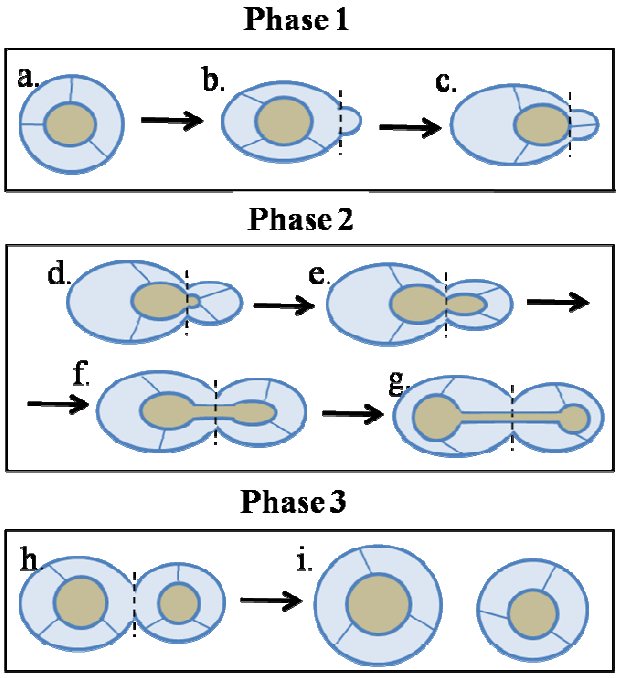

Figure 5.4 **Schematic summarizing the proposed mechanism for ER inheritance in *S. cerevisiae*. Dotted lines represent mother-daughter neck. The three subdomains are shown similarly to Figure 4.1 in section 4.2.1. Budding progression follows the alphabetic order of the labels.**

Figure 5.4 summarizes the proposed mechanism for ER segregation during the budding of yeast cells. The top panel of images represents what will be called 'Phase 1' of cell division throughout the remainder of this thesis. Phase 1 includes the progression from G1 phase, through S phase, and into G2 phase, as a bud is formed during DNA synthesis and then continues to grow. The only ER inheritance occurring during Phase 1 is the partitioning of the peripheral and tubular ER network. The second panel illustrates what is referred to as 'Phase 2' of cell division. This step

includes the nucleus and perinuclear ER partitioning during mitosis (M phase). The final stage of cell division, 'Phase 3' in the bottom panel of Figure 5.4, consists of the final stages of mitosis as the mother and daughter cell segregate (cytokinesis) and return to G1 phase. Further details of each of the three stages of cell division with respective experimental results are described in subsequent sections.

Time series analysis was used to compute the time scales for each step of cell division illustrated in Figure 5.4. A sample of yeast cells (n=27) were imaged every 2-8 minutes throughout cell division. The times of occurrence for individual cells to progress through each stage were recorded and are shown in Figure 5.5.

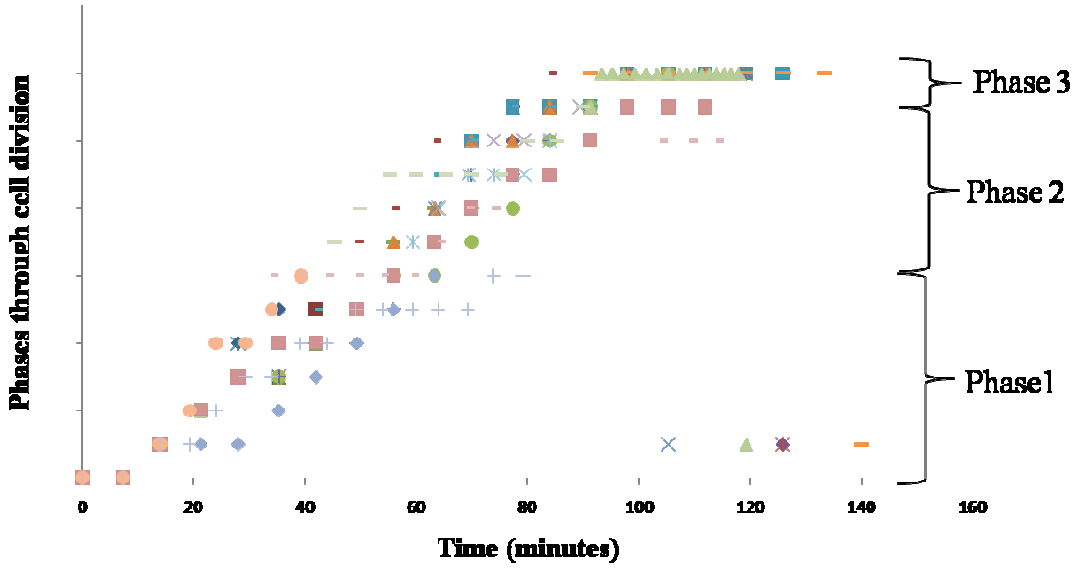

Figure 5.5 **Time series results for sample of yeast cells (n=27) undergoing cell division. Results show the range of time scales for each of the phases in cell division. Individual cells are represented by the different symbols and colors.**

Figure 5.5 displays the results for the time series analysis of a population of yeast cells. The mean time scales for each of the phases of cell division are summarized in Table 5.1.

Table 5.1 Time scales for 3 phases of cell division in a population of yeast cells.

Budding Phase	Time Scale ± 90% CI (minutes)
Phase 1	55 ± 8
Phase 2	35 ± 5
Phase 3	18 ± 7
Total Cell Cycle	108 ± 7

The total time observed for cell division of a population of yeast cells is consistent with literature reports that the doubling time for yeast is between 90 and 120 minutes (Herskowitz, 1988). The individual step time scales indicate that Phase 1 is the limiting step in the yeast budding cell cycle.

5.3.1 Phase 1 of Cell Division: Peripheral and Tubular ER segregation

Partitioning of the tubular network and peripheral ER into the daughter cell has been described as a step-wise process as shown in Figure 5.4 (Lowe and Barr, 2007; Loewen *et al*., 2007). Previous experiments have indicated that the peripheral ER first extends into the bud and is then anchored at the growing tip of the bud, referred to as the exocyst, where a complex of proteins is localized. At this point, the peripheral ER extends and expands along the cell periphery to fill the entire bud. The ER tubules extend into the bud and also attach to the periphery of the bud. Following this attachment, the ER tubules are distributed in the bud to form a tubular and peripheral ER network within (Lowe and Barr, 2007; Loewen *et al*., 2007). In an

effort to confirm the results of Part 1 cell division found in literature, live budding yeast cells expressing ER resident fusion proteins were analyzed with confocal microscopy. Figure 5.6 shows fluorescent images of different yeast cells expressing BiP-mCherry and Nup49-Venus throughout the first stages of Phase 1 of cell division.

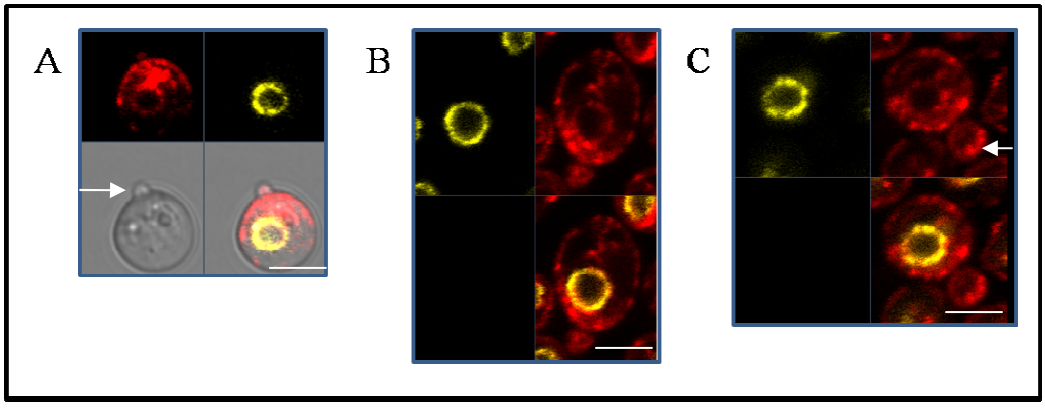

Figure 5.6 Three representative time points of Phase 1 of cell division for different yeast cells expressing BiP-mCherry (red) and Nup49-Venus (yellow). Bud emergence in (A) is indicated by the white arrow. Exocyst in (C) is indicated by the white arrow. Zeiss5 DUO confocal microscope, Plan-Apochromat 63x/1.40 Oil DIC M27 objective lens. Scale bars are ~5µm.

Figure 5.6 (A) represents the time point when the bud is just beginning to emerge from the mother cell. Bud emergence is shown with an arrow in the DIC transmitted light image of this figure. At this first time point of cell division, a relatively high concentration of BiP-mCherry accumulates at the bud emergence site, while the Nup49-Venus marking the perinuclear ER remains in the center of the mother cell. As the bud begins to increase in size, shown in Figure 5.6 (B), BiP-mCherry fills the entire area of the bud, while Nup49-Venus remains localized around the nucleus in the

center of the mother cell. The next time point, Figure 5.6 (C), shows the bud growing even larger and the BiP distribution concentrating at the exocyst (tip of the bud) indicated by the arrow. In all three images, the NE, marked by the NPC fusion protein, and the perinuclear ER, which is continuous with the NE, are not partitioned as the bud emerges. The only change in ER morphology is present in the peripheral network of the ER, indicated by the luminal protein BiP localization.

The most noteworthy characteristic of these first three time points are the ER dynamics of the growing bud. The peripheral network of the bud has been found to often appear to be more dynamic due to the ongoing formation of the reticular network of ER tubules (Du *et al*., 2004). In Figure 5.6, these ER bud dynamics are shown by the shift in localization of BiP-mCherry from an isotropic distribution throughout the bud in Figure 5.6 (B) to a polarized distribution of BiP-mCherry concentrated at the exocyst in Figure 5.6 (C). During bud growth, the localization of the ER proteins are known to switch from an isotropic to a polarized distribution through a process known as *polarized growth* (Lowe and Barr, 2007). To further analyze this particular shift in ER protein concentration, the Figure 5.7 displays bud growth of a single budding yeast cell over time.

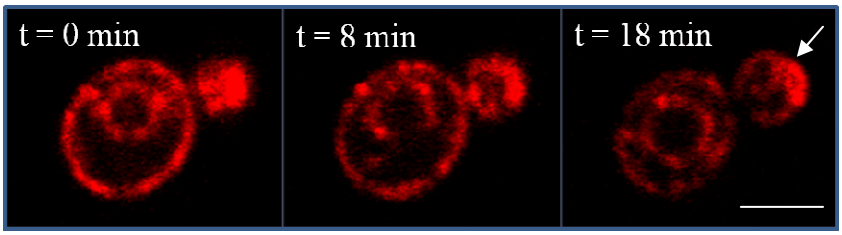

Figure 5.7 Shift in distribution of BiP-mCherry in the bud of a yeast cell. Zeiss5 DUO confocal microscope, Plan-Apochromat 63x/1.40 Oil DIC M27 objective lens. Scale bars are ~5µm.

Figure 5.7 displays the shift in ER (BiP-mCherry) distribution over three time points in a cell division time series experiment of a yeast cell. Qualitatively, it is apparent that the BiP-mCherry distribution shifts from uniform in the first image (t=0 min) to more polarized in the last image (t=18 min) located at the exocyst of the bud, indicated by the white arrows. Surface plots were constructed for a region of interest around the growing bud for these three time points. The results are displayed in Figure 5.8.

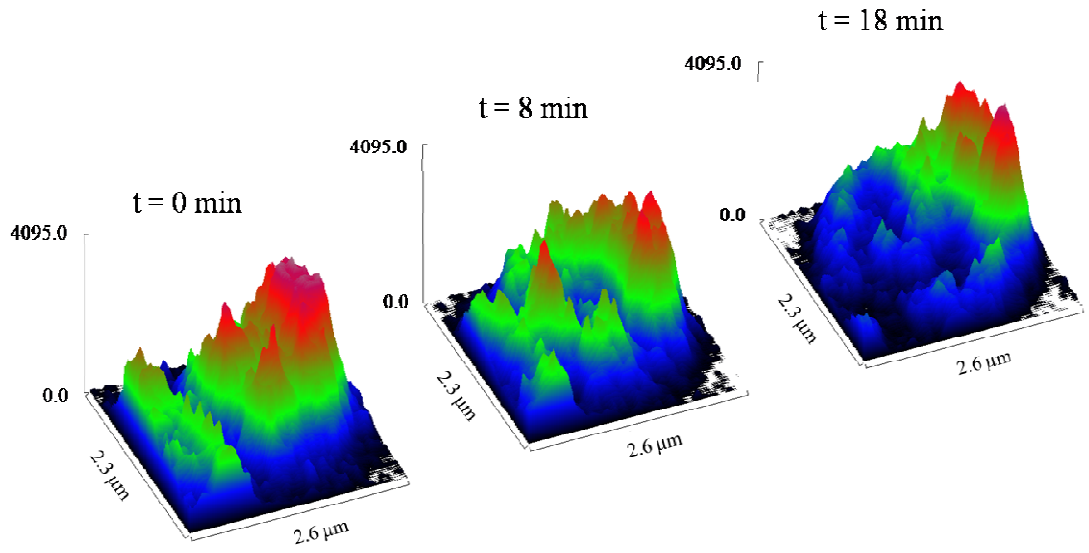

Figure 5.8 Surface plots for each time point for a region of interest around the growing bud shown in Figure 5.7. The z-axis is the gray scale intensity of each pixel in the region of interest (ranging from 0 to 4095) and the x and y plane represents the area of the region of interest (μm^2).

The surface plots provide a more quantitative perspective of the BiP-mCherry intensity distributions in the bud over three time points. At the first time point (t=0 min) the BiP localization is a relatively isotropic distribution with peaks present throughout the region of interest. In the transition to the next two time points (t = 8 min and t= 18 min), the BiP surface plots indicate a shift to a more polarized distribution of intensity peaks, located at the upper right area of the region of interest, which has been proposed to be the exocyst of the bud. This dynamic ER trend in the beginning of Phase 1 of cell division was consistently observed in the majority of time series through this phase of cell division for yeast cells expressing BiP-mCherry.

After the polarized localization of ER resident proteins, the bud continues to grow. The last two times points in Phase 1 of cell division are shown in Figure 5.9.

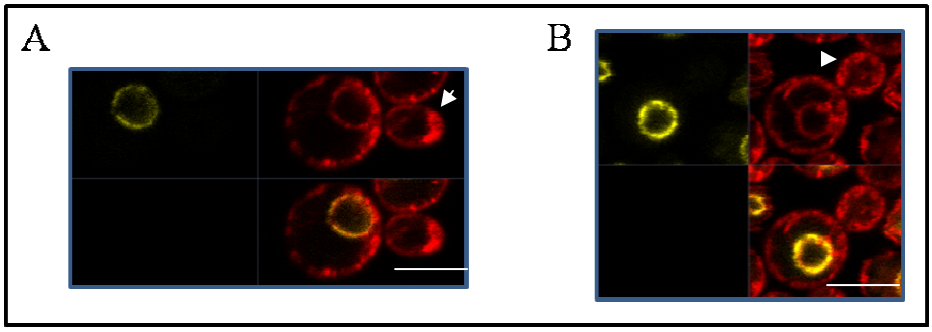

Figure 5.9 The last two time points in Phase 1 of cell division of yeast cells expressing BiP-mCherry (red) and Nup49-Venus (yellow). White arrowheads indicate the buds of the dividing yeast cells. Zeiss5 DUO confocal microscope, Plan-Apochromat 63x/1.40 Oil DIC M27 objective lens. Scale bars are ~5µm.

In Figure 5.9 (A), the bud continues polarized growth as the BiP-mCherry accumulates at the exocyst. Another localization pattern shown in (A) is the relatively high concentration of BiP-mCherry at the mother-daughter neck of the budding yeast cell. The NPC fusion protein Nup49-Venus remains localized around the nucleus in the mother cell. The next time point of Phase 1 in cell division is captured in Figure 5.9 (B). The high concentration of BiP-mCherry at the mother-daughter neck remains the same; however, the localization of BiP changes again as the polarized distribution shifts to an even distribution around the perimeter of the bud, forming the peripheral network. The results for the localization of the ER resident protein shown above are consistent with literature findings for this first phase of cell division (Du *et al*., 2004; Loewen *et al*., 2007; Lowe and Barr, 2007).

In summary, Phase 1 of cell division in budding yeast cells is characterized by the ER role in bud emergence, ER polarized growth and bud dynamics, and a consistent localization of the perinuclear ER observed only in the mother cell. The approximate time scale associated with Phase1 of cell division is 55 minutes.

5.3.2 Phase 2 of Cell Division: Perinuclear Division

Phase 2 of cell division of yeast cells includes nuclear division during mitosis. As previously discussed, the three ER subdivisions are uniquely segregated into the daughter cell during yeast budding. Studies have also shown that the yeast NE and the perinuclear ER are divided concurrently, as they position the nucleus at the neck of the dividing cell so that it will be separated equally in the mother and daughter cells (Lowe and Barr, 2007). This paired division has been explained by the proposed mechanism involving the perinuclear ER proteins actually tethering to nuclear components during nuclear division (Voeltz and Prinz, 2007). In order to track the localization of the perinuclear ER during cell division, the NPC protein, Nup49-Venus, was used to mark this subdivision. Because the NPC spans both the NE and perinuclear ER and these membranes are assumed to be continuous, it is expected that the perinuclear ER will divide simultaneously with the NE. Also, previous research has shown Nup49-GFP localizes correctly to the NPC and a time series analysis using confocal light microscopy has shown successive changes in NE shape during cell division (Belgareh and Doye, 1997). The changes in NE during yeast budding is summarized in the schematic in Figure 5.10.

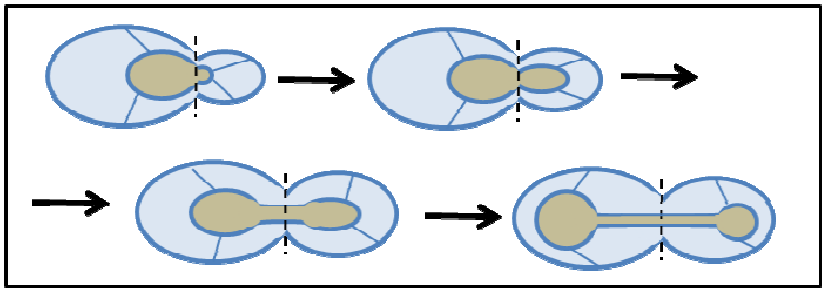

Figure 5.10 Schematic of NE division in budding yeast cells for Phase 2 of cell division. This phase represents the nuclear division occurring during mitosis in the cell cycle. This figure was adapted from Belgareh and Doye, 1997.

Throughout cell division, the NE inserts into the neck of the budding yeast cell, followed by nuclear elongation and migration into the bud, with a final step consisting of a bi-lobed shape of the nucleus during later time points in cell division (Belgareh and Doye, 1997).

In order to analyze Phase 2 of cell division, live yeast cells were imaged expressing BiP-mCherry (ER lumen) and Nup49-Venus (NPC) to fully elucidate paired perinuclear ER and NE division. In the images in Figure 5.11 and 5.12, the yellow signal of Nup49-Venus often overlaps with the red signal of BiP-mCherry, which indicates the continuity between the NE and the perinuclear ER. The results for Phase 2 of cell division are shown below in Figure 5.11, which displays the first four time points of this phase of cell division.

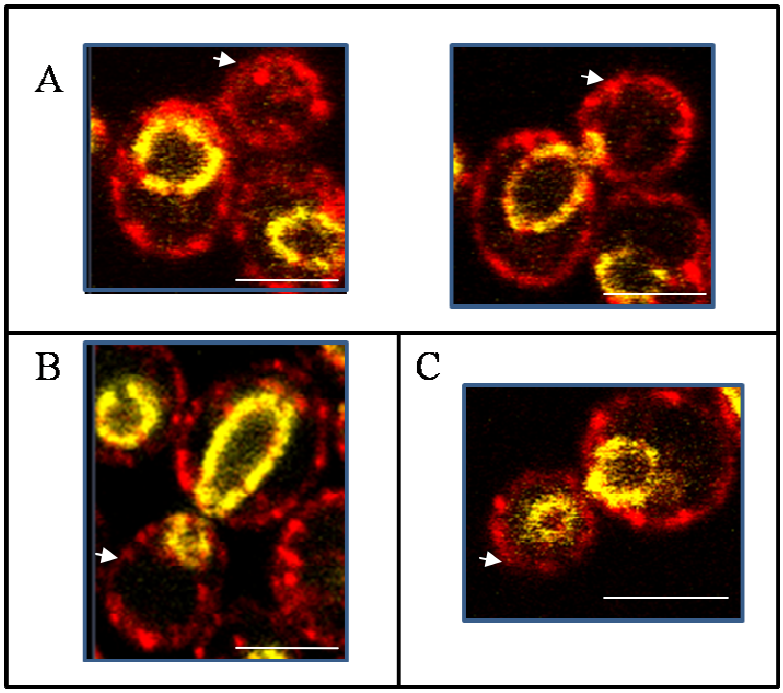

Figure 5.11 First four representative time points of the second phase of cell division of different yeast cells expressing BiP-mCherry (red) and Nup49-Venus (yellow). Arrowheads in the four images indicate the growing buds. Zeiss5 DUO confocal microscope, Plan-Apochromat 63x/1.40 Oil DIC M27 objective lens. Scale bars are ~5µm.

Figure 5.11 (A) shows two time points of the same yeast cell dividing in early Phase 2 division. In the first image on the left, the Nup49-Venus (marking the NE and perinuclear ER) moves towards the mother-daughter neck of the budding cell. The second image of the same cell on the right of Figure 5.11 (A) shows the NE and perinuclear ER beginning to cross over the mother-daughter neck into the bud. There still remains a higher concentration of peripheral ER at the neck, as well as forming an ER network around the periphery of the bud. Figure 5.11 (B) is a different yeast cell at

a later time point in Phase 2 of cell division. The perinuclear ER has extended even further into the bud, forming a slight circular membrane around the nucleus. At even later time points in Phase 2 of cell division, shown in Figure 5.11 (C), the perinuclear ER and NE have formed similar sized small spheres on either side of the mother-daughter neck, resembling a dumbbell formation. The peripheral ER remains at the neck in the mother cell of Figure 5.11 (C) and around the periphery of the daughter cell.

The second half of Phase 2 cell division includes the elongation and further segregation of the perinuclear ER. Figure 5.12 displays this phase of cell division.

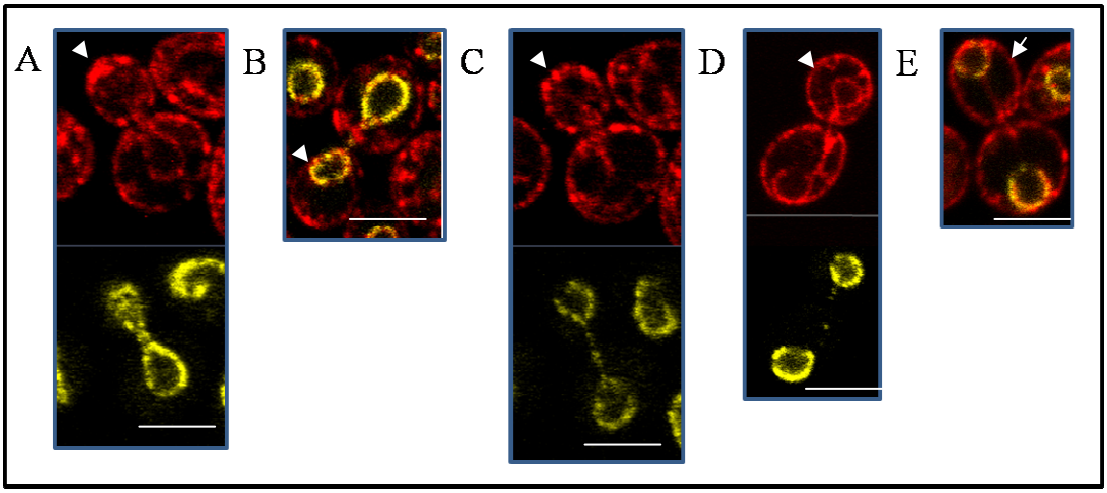

Figure 5.12 Five representative time points of the second phase of cell division of different yeast cells expressing BiP-mCherry (red) and Nup49-Venus (yellow). White arrowheads indicate the growing bud of each yeast cell. Zeiss5 DUO confocal microscope, Plan-Apochromat 63x/1.40 Oil DIC M27 objective lens. Scale bars are ~5µm.

As the yeast cell begins to divide further, the perinuclear ER begins to elongate between the mother and daughter cells, as observed in the two time points of Figure 5.12, (A) & (B). As the nuclei in the mother and daughter cells beginning to separate, the perinuclear ER figure-eight shape elongates into a bi-lobed configuration, clearly shown in (B). The next time point, shown in Figure 5.12 (C), is defined by the nuclei of the mother and daughter, which move to opposite ends of the cells. The two nuclei are connected by a tubule of both Nup49-Venus and BiP-mCherry, suggesting that both the ER and the NE are localized along this tubule across the length of the cells. As the yeast cells reach the final stages of cell division, the NPC proteins are completely partitioned into the mother and daughter cells and are only localized around the nuclei of each cell. This time point of cell division is shown in Figure 5.12 (D). Due to the continuity between the NE and the perinuclear ER, this suggests that the perinuclear ER is also partitioned completely into the mother and daughter cells. In contrast, ER tubules remain in contact between the mother and daughter nuclei, shown in (D) and more clearly defined in Figure 5.12 (E).

In summary, Phase 2 of cell division is described by the simultaneous perinuclear and NE partitioning during yeast budding during a period of approximately 35 minutes.

5.3.3 Phase 3 of Cell Division: Final Segregation

The third and final step of cell division is distinguished by the complete separation of the mother and daughter cells. In this phase of budding, the ER morphology and ER resident proteins resume their typical ER localization patterns. At this point, the newly partitioned daughter cell is able to grow to the required size for its own bud initiation. As previously indicated, this stage lasts approximately 18

minutes. Figure 5.13 displays a time series of a cell at the very end of cell division, and transitioning back into the cell cycle as a new bud is formed.

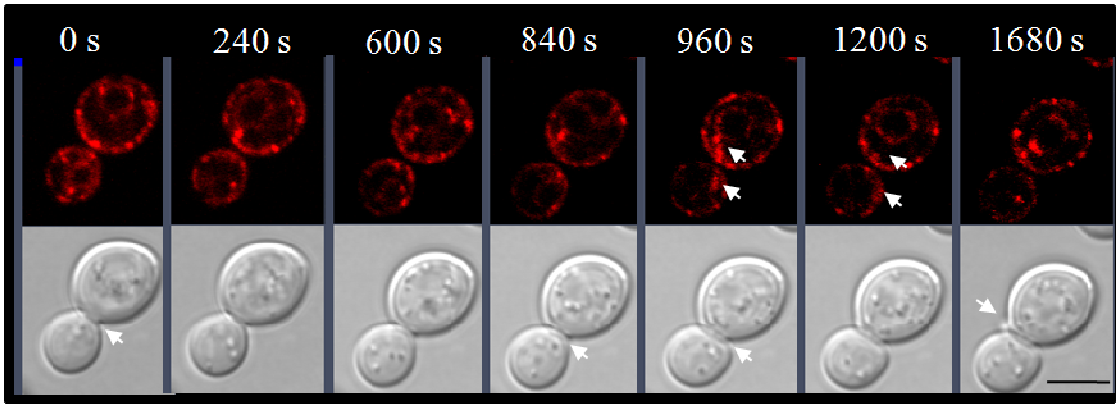

Figure 5.13 Time series of a yeast cell undergoing Phase 3 of cell division. Arrowheads indicate areas of further discussion. The top row of images are yeast cells expressing BiP-mCherry and the bottom row are the DIC transmitted images of the same cells. Zeiss5 DUO confocal microscope, Plan-Apochromat 63x/1.40 Oil DIC M27 objective lens. Scale bars are ~5µm.

The time series begins as nuclear division between the daughter and mother cell is complete, although the yeast cells are still connected (indicated by arrow in first DIC transmitted light image). As time progresses to 840 seconds, the yeast cells are preparing for complete separation, yet still connected at the point indicated by the arrowhead in the image. At 960 seconds, the DIC light image indicates that complete separation occurs between the mother and daughter cell. Although separated, both the mother and daughter cells consist of ER tubules that appear to almost connect the detached pair. At the next time point, both cells seem to have transitioned back to normal ER patterns of BiP-mCherry. This normality continues until the time point

1680 seconds (28 minutes) when a new bud emerges from the mother cell, indicated by the arrow in the DIC transmitted light image. In summary, Phase 3 of cell division includes the complete separation of the mother and daughter cells and eventual normal distribution patterns of ER proteins.

5.4 Proposed Mechanisms for Control of ER Inheritance

There are several existing proposals for mechanisms controlling the unique segregation of the three ER subdomains. One suggestion is the existence of selective diffusion barriers to prevent the movement of ER resident proteins between the peripheral and perinuclear ER domains (Voeltz and Prinz, 2007). Another proposal regarding localization of ER resident proteins is the existence of a septin-dependent diffusion barrier located at the neck of the budding yeast cells (Voeltz and Prinz, 2007). The purpose of the barrier is to slow diffusion of ER resident proteins between the continuous ER structure of the mother and daughter cells (Voeltz and Prinz, 2007). The high concentration of BiP-mCherry present in the mother cells at the mother-daughter neck, shown in Figure 5.14, is an indication that the proposed barrier between ER subdomains or between mother-daughter cells might possibly exist.

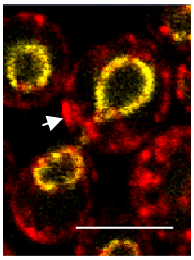

Figure 5.14 Image of a dividing yeast cell expressing BiP-mCherry (red) and Nup49-Venus. The high concentration of BiP-mCherry at the mother-daughter neck is indicated with the arrowhead. Zeiss5 DUO confocal microscope, Plan-Apochromat 63x/1.40 Oil DIC M27 objective lens. Scale bars are ~5µm.

Although this and other images appear to support a barrier hypothesis, two-dimensional images do not provide conclusive evidence to either confirm or disprove that three-dimensional spatial barriers exist within three-dimensional yeast cells. The limitations of two-dimensional images are discussed further in Chapter 8.

It has also been proposed that yeast cells that are smaller in size must grow during G1 phase before initiating the budding process (Herskowitz, 1988). To test this hypothesis, the ratio of the daughter cell area to the mother cell area was computed at three different time points in cell division. The sizes of daughter and mother cells of a population of 102 dividing yeast cells expressing BiP-mCherry and 89 yeast cells expressing KGFP were analyzed. The results are shown in Figure 5.15.

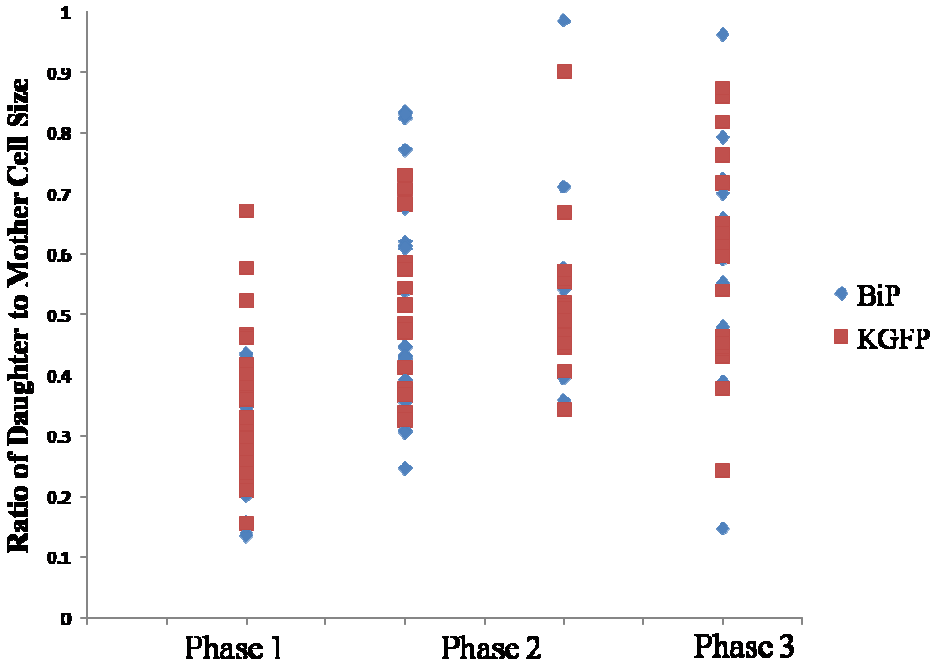

Figure 5.15 Distribution of daughter:mother cell size ratios of BiP-mCherry and KGFP individually expressed in cells at different time points during cell division. Step 1 includes cell size ratios when protein was concentrated at the exocyst. Step 2 includes the start of nuclear division in the second set of data and at the stage with ER tubules connecting nuclei in the third set of data. Step 3 includes the final separation of the yeast cells.

The variance of the data in Figure 5.15 indicates that there is no significant difference in daughter:mother cell size ratio over the three phases in cell division. However, this is most likely due to the limitations of two-dimensional imaging. Each image captured in cell division was focused on the location of the ER of the yeast cells, which is not consistently located at the midsection of the yeast cells. Therefore, this data neither

prove nor disprove the proposal of controlled daughter cell size as a mechanism for ER inheritance during the cell cycle.

Due to the linear nature of the extension of the ER during ER inheritance in budding yeast cells, it has been suggested that the cytoskeleton plays a role in cell division (Du *et al*., 2004). The cytoskeleton of yeast includes both microtubules and actin. The proposed mechanism for cytoskeleton involvement includes the ER following the cytoskeleton across the mother-daughter neck and anchors to the tip of the growing bud, the exocyst. The role of the cytoskeleton is discussed further in Chapter 7. It has been hypothesized that the translocon, Sec61, interacts with the exocyst, which provide an additional mechanism for the ER to anchor at the bud tip (Lowe and Barr, 2007). The role of the exocyst is further discussed in future work (Chapter 8).

Chapter 6

HETEROGENEOUS SPATIAL LOCALIZATION OF ER RESIDENT PROTEINS

The main goal of this research is to confirm our hypothesis that spatial heterogeneity exists between the proteins of the ER lumen, membrane and nuclear pore complex (NPC) during cellular division in *Saccharomyces cerevisiae*. It is believed that this spatial heterogeneity exists and is a direct consequence of protein function. The structure and morphology of the ER has been introduced in Chapter 4, selective ER resident and NPC protein functions and inherent concentrations in Chapters 1 and 4, and the technology associated with fusing proteins of interest with fluorescent protein variants in Chapter 2 and 3. In addition, the yeast budding cell cycle has been analyzed by time course analysis and our data on mother-daughter division have been categorized into three distinct phases. Having established the groundwork as well as preliminary results, this chapter focuses on the apparent heterogeneous spatial localization of selective proteins throughout the budding cycle. The main proteins analyzed include luminal protein BiP, soluble GFP retained in the ER lumen, ER membrane protein Sec61, and Nup49 of the NPC complex.

6.1 Quantitative Methods of Analysis

Image Processing and Analysis in Java (ImageJ, National Institutes of Health) was used to quantify the spatial heterogeneity of proteins in our system. Regions of interest (ROI) were selected in order to define specific areas of interest from which the mean intensity and area were measured using Image J.

Image J has the ability to remove outlier pixels, or background noise. A threshold was calculated within Image J to remove the outlier bright pixels, resulting in more resolved images used for analysis. All images analyzed in this chapter were subjected to the same threshold resulting in the removal of noise.

An algorithm created by Pierre Bourdoncle (Institut Jacques Monod, Service Imagerie, Paris) entiled *Colocalization* has been used for data analysis in this chapter. This algorithm highlights colocalized points of two 8-bit images. If we account for our raw data as a population of cells that simultaneously express fusion proteins of GFP variants, mCherry and Venus, each population of cells results in a red frame (e.g. mCherry) evaluated at the wavelength of 546nm and a green frame (e.g. Venus) evaluated at 488nm. Using the *Colocalization* algorithm, comparison for our data from each channel (e.g. 546nm and 488nm) produce results with colocalized points in white. Parameters include colocalized points displayed at a value set to 255 and a default threshold of 50. Prior to colocalization analysis, images were first converted to binary mode which normalizes all pixels to either 1, if fluorescence is detected or 0, if no fluorescence exists. This function in Image J converts each pixel to either a black (e.g. 1) or white (e.g. 0) color. Modification of the raw data using a binary method ultimately eliminates each fluorescent protein variant's fluorescent intensity as an error of colocalization.

6.2 BiP and Nup49 Colocalization

As previously discussed, Nup49-Venus was used in this research to mark the nuclear pore complex (NPC) in yeast cells, which spans both the perinuclear ER and the nuclear envelope (NE). From a qualitative analysis, the BiP-mCherry (ER lumen) and the Nup49-Venus (NPC) appear to be consistently colocalized in all

results presented in Chapter 5. This section will prove by quantitative methods colocalization exists between these two proteins.

Results from Chapter 5 implied that changes in spatial localization of selective proteins of interest occurred primarily in the peripheral ER of the mother and daughter cells during the first phase of cell division. In contrast, the perinuclear ER remained localized in the mother cell only. A single *S. cerevisiae* yeast cell simultaneously expressing BiP-mCherry and Nup49-Venus has been analyzed in order to determine the level of colocalization present in the mother cell at this time point. Figure 6.1 shows an image of the yeast cell prior to quantitative analysis.

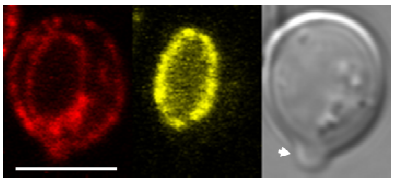

Figure 6.1 Yeast cell expressing BiP-mCherry (red), Nup49-Venus (yellow) and a DIC transmitted light image. Zeiss5 DUO confocal microscope, Plan-Apochromat 63x/1.40 Oil DIC M27 objective lens. Scale bar is ~5µm.

This yeast cell is undergoing the beginning stages of bud emergence, as indicated by the arrow in the DIC transmitted light image. Each channel (i.e. 546 nm and 488 nm) representative of BiP-mCherry and Nup49-Venus, respectively, was converted to binary and colocalized points were defined. Figure 6.2 displays the same BiP-mCherry and Nup49-Venus image in RG binary as well as resulting colocalized points.

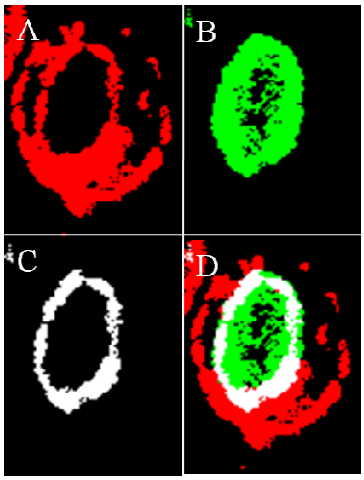

Figure 6.2 RG Binary images of (A) BiP-mCherry, (B) Nup49-Venus, (C) colocalized points, and (D) a merged image.

The image in Figure 6.2 (D) illustrates the colocalized points of the perinuclear ER and the NE surrounding the nucleus during the bud emergence step of cell division, indicated by the arrow in Figure 6.1. The number of pixels in the BiP-mCherry binary image that are colocalized with Nup49-Venus was counted and compared to the total number of pixels in the BiP-mCherry image. This fraction was calculated and represents the concentration of BiP located in the perinuclear ER. For Figure 6.2, 36% of the BiP-mCherry signal was found in the perinuclear ER. The majority of the BiP-mCherry appears to be localized at the bud emergence site, and not in the perinuclear ER domain.

At later time points in cell division, during Phase 2, the nucleus begins to divide between the mother and daughter cell. Nup49-Venus was used to mark the

perinuclear ER inheritance during this phase of cell division. A single budding cell at this time point in division is shown in Figure 6.3.

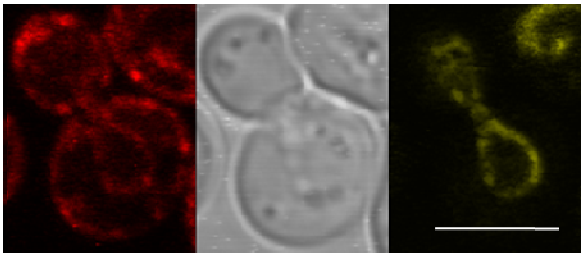

Figure 6.3 A yeast cell expressing BiP-mCherry (red) and Nup49-Venus (yellow) and a DIC transmitted light image. Zeiss5 DUO confocal microscope, Plan-Apochromat 63x/1.40 Oil DIC M27 objective lens. Scale bar is ~5µm.

The budding yeast cell in Figure 6.3 is undergoing nuclear division in Phase 2 of cell division. In Figure 6.4 binary and colocalized images are depicted.

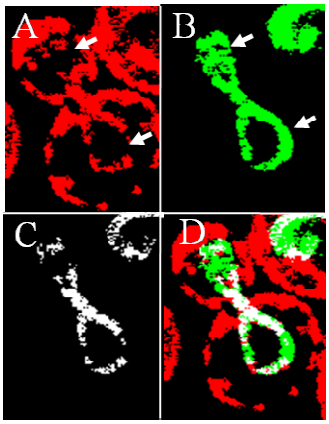

Figure 6.4 RG Binary images of (A)BiP-mCherry, (B) Nup49-Venus, (C) colocalized points, and (D) a merged image.

Figure 6.4 indicates that spatial heterogeneity exists between the fusion proteins, BiP and Nup49. Based on the nuclear/ER structure and protein function, BiP and Nup49 fusion proteins should be localized around the nuclei of the dividing mother and daughter cells. However, it appears that BiP is not homogeneously distributed around either the mother nucleus or the daughter nucleus, indicated by the arrows in the binary images. In Figure 6.4, the fraction of BiP-mCherry localized in the perinuclear ER is 21%.When comparing this percentage with those reported for Figure 6.2, less of the BiP-mCherry is localized in the perinuclear ER. A possible explanation is that BiP is required in other subcompartments of the ER. Specifically, its function dictates that BiP, an ER resident protein involved in karyogamy, must leave the perinuclear ER in order to be partitioned into the bud. This phenomenon results in a lower concentration of BiP-mCherry colocalized with the NuP49-Venus during nuclear division of Phase 2.

Images of yeast cells that were at even later time points in cell division, such as the cells transitioning from Phase 2 to Phase 3 of cell division, were also analyzed, as in Figure 6.5.

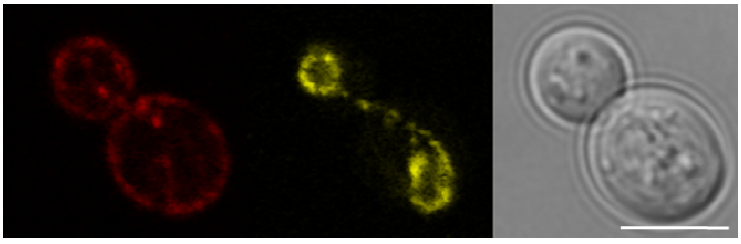

Figure 6.5 A yeast cell simultaneously expressing BiP-mCherry (red) and Nup49-Venus (yellow), and a DIC transmitted light image. Zeiss5 DUO confocal microscope, Plan-Apochromat 63x/1.40 Oil DIC M27 objective lens. Scale bar is ~5µm.

This yeast cell is at the end of Phase 2 of cell division, as there is an ER tubule beginning to segregate into the separate cells and the DIC transmitted light image shows almost complete separation of the cells. Conversion to RG binary followed by data analysis results in the colocalization of the two images, as shown in Figure 6.6.

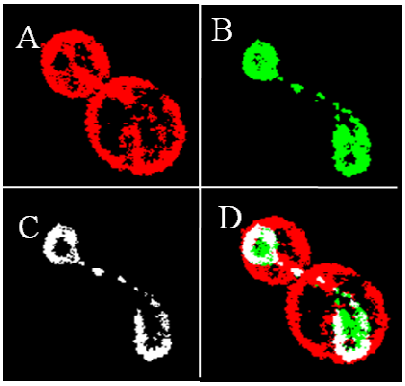

Figure 6.6 RG Binary images of (A)BiP-mCherry, (B) Nup49-Venus, (C) colocalized points, and (D) a merged image.

The white colocalized points are spatially located around the nuclei of both the mother and daughter cells, as well as along the ER tubule connected the two nuclei. The fraction of BiP-mCherry localized in the perinuclear ER in Figure 6.6 is is 25%. In this dividing cell, the small fraction of colocalized BiP is consistent with the hypothesis that BiP to the nuclear ER is consistent with the hypothesis that BiP must leave the perinuclear ER for adequate ER inheritance to occur in the daughter cell.

There are several intrinsic limitations to using the *Colocalization* algorithm that must be mentioned. The first concerns 12-bit images which were obtained from the confocal microscope and the conversion to 8-bit images in order to remain compatible with the algorithm, causing a significant amount of data loss.

Another restriction inherent within the algorithm is the default threshold when calculating colocalized pixels. A more adequate method must be chosen which does not introduce bias of the analyzer nor variability due to confocal parameter settings. One must calculate a more suitable threshold to be used for each image being analyzed.

Having analyzed the heterogeneous distribution of BiP, an ER luminal protein, and Nup49, a NPC protein, the next analysis performed was for three different ER resident proteins.

6.3 Spatial Localization of ER Proteins Due to Function

Three main ER resident proteins were examined in order to determine the spatial heterogeneity associated with ER proteins. These three proteins of interest include (i) BiP-mCherry, an ER luminal protein that is involved in multiple critical processes within the cell; (ii) KGFP, an ER luminal protein that has no known inherent function; and (iii) Sec61-Venus, an ER membrane protein involved in both translocation and ER-associated degradation. Each fusion protein was analyzed in separate *S. cerevisiae* strains as a sole fluorescently tagged protein. Three different time points in cell division were analyzed for each protein of interest. The first phase concerns the concentration of protein gathering at the bud emergence site. The second phase focuses on the amount of fusion protein which collects at the exocyst, a specific site in the daughter cell located at the tip of the bud. Finally, we have monitored the protein concentration of interest in the mother cell which is localized in the mother-daughter neck during nuclear division. The mean intensity and integrated density values (explained in section 6.1) were calculated for proteins of interest at each of these three time points in cell division. The variance associated with results for

proteins at each phase analyzed are displayed in merged histograms for comparative purposes.

6.3.1 Protein Concentrations at Bud Emergence

Three separate populations of yeast cells, all undergoing the initial phase of bud emergence, were analyzed for BiP-mCherry (n=41), KGFP (n=44), and Sec61-Venus (n=18). Individual yeast cells were analyzed by selection of a region of interest (ROI) around the mother cell (ROI_M) and an ROI around the site of bud emergence (ROI_{BS}), depicted in Figure 6.7.

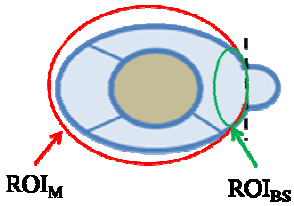

Figure 6.7 Schematic illustrating the selected ROI of the mother cell (ROI_M) and the ROI of the bud emergence site (ROI_{BS}).

The mean intensity of pixels in each ROI was then computed. The ratio of the site of bud emergence ROI_{BS} mean intensity (MI) to the mother cell ROI_M mean intensity was calculated, as in

$$Ratio1 = \frac{MI\ (ROI_{BS})}{MI\ (ROI_M)}$$

This ratio was compared to that in all yeast cells in each population (n1 = 41, n2=44, n3=18). Distributions were then plotted in a merged histogram. Results for each sample are displayed in Figure 6.8.

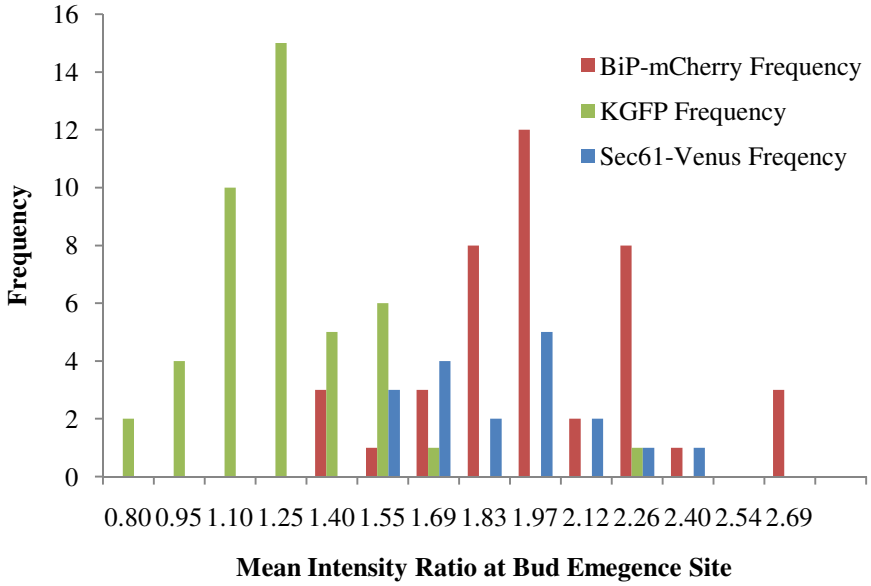

Figure 6.8 Merged histograms illustrate for the distribution of mean intensity ratio found at the bud emergence site for each protein observed ($MIROI_{BS}/MIROI_{M}$). Red bars indicate the distribution for BiP-mCherry; green bars represent distribution for KGFP; and blue bars represent Sec61-Venus expressed and analyzed in separate *S. cerevisiae* strains.

The merged histograms displayed in Figure 6.8 represent the distribution of mean intensity ratios ($MIROI_{BS}/MIROI_{M}$) calculated for each protein of interest at the bud emergence site. The histograms indicate that the mean intensity ratios for BiP-mCherry and Sec61-Venus located at the bud emergence site are similarly distributed around the respective means of 1.92 ±0.05 for BiP-mCherry and 1.81 ± 0.06 for Sec61-Venus. The mean values signify that BiP and Sec61 are almost twice as intense at the bud emergence site than across the entire mother cell. In contrast, the mean

intensity ratio distribution for KGFP was negatively shifted to the left, with a mean of 1.19 ± 0.04, implying that KGFP has almost the same average intensity at the bud emergence site as it does in the entire mother cell. A two-sample t-test with a 95% confidence interval was performed to statistically determine the differences in mean intensity ratios for BiP-mCherry, Sec61-Venus, and KGFP. The null hypothesis was defined as $\mu_1 - \mu_2 = 0$ and the alternative hypothesis was defined as $\mu_1 - \mu_2 > 0$. The observed levels of significance for comparing both BiP-mCherry and Sec61-Venus to KGFP mean ratios were equal to zero, indicating that the null hypothesis can be rejected. Therefore, both BiP-mCherry and Sec61-Venus mean intensity ratios are significantly different than that of KGFP. In contrast, when comparing the ratios of BiP-mCherry and Sec61-Venus, the observed level of significance was 0.076, which is greater than the selected alpha value of 0.05. Therefore, the mean intensity ratios of BiP-mCherry and Sec61-Venus are not significantly different. This quantitative analysis indicates that the ER protein assembly at the bud emergence site is a direct result of the luminal functionality of BiP and the functionality of ER membrane Sec61.

6.3.2 Protein Concentrations at the Exocyst

Three separate populations of yeast cells consisting of growing buds during Phase 1 of cell division were analyzed for BiP-mCherry (n=42), KGFP (n=41), and Sec61-Venus (n=34) expression and localization. Each individual yeast cell was analyzed by selecting an ROI around the growing bud (ROI_{bud}) and an ROI around the exocyst (ROI_{exo}), as depicted in Figure 6.9.

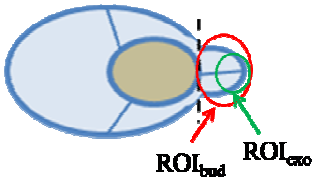

Figure 6.9 Schematic illustrating the selected ROI of the bud (ROI_{bud}) and the ROI of the exocyst (ROI_{exo}).

The ratio of the exocyst mean intensity (MI) to the bud cell mean intensity was calculated from

$$Ratio2 = \frac{MI\ (ROI_{exo})}{MI\ (ROI_{bud})}$$

Distributions of each fusion protein were merged to one histogram displayed in Figure 6.10.

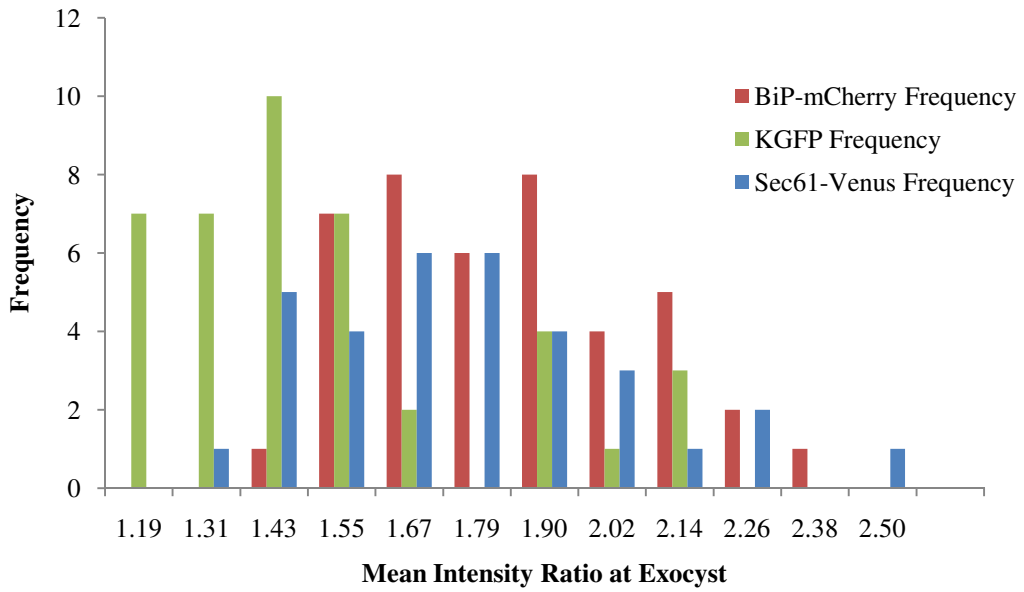

Figure 6.10 Merged histograms illustrate for the distribution of mean intensity ratio found at the exocyst for each protein observed ($MIROI_{exo}/MIROI_{bud}$). Red bars indicate the distribution for BiP-mCherry; green bars represent distribution for KGFP; and blue bars represent Sec61-Venus expressed and analyzed in separate *S. cerevisiae* strains.

The merged histograms displayed in Figure 6.10 represent the distribution of mean intensity ratios found for each protein of interest at the exocyst of the bud ($MIROI_{exo}/MIROI_{bud}$). The histograms indicate that the mean intensity ratios for BiP-mCherry and Sec61-Venus located at the bud exocyst are also similarly distributed around the respective means of 1.78 ± 0.04 for BiP and 1.72 ± 0.05for Sec61. Therefore BiP and Sec61 are ~1.7 times more intense at the exocyst of the bud than

across the entire daughter cell. In contrast, the mean intensity ratio distribution for KGFP is again negatively shifted to the left, with a mean of 1.45 ± 0.04. The same two-sample t-test with a 95% confidence interval was performed to statistically determine the differences in mean intensity ratios for BiP-mCherry, Sec61-Venus, and KGFP. The observed levels of significance for comparing both BiP-mCherry and Sec61-Venus to KGFP mean ratios were equal to zero, indicating that the null hypothesis can be rejected. Therefore, both BiP-mCherry and Sec61-Venus mean intensity ratios are significantly different than that of KGFP at the exocyst. In contrast, when comparing the ratios of BiP-mCherry and Sec61-Venus, the observed level of significance was 0.212, which is greater than the selected alpha value. Therefore, the mean intensity ratios of BiP-mCherry and Sec61-Venus are not significantly different. It is concluded that protein function of BiP and Sec61 plays an important role in terms of localization to the exocyst during bud growth.

6.3.3 Protein Concentrations at Mother-Daughter Neck During Mitosis

As yeast cells undergo mitosis, referred to as nuclear division, it was observed that ER resident proteins accumulate at the mother-daughter neck in the mother cell. This indicates a possible structural barrier, or mechanism, that limits the ER inheritance during the cell cycle. Three separate populations of yeast cells in the mitosis stage (Phase 2) of cell division were analyzed for BiP-mCherry (n=36), KGFP (n=28), and Sec61-Venus (n=25). Each individual yeast cell was analyzed by selecting an ROI around the mother cell (ROI_M) and an ROI around the mother-daughter neck (ROI_{neck}), as depicted in Figure 6.11.

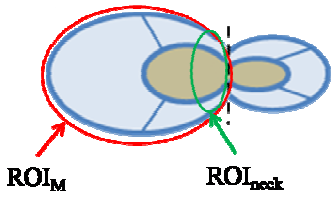

Figure 6.11 Schematic illustrating the selected ROI of the mother cell (ROI_M) and the ROI of the mother-daughter neck (ROI_{neck}).

The ratio of the neck mean intensity (MI) to the mother cell mean intensity was calculated using

$$Ratio3 = \frac{MI\ (ROI_{neck})}{MI\ (ROI_M)}$$

Distributions of each fusion protein were merged to one histogram displayed in Figure 6.12.

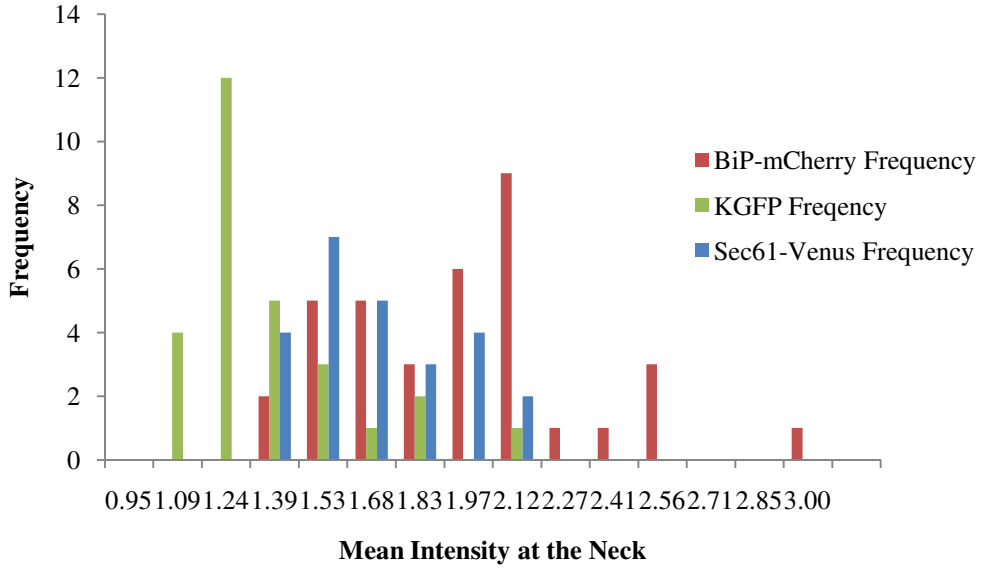

Figure 6.12 Merged histograms illustrate for the distribution of mean intensity ratio found at the exocyst for each protein observed ($MIROI_{neck}/MIROI_{bud}$). Red bars indicate the distribution for BiP-mCherry; green bars represent distribution for KGFP; and blue bars represent Sec61-Venus expressed and analyzed in separate *S. cerevisiae* strains.

The same conclusions were drawn from this quantitative analysis for BiP-mCherry, Sec61-Venus, and KGFP within yeast cells undergoing mitosis. Comparison of the intensity ratios at the mother-daughter neck, indicates that the KGFP distribution is again negatively shifted at a mean of 1.30 ± 0.04, whereas BiP and Sec61 are similarly distributed around the respective means of 1.89 ± 0.06 and 1.62 ± 0.05. To statistically determine the differences in mean intensity ratios, the same two-sample t-test with a 95% confidence interval was performed. The observed levels of significance for

comparing mean intensity ratios of BiP-mCherry, Sec61-Venus, and KGFP are all equal to zero. This analysis indicates that there are significant differences in all three mean intensities for the three proteins localized at the mother-daughter neck. This result can be explained either based on protein functionality or mechanism during budding. The difference in protein functions of luminal BiP, ER membrane Sec61, and luminal KGFP could result in the significantly different concentrations at the mother-daughter neck. A second proposal involves the potential barrier existing between the two cells during division. This barrier, which is part of the mechanism during mitosis, could result in build-up of different fractions of proteins at the mother-daughter neck. This proposal is consistent with qualitative results, which shows protein accumulation at the neck during mitosis being relatively conserved among these three different ER resident proteins.

To gather more reliable results in the future, analysis must be perfomed on a larger population of budding yeast cells. In addition, there is not an experimental method to ensure that the same ROI is used for each intensity reading. Thus, the construction of a new yeast strain that simultaneously expresses KGFP and BiP would make this analysis attainable.

6.4 Spatial Heterogeneity Exists between Membrane and Luminal ER proteins

BiP (ER luminal protein) and Sec61 (ER membrane protein) were shown to be localized similarly at the bud emergence site, the bud exocyst, and at the mother-daughter neck. However, when analyzing yeast cells that express both BiP-mCherry and Sec61-Venus simultaneously, a more detailed and direct comparison of spatial localization was made.

During Phase 1 of cell division, when a bud is first formed, it has already been established that both BiP and Sec61 are concentrated at the bud emergence site. To determine if these two proteins differ in localization elsewhere in this phase of budding, an analysis of a single yeast cell expressing both BiP-mCherry and Sec61-Venus was performed, shown in Figure 6.13.

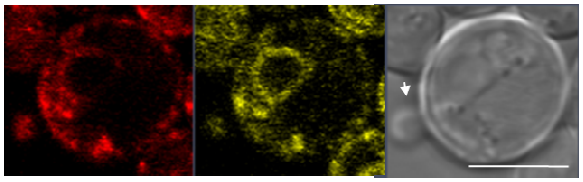

Figure 6.13 Yeast cell expressing BiP-mCherry (red) and Nup49-Venus (yellow), and a DIC transmitted light image. A white arrow head indicates the formation of a bud. Zeiss5 DUO confocal microscope, Plan-Apochromat 63x/1.40 Oil DIC M27 objective lens. Scale bar is ~5µm.

Fluorescence images of the yeast cell in Figure 6.13 were converted to RG binary then spatial heterogeneity was determined. Results are shown in Figure 6.14.

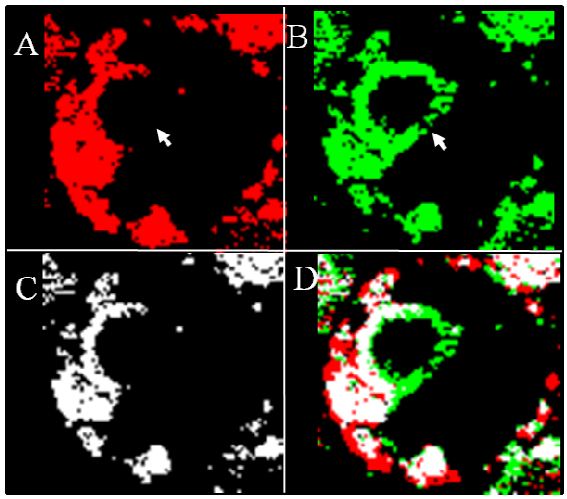

Figure 6.14 RG binary images of (A) BiP-mCherry, (B) Sec61-Venus, (C) spatial homogeneous localization is indicated by the white pixels, and (D) merged image. Arrowheads represent regions of heterogeneity.

Figure 6.14 indicates that there is spatial heterogeneity around the perinuclear ER. In the BiP-mCherry binary image, an arrow marks the region of the ER that is not localized similarly to the arrow in the Sec61-Venus binary image.

A second example of this heterogeneity is shown in a time series, which captures a single yeast cell transitioning from Phase 1 of cell division to Phase 2 of cell division, shown in Figure 6.15.

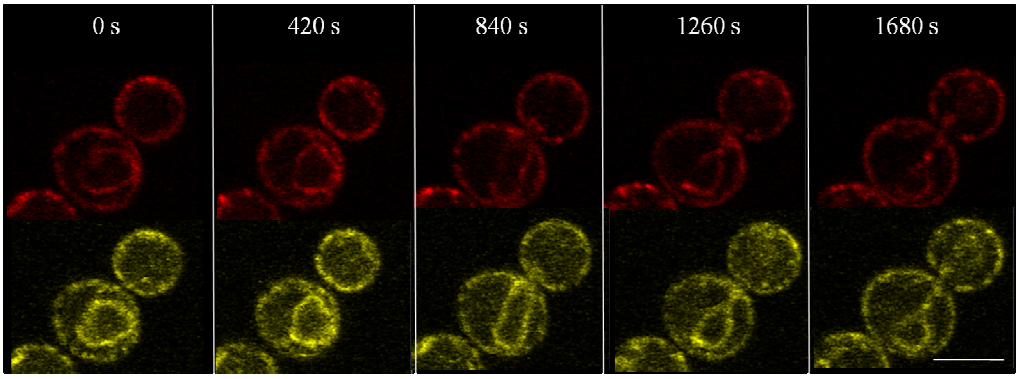

Figure 6.15 Time series of a yeast cell expressing BiP-mCherry (red) and Nup49-Venus (yellow). Zeiss5 DUO confocal microscope, Plan-Apochromat 63x/1.40 Oil DIC M27 objective lens. Scale bar is ~5µm.

The yeast cell begins mitosis in the third panel, at the time point of 840 seconds. When qualitatively observing this yeast cell, it appears that both BiP-mCherry and Sec61-Venus are colocalized. However, converting the image to binary and comparing the fluorescence of each pixel in two images indicates that there exists spatial heterogeneity between BiP and Sec61. Results are shown in Figure 6.13.

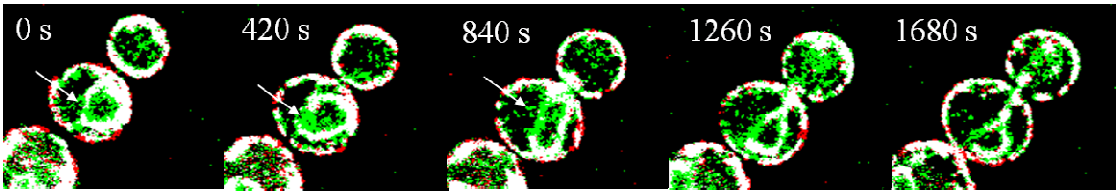

Figure 6.13 Merged RG binary images of BiP-mCherry (red) and Sec61-Venus (green). Spatial homogeneous localization is indicated by the white pixels in the merged images. Arrowheads represent regions of heterogeneity.

As the yeast cell progresses form Phase 1 of cell division into mitosis during Phase 2 of cell division, the spatial heterogeneity increases in the mother cell. In the first time point (0 seconds), an arrow marks the very small region of heterogeneity. Over the next two time points (420 and 840 seconds), this lack or decreased concentration of BiP-mCherry increases over a larger area. At later time points (1260 and 1680 seconds), there are various points of spatial heterogeneity throughout both the mother and daughter cells.

6.5 Heterogeneous ER Protein Localization Conclusions

In conclusion, spatial heterogeneity has been proven for ER luminal, ER membrane, and NPC proteins in budding yeast cells. Colocalization does exist between BiP-mCherry and Nup49-Venus throughout cell division. This spatial homogeneity exists around the nuclei of the mother and daughter cells and along ER tubules connecting the nuclei at later time points. However, through the transition from bud initiation to nuclear division, the fraction of colocalized BiP-mCherry pixels

decreases. It has been proposed that a portion of the BiP localized around the nucleus is removed from the perinuclear ER and placed into other ER subdomains during cell division. ER resident protein intensities were analyzed at different locations in budding yeast cells. Using KGFP, which has no function in the ER, as a control, it was determined that the concentration of ER proteins (BiP and Sec61) at both the bud emergence site and the exocyst depends on protein functionality. In contrast, the accumulation of proteins at the mother-daughter neck during nuclear division is not dependent on protein function within the ER. Finally, yeast cells expressing both BiP and Sec61 simultaneously yield spatial heterogeneity at different time points in cell division, specifically within the perinuclear ER.

Chapter 7

ROLE OF CYTOSKELETON IN CELL DIVISION

7.1 Introduction

It has been suggested that the cytoskeleton has an important role in ER inheritance of budding yeast cells. Yeast cells, like all eukaryotes, contain a cytoskeleton that serves as the infrastructure in order to maintain cell shape and cell motility. The yeast cytoskeleton is comprised of microtubules, filamentous actin cables, and actin patches, each associated with selective functions. In higher eukaryotic cells, ER dynamics are controlled predominantly by microtubules while actin's contribution is much less. Experiments have been performed in animal cells that show the disruption of microtubules which results in a gradual collapse of the peripheral ER and formation of large patches located in the cytoplasm or aggregates around the nucleus (Du *et al*., 2004). The role of microtubules in mammalian ER dynamics and morphology is dependent on microtubule-associated motors and the polymerization of microtubules (Du *et al*., 2004).

In contrast, our system of interest, S. *cerevisiae* cells, require actin to serve as the structure which protein complexes follow to the daughter cell during l division, while microtubules play a far less important role (Du *et al*., 2004). There are three types of cytoplasmic microtubules in yeast, referred to as α, β, and γ (Prinz *et al*., 2000). Studies have shown that the NE in budding yeast is partitioned through a multi-stage process involving microtubule-dependent transport for extension into the daughter cell, whereas ER segregation does not depend on the microtubules for

partitioning (Du *et al*., 2004). Prolonged disruption of microtubules has been examined and did not result in detectable effects of either inheritance or dynamics of the peripheral ER (Prinz et al 2000; Du *et al*., 2004). However, because the NE and perinuclear ER are continuous structures, we find it interesting that their inheritance may be controlled by different mechanisms.

Assuming that microtubules are not required for ER inheritance, actin appears to be the most likely candidate that directs biogenesis of the ER. Recent studies have shown that ER inheritance involves ER tubules forming and segregating in budding cells along actin cables present in the cell (Du *et al*., 2004). A diagram illustrating this concept is shown in Figure 7.1.

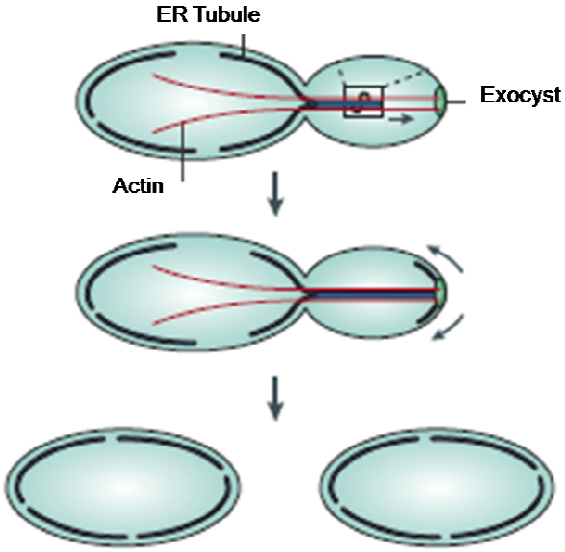

Figure 7.1 Actin creates a pathway for inheritance of peripheral ER and ER tubules in budding yeast cells. This image has been modified from Lowe and Barr, 2007.

Figure 7.1 summarizes the proposed role of actin in yeast during cell division. As the peripheral ER is partitioned into the daughter cell, ER tubules traverse along actin cables, across the mother-bud axis by the use of motor proteins (not shown in Figure 7.1). Upon reaching the bud tip, ER tubules are anchored at the exocyst, followed by the spread of the ER along the cell periphery which forms the cortical ER network within the daughter cell (Lowe and Barr, 2007). The linear extension of the ER into the bud, illustrated in the live cell images of Chapter 5, suggests that the actin cytoskeleton does play an important role in ER partitioning. Actin's role has also been verified by genetic screening for the myosin motor protein Myo4p, which has been shown to be required for delivery of the peripheral ER into the daughter cells (Du *et al*., 2004).

Studies have shown that actin depolymerization dramatically reduces the dynamics of the peripheral ER of the bud and immobilizes ER tubules extending into the bud (Prinz *et al*., 2000; Du *et al*., 2004). However, imaging of individual cells has revealed that the majority of ER tubules are not aligned with cortical actin cables in yeast (Du *et al*., 2004). One explanation is that ER structures are already formed in a yeast cell and can be maintained without actin-dependent mechanisms (Du *et al*., 2004). It is also possible that ER inheritance only occurs through the small number of ER tubules that do colocalize with actin cables (Du *et al*., 2004).

7.2 Experimental Methods

7.2.1 Phalloidin Staining Protocol

To observe the localization of actin compared to ER resident proteins throughout different time points in cell division, yeast cells expressing BiP-mCherry

were fixed with paraformaldehyde, which halts intracellular dynamic, and then stained with fluorescein phalloidin stain. A modified phalloidin staining protocol has been adapted from Tatchell, K. and Robinson, L.C. "Use of Green Fluorescent Protein in Living Cells" Methods in Enzymology. *Guide to Yeast Genetics and Molecular and Cell Biology Part C.*

750 µL of *S. cerevisiae* cell culture was grown in synthetic media for 1 hour at mid-log phase. 1-2 ODs were fixed with the addition of paraformaldehyde (4%) directly to a 1 mL cell culture. The sample was covered with foil, inverted,, and then allowed to sit at room temperature for 30 minutes. Cells were harvested by centrifugation for 4 minutes at 2000 rcf, then washed 3 times with 500 µL of PBS, and finally resuspended in 200 µL of PBS. 10µL of phalloidin (Molecular Probes Cat# F432, 6.6µM in MeOH) was added to 100µL of sample. The sample was then incubated at room temperature (in the dark) for one hour, followed by 5 washes with 1 mL of PBS. Cells were then resuspended in 1 drop of Anti Slow Fade Gold™ (Invitrogen). 3µL of sample were immediately plated on a 2% agarose microslide. Plates were stored at 4°C, in the dark, until use.

7.2.2 Depolymerization of Actin with Latrunculin A

Filamentous actin (F-actin) was destabilized by adding latrunculin A (LatA) to a growing culture of yeast cells. Our protocol was derived from that of Fehrenbacher *et al*. (2002). A 1 mL culture of yeast cells was grown in midlog phase for one hour. Latrunculin A (2 mM stock in DMSO; Invitrogen) was added to the culture in order to achieve a final concentration of 500 µM. An equivalent amount of LatA-free DMSO was added to an additional culture as a control. Both cultures were incubated at room temperature for 20 minutes and then washed twice with 1 mL of SC

media. Cells were immediately plated on a 2% agarose slide to be analyzed on the confocal microscope.

7.2.3 Disruption of Microtubules with Nocodazole

The cytoskeleton network of microtubules in yeast was disrupted by adding nocodazole to the cell culture. This protocol was derived from that of Prinz *et al*. (2000). A 1 mL culture of yeast cells was grown in midlog phase for one hour. Nocodazole (20mM stock in DMSO; Sigma Aldrich) was added to the culture in order to achieve a concentration of 20 µg/mL. The culture was then placed in the 30°C shaker at 250 rpm for 30 minutes. Cells were washed twice with 1 mL of SC media, and then immediately plated on a 2% agarose slide to be analyzed on the confocal microscope.

7.3 Actin Localization

Both actin patches and actin cables consist of F-actin structures that exist in budding yeast cells throughout cell division (Huckaba *et al*., 2004). Actin patches are known to be localized in both the bud and the mother-daughter neck (Huckaba *et al*., 2004). In contrast, actin cables run along the mother-bud axis and are often thought to serve as tracks for the movement of vesicles, mRNA, mitochondria, Golgi and vacuoles from the mother to the daughter (Huckaba *et al*., 2004).

Previous research studying actin localization patterns in yeast cells suggests that actin plays a role in several stages of cell division. To compare these results, yeast cells expressing BiP-mCherry (ER lumen) were stained with phalloidin to mark actin cortical patches. The protocol for the staining is described in section 7.2.1. Actin patches are known to first localize in a cluster at the site of bud

emergence, with cables oriented towards the bud site (Karpova *et al*., 1998, Amberg, 1998).

At early time points of cell division, actin patches are clustered at the tip of the bud (Karpova *et al*., 1998). Results for the phalloidin staining of budding yeast cells expressing BiP-mCherry are shown in Figure 7.2.

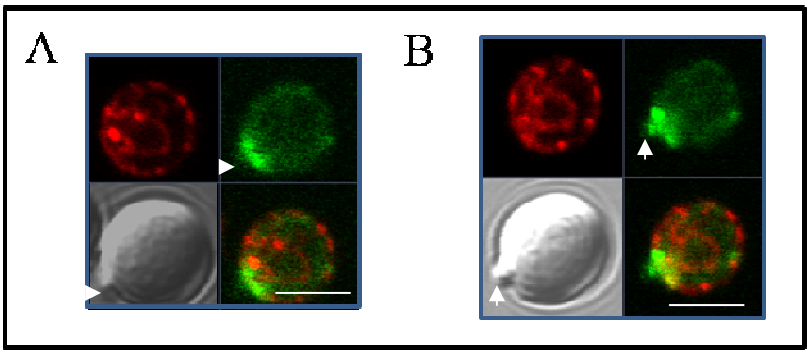

Figure 7.2 Early time points of cell division of fixed yeast cells expressing BiP-mCherry (red) and stained with phalloidin (green). White arrowheads indicate the buds' emergence from mother cell. Zeiss5 DUO confocal microscope, Plan-Apochromat 63x/1.40 Oil DIC M27 objective lens. Scale bars are ~5µm.

Figure 7.2 clearly shows that high concentrations of actin patches and BiP-mCherry are located at the site of bud emergence. However, in Figure 7.2 (A), there is only an assembly of actin at the bud site, while BiP-mCherry is also distributed throughout the cell. In cells that have a larger bud forming, shown in Figure 7.2 (B), both the actin and ER are localized at the bud emergence site. This is indicated by the concentration of phalloidin-stained actin (green) and BiP-mCherry (red).

Studies have shown that as the bud grows to a 'medium size', actin patches become randomly distributed throughout bud (Karpova *et al*., 1998). The

distribution of cortical patches in the bud suggests a role in bud growth (Amberg, 1998). Previous research has also shown that following bud initiation and continued growth, there is a shift to a polarization of the actin cytoskeleton (Lowe and Barr, 2007). Results of yeast cells analyzed at this stage of cell division are shown in Figure 7.3.

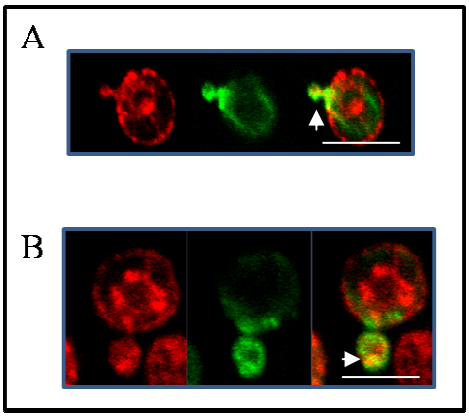

Figure 7.3 Two time points of the cell division of fixed yeast cells expressing BiP-mCherry (red) and stained with phalloidin (green). White arrowheads indicate the growing buds in each yeast cell. Zeiss5 DUO confocal microscope, Plan-Apochromat 63x/1.40 Oil DIC M27 objective lens. Scale bars are ~5µm.

In Figure 7.3 (A), it is apparent that the bud is filled with both the phalloidin stained actin (green) and the BiP-mCherry (red). However, the actin is extended further into the bud than the ER, which suggests the actin plays a role in guiding the ER into the bud. At a later time point in cell division, Figure 7.3 (B), there is an apparent accumulation of both BiP and actin at the exocyst in the bud. Literature studies have shown larger buds, at later time points in division, with actin patches evenly distributed throughout both the mother and daughter cells (Karpova *et al.*,

1998). In the final stages of cell division, actin patches gather at the site of cell division, the mother-daughter neck (Karpova *et al*., 1998). This localization implies that cytoskeleton actin has a role in cytokinesis (Amberg, 1998). Phalloidin staining of BiP-mCherry expression yeast cells shows the localization of actin and the ER at later time points in cell division.

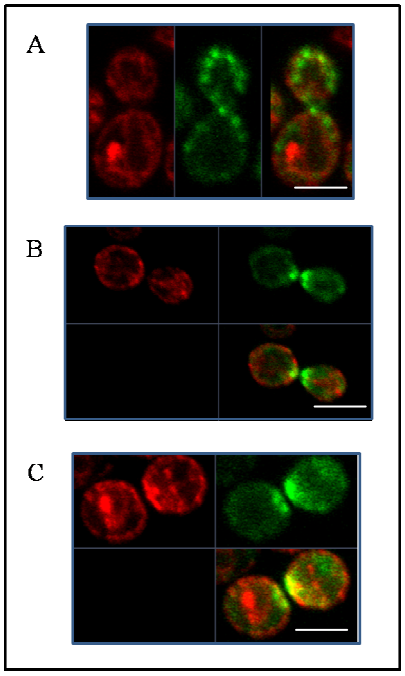

Figure 7.4 Fixed yeast cells expressing BiP-mCherry and phallodin stained actin at later time points in cell division. Zeiss5 DUO confocal microscope, Plan-Apochromat 63x/1.40 Oil DIC M27 objective lens. Scale bars are ~5µm.

At later time points in cell division, Figure 7.4 (A) illustrates how the actin cortical patches are distributed in both the mother and daughter cells. Yeast cells undergoing cytokinesis are shown in both Figure 7.4 (B) and (C). In accordance with previous

research, the actin is localized at the neck of the mother and daughter cells. This suggests that actin does play a significant role in cytokinesis in yeast cells.

7.4 Disruption of the Cytoskeleton Network of Microtubules

In higher eukaryotes, such as mammalian cells, the ER structure and organization are dependent on microtubules (Fehrenbacher *et al*., 2002). It has been previously shown that the ER colocalizes with microtubules and extends into the periphery of the cells as a microtubule-dependent process (Fehrenbacher *et al*., 2002). In contrast, budding yeast microtubules tend to have less of a role in ER dynamics and inheritance. There are a total of four tubulin genes in budding yeast, two α-tubulins, one β-tubulin, and one γ-tubulin (Andresen *et al*., 2004). There have been fusion proteins created for Tub1 and Tub3 with GFP variants to view in live yeast cells (Andresen *et al*., 2004). However, these constructs were not available at the time this research was executed. Therefore, in order to examine the role of microtubules in ER inheritance and ER protein localization, yeast cells were incubated in medium containing nocodazole. This reagent is known to depolymerize the microtubule network in eukaryotes. Studies have tracked the localization of ER membrane protein, Sec63-GFP; however, experiments have never examined the effect on ER resident and NPC proteins expressed in yeast cells (Prinz *et al*., 2000).

We have performed experiments which depolymerized microtubules in yeast cells expressing BiP-mCherry and Nup49-Venus. The fluorescence images obtained after disruption of the microtubules are presented in Figure 7.5.

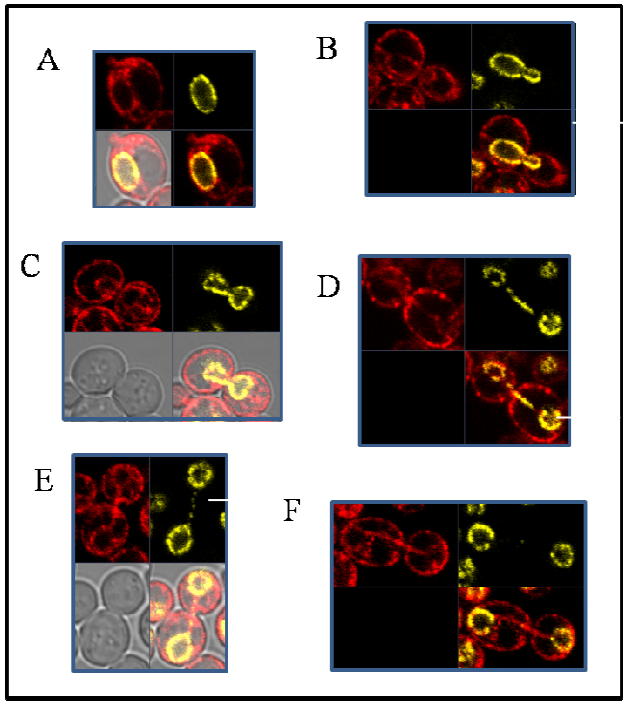

Figure 7.5 Live cell imaging results after disruption of microtubules with nocodazole in yeast cells expressing BiP-mCherry and Nup49-Venus. Zeiss5 DUO confocal microscope, Plan-Apochromat 63x/1.40 Oil DIC M27 objective lens. Scale bars are ~5µm.

In Figure 7.5, results show that disruption of microtubules in live budding yeast cells did not disrupt the process of ER inheritance. Figure 7.5 (A) shows successful bud initiation. Figures (B) through (F) indicate that nuclear division was initiated and continued until complete separation of the mother and daughter cells. This result is consistent with previous literature, which reported that disruption of microtubules in yeast cells expressing Sec63-GFP did not disrupt the structure or maintenance of the

ER (Prinz *et al*., 2000). Therefore, we conclude that microtubules are not required for ER inheritance in budding yeast cells.

7.5 Depolymerization of Actin Cytoskeleton

To examine the role of actin in ER inheritance, yeast cells were inoculated with latrunculin A (Lat A). Images of live cells were taken with the confocal microscope following the induction of LatA for the period of time specified in section 7.3. By examination of several populations, including a total of ~320 cells, we have determined that the concentration of LatA used in this experiment was 65% effective at actin cytoskeleton depolymerization. Therefore, a population of dividing cells existed with the ability to successfully segregate the ER and another population that could not complete cell division. Figure 7.6 is an example of a yeast cell unaffected by the LatA addition.

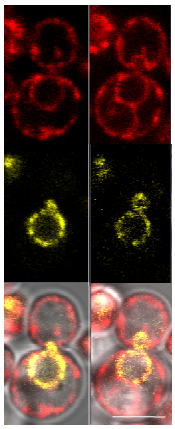

Figure 7.6 Time series of a yeast cell expressing BiP-mCherry and Nup49-Venus through mitosis after LatA was introduced during an attempt to disrupt actin cytoskeleton. Zeiss5 DUO confocal microscope, Plan-Apochromat 63x/1.40 Oil DIC M27 objective lens. Scale bar is ~5µm.

It is apparent that this yeast cell, as well as ~35% of the cells in the sample population, was not at all affected by LatA. The inheritance of the perinuclear ER continues normally, with protein localizations similar to those reported in Chapter 5. Figure 7.7 includes a sample of cells that were affected by the LatA, indicated with white arrowheads.

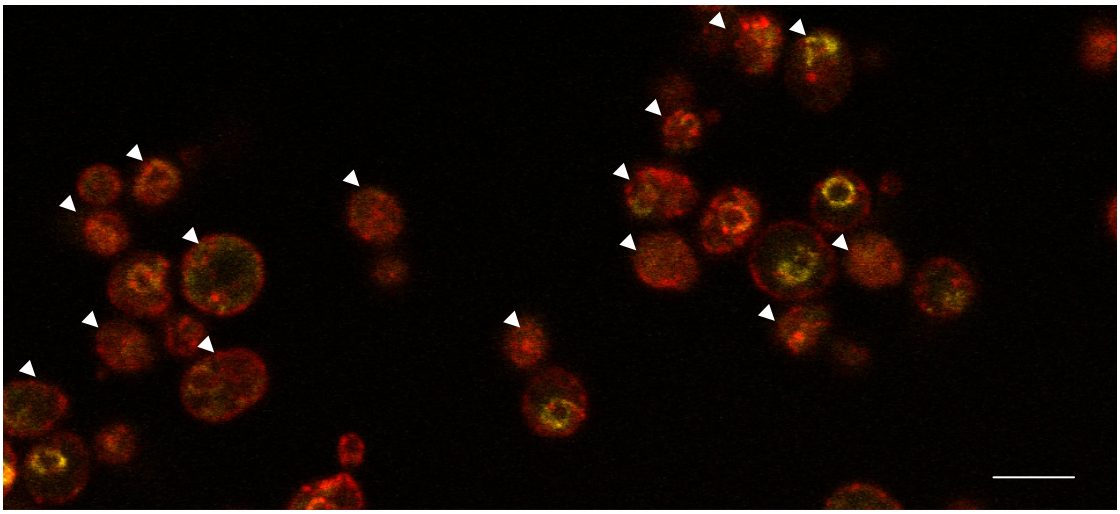

Figure 7.7 Live cell images of yeast cells expressing BiP-mCherry and Nup49-Venus after LatA was introduced in order to disrupt actin cytoskeleton. Zeiss5 DUO confocal microscope, Plan-Apochromat 63x/1.40 Oil DIC M27 objective lens. Scale bar is ~5µm.

In contrast to the results shown in Figure 7.6, the yeast cells imaged in Figure 7.7 were affected by the LatA. It appears that without the cytoskeleton infrastructure, the ER structure in the mother and daughter cell has been completely disrupted. There appears to be no organized segregation occurring in the mother and daughter cells.

A previous study examined the localization of ER membrane protein Sec63-GFP, when the actin cytoskeleton was depolymerized with LatA. Results

indicated that the actin cytoskeleton appeared to be required for ER dynamics. Upon introduction of LatA, ER dynamics were immediately reduced (Prinz *et al*., 2000). Previous research involving perturbations in the actin cytoskeleton resulted in the delay of bud formation, with eventual altered growth conditions (Lowe and Barr, 2007). Results from scanned images of yeast cells shown in Figure 7.7 suggest that depolymerizing actin does halt ER dynamics and disrupts ER inheritance during cell division. However, this experiment was not optimized for the yeast cells examined in this research. As previously stated, only 65% of yeast cells appeared to be affected by the introduction of LatA. Among the population of disrupted cells, a fraction were found to have only ER dynamics disturbed, while the other fraction of cells appeared to have changes in localization of both ER and NPC proteins. Future work includes determining the optimal concentration of LatA that will depolymerize F-actin. In addition, a more quantitative analysis and time series experiments should be performed to conclude the exact role of the actin cytoskeleton in ER inheritance.

Chapter 8

CONCLUSIONS AND FUTURE WORK

The endoplasmic reticulum (ER) of yeast, *S. cerevisiae*, is an essential organelle responsible for multiple critical processes of the cell. Structurally, this organelle is comprised of three main subdomains: the peripheral ER, the perinuclear ER, and a network of ER tubules. Our motivation has been to study the organelle biogenesis of the ER during mother-daughter budding in order to understand the mechanisms associated with ER inheritance during cellular division. We hypothesize that ER resident proteins distribute in a heterogeneous fashion throughout the continuous ER, and that effects of spatial distribution are a result of a protein's specific function.

Confocal light microscopy has been used to continuously monitor fluorescently tagged proteins of interest throughout the life cycle of budding yeast, *S. cerevisiae*. Proteins examined in this research include ER luminal proteins BiP and KGFP, ER membrane protein Sec61, and nuclear pore complex (NPC) protein Nup49, which is embedded in the NPC as it spans across the perinuclear ER and nuclear envelope.

8.1 Three Phases of ER Inheritance

We have classified ER inheritance as a stepwise process that can be identified as three separate phases during which the different ER subdomains segregate separately. Phase 1 includes alterations in the positioning of proteins in the

peripheral ER as a bud is formed and begins to grow. High concentrations of ER protein (BiP-mCherry, Sec61-Venus) were observed at the site of bud emergence and at the exocyst, referred to as the tip of the growing bud. This phase of cellular division was found to last approximately 55 minutes. Phase 2 consists of nuclear division as the perinuclear ER is segregated, in conjunction with the NPC, between the mother and daughter cells. There appears to be a barrier at the mother-daughter neck which results in a buildup of increased concentration of ER proteins localized at the neck of the mother cell. This phase of cell division occurred in approximately 35 minutes. Phase 3 includes complete separation of cells followed by a homogeneous spatial distribution of ER resident and NPC proteins. This phase of cell division has been observed during the time period of approximately 15 minutes.

8.2 Colocalization Between BiP-mCherry and Nup49-Venus

In addition to monitoring spatial localization of ER proteins during organelle inheritance, ER resident and NPC proteins were compared in order to quantify heterogeneity. We believe that spatial heterogeneity exists as a consequence of protein function during organelle biogenesis. Therefore, our first analysis was performed in order to quantify the colocalization between BiP-mCherry and Nup49-Venus which were simultaneously expressed in budding yeast cells. As cells transition from Phase 1 of cell division into Phase 2 (nuclear division), the concentration of BiP-mCherry colocalized with Nup49-Venus decreased significantly. Our results suggest that BiP's function requires trafficking from the perinuclear ER in order to be partitioned during budding of mother-daughter cells. Thus, we propose that BiP not only plays an important role in the mating of yeast, through its involvement in

karyogamy (Rose *et al*., 1989), but it also plays a pivotal role in ER inheritance of budding yeast cells.

8.3 Protein Function Dictates ER Protein Spatial Localization

Three ER resident proteins have been examined in order to determine the spatial heterogeneity associated with ER proteins. KGFP, a soluble GFP retained in the ER, participates in no known cellular function, was used as a control when determining if protein function dictates spatial localization. ER resident proteins examined include ER luminal protein, BiP-mCherry, and ER membrane protein, Sec61-Venus. Mean intensities of protein concentrations were measured during the three phases of cellular division. When compared to BiP-mCherry and Sec61-Venus, a significantly lower fraction of KGFP was observed at the bud emergence site in Phase 1, the exocyst of the growing bud in Phase 1. In contrast, at the mother-daughter neck during mitosis of Phase 2, there are significant differences in the fractions of all three ER resident proteins. This indicates that either protein function or the mechanism involving a mother-daughter neck barrier results in build-up at the mother-daughter neck. Therefore, in comparison to endogeneous proteins of yeast, we have concluded that the luminal function of BiP, and the membrane function of Sec61, dictates their spatial localization in the three examined time points of cellular division.

Previous studies have shown that the exocyst plays an important role in cell division of budding yeast. Specifically, the protein Sec3p, one component of the exocyst complex, is required for anchorage of the peripheral ER as it enters the daughter bud and is also essential for a polarized distribution of proteins within the bud (Du *et al*., 2004, Boyd *et al*, 2004). Experiments using GFP tagged Sec3p have shown that a loss of Sec3p results in significant delays of peripheral ER inheritance

(Du *et al*., 2004). It has also been suggested that the ER membrane protein Sec61, which is a core component of the translocon, is involved in anchoring the ER to the exocyst. Over-expression of Sec3p causes Sec61 to accumulate at the bud tip without affecting the localization of other ER-resident proteins (Du *et al*., 2004). Future work includes implementation of a GFP-tagged Sec3p to monitor the specific location of the exocyst. In addition, we would then be able to quantify the effects on the spatial distribution of BiP-mCherry and Sec61-Venus when Sec3p is either lost or over-expressed.

8.4 Spatial Heterogeneity Between ER Luminal and ER Membrane proteins

ER luminal protein BiP and the ER membrane protein Sec61 have been examined in order to determine the existence of spatial heterogeneity throughout ER inheritance. At different stages of cell division, BiP-mCherry and Sec61-Venus experience spatial heterogeneity specifically within the perinuclear ER. As previously stated, future work would include examining the dependence of BiP-mCherry and Sec61-Venus spatial localization in relation to the exocyst during cell division.

A few limitations exist within our experimental system with respect to quantification of confocal images. One issue was addressed in Chapter 6 concerning two-dimensional imaging. When comparing individual yeast cells within a population, it is difficult to effectively evaluate the differences of protein location in three-dimensions when data are from a two-dimensional image. Future studies will use confocal microscopy to reconstruct three-dimensional images by combining a stack of many optical slices through a dividing yeast cell. A second concern regarding data analysis was discussed in Chapter 7 concerning the inconsistency associated with

defining the region of interest. The use of strains expressing multiple fusion proteins will allow for more consistent and reliable results.

8.5 Role of Actin Cytoskeleton in ER inheritance

Finally, disruption of yeast microtubules and actin cytoskeleton was performed in order to determine the mechanism controlling ER inheritance. Actin depolymerization proved to disrupt ER morphology and the protein distribution in budding yeast cells. Therefore, in contradiction to previous studies of yeast, we infer that actin plays a pivotal role in ER biogenesis. Future studies will optimize the disruption of actin and quantify the spatial effects of proteins after actin depolymerization.

In conclusion, our results offer a better understanding of how various ER resident proteins have distinct localization patterns. Spatial heterogeneity is believed to be dependent on the unique functions of various proteins during ER inheritance of budding yeast cells. Continuous studies of the ER and associated proteins will provide further information concerning the importance and mechanism of ER organelle inheritance in budding yeast cells.

REFERENCES

Albertazzi, L., Arosio, D., Marchetti, L., Ricci, F., & Beltram, F. (2009). Quantitative FRET analysis with the E^0GFP-mCherry fluorescent protein pair. *Photochemistry and Photobiology, 85*(1), 287-297.

Alder, N. N., Ying Shen, Jeffrey L. Brodsky, Linda M. Hendershot, & Arthur E. Johnson. (2005). The molecular mechanisms underlying BiP-mediated gating of the Sec61 translocon of the endoplasmic reticulum. *The Journal of Cell Biology, 168*(3), 389-399.

Amberg, D. C. (1998). Three-dimensional imaging of the yeast actin cytoskeleton through the budding cell cycle. *Molecular Biology of the Cell, 9*(12), 3259-3262.

Amberg, D., Daniel J. Burke, & Jeffrey N. Strathern. (2005). In David Crotty (Ed.), *Methods in yeast genetics: A cold spring harbor laboratory course manual* (2005th ed.). New York: Cold Spring Harbor Laboratory Press.

Andresen, M., Schmitz-Salue, R., & Jakobs, S. (2004). Short tetracysteine tags to {beta}-tubulin demonstrate the significance of small labels for live cell imaging. *Molecular Biology of the Cell, 15*(12), 5616-5622.

Belgareh, N., & Doye, V. (1997). Dynamics of nuclear pore distribution in nucleoporin mutant yeast cells. *J.Cell Biol., 136*(4), 747-759.

Boyd, C., Hughes, T., Pypaert, M., & Novick, P. (2004). Vesicles carry most exocyst subunits to exocytic sites marked by the remaining two subunits, Sec3p and Exo70p . *J.Cell Biol., 167*(5), 889-901.

Brodsky, J. L., Werner, E. D., Dubas, M. E., Goeckeler, J. L., Kruse, K. B., & McCracken, A. A. (1999). The requirement for molecular chaperones during endoplasmic reticulum-associated protein degradation demonstrates that protein export and import are mechanistically distinct. *Journal of Biological Chemistry, 274*(6), 3453-3460.

Cherry JM, Ball C, Weng S, Juvik G, Schmidt R, Alder C, Dunn B, Dwight S, Riles L, Mortimer RK, Botstein D Nature 1997 387 (6632 Suppl): 67-73 Genetic and physical maps of Saccharomyces cerevisae.

Corsi, Ann K., Randy Schekman. (1997). The lumenal domain of Sec63p stimulates the ATPase activity of BiP and mediates BiP recruitment to the translocon in saccharomyces cerevisiae. *The Journal of Cell Biology, 137*(7), 1483-1493.

Davis, T. N. (2004). Protein localization in proteomics. *Current Opinion in Chemical Biology, 8*, 49-53.

Deng, M., & Mark Hochstrasser. (2006). Spatially regulated ubiquitin ligation by an ER/nuclear membrane ligase. *Nature, 443*, 827-831.

Du, Y., Ferro-Novick, S., & Novick, P. (2004). Dynamics and inheritance of the endoplasmic reticulum. *J Cell Sci, 117*(14), 2871-2878.

Fehrenbacher, K. L., Davis, D., Wu, M., Boldogh, I., & Pon, L. A. (2002). Endoplasmic reticulum dynamics, inheritance, and cytoskeletal interactions in budding yeast. *Molecular Biology of the Cell, 13*(3), 854-865.

Fewell, S. W., Travers, K. J., Weissman, J. S., & Brodsky, J. L. (2001). THE ACTION OF MOLECULAR CHAPERONES IN THE EARLY SECRETORY PATHWAY. *Annual Review of Genetics, 35*(1), 149-191.

Foster, B. (1997). *Optimizing light microscopy for biological and clinical laboratories*. Dubuque, Iowa: Kendall/Hunt Publishing Company.

Ghaemmaghami, S., Won-Ki Huh, Kiowa Bower, Russell W. Howson, Archana Belle, Noah Dephoure, et al. (2003). Global analysis of protein expression in yeast. *Nature, 425*, 737-741.

Gia K. Voeltz, & Prinz, W. A. (2007). Sheets, ribbons and tubules — how organelles get their shape. *Nature Reviews Molecular Cell Biology, 8*, 258-264.

Gietz, R.D. and R.A. Woods. (2002). TRANSFORMATION OF YEAST BY THE Liac/SS CARRIER DNA/PEG METHOD methods in enzymology.*350*, 87-96.

Goldstein, Alan L. and John H. McCusker. (1999). Three new dominant drug resistance cassettes for gene disruption in saccharomyces cerevisiae. *Yesat, 15*, 1541-1553.

Hammond, C., & Helenius, A. (1995). Quality control in the secretory pathway. *Current Opinion in Cell Biology, 7*(4), 523-529.

Hampton, R. Y. (2002). ER-associated degradation in protein quality control and cellular regulation. *Current Opinion in Cell Biology, 14*(4), 476-482.

Hennessy, F., William S. Nicoll, Richard Zimmermann, Michael E. Cheetham, & Gregory L. Blatch. (2005). Not all J domains are created equal: Implications for the specificity of Hsp40-Hsp70 interactions. *Protein Science, 14*, 1697-1709.

Herskowitz, I. (1988). Life cycle of the budding yeast saccharomyces cerevisiae. *Microbiological Reviews, 52*(4), 536-553.

Huckaba, T. M., Gay, A. C., Pantalena, L. F., Yang, H., & Pon, L. A. (2004). Live cell imaging of the assembly, disassembly, and actin cable-dependent movement of endosomes and actin patches in the budding yeast, saccharomyces cerevisiae. *J.Cell Biol., 167*(3), 519-530.

Jakobs, S., Subramaniam, V., Schönle, A., Jovin, T. M., & Hell, S. W. (2000). EGFP and DsRed expressing cultures of escherichia coli imaged by confocal, two-photon and fluorescence lifetime microscopy. *FEBS Letters, 479*(3), 131-135.

Kabani, M., Stephanie S. Kelley, Michael W. Morrow, Diana L. Montgomery, Renuka Sivendran, Mark D. Rose, et al. (2003). Dependence of endoplasmic reticulum-associated degradation of the peptide binding domain and concentration of BiP. *Molecular Biology of the Cell, 14*, 3437-3448.

Karpova, T. S., McNally, J. G., Moltz, S. L., & Cooper, J. A. (1998). Assembly and function of the actin cytoskeleton of yeast: Relationships between cables and patches . *J.Cell Biol., 142*(6), 1501-1517.

Kersteen, E. A., & Ronald T. Raines. (2003). Catalysis of protein folding by protein disulfide isomerase and small-molecule mimics. *Antioxidants & Redox Signaling, 5*(4), 413-424.

Laboissière, M. C. A., Sturley, S. L., & Raines, R. T. (1995). The essential function of protein-disulfide isomerase is to unscramble non-native disulfide bonds. *Journal of Biological Chemistry, 270*(47), 28006-28009.

Lippincott-Schwartz, J. (2004). Dynamics of secretory membrane trafficking. *Annals of the New York Academy of Sciences, 1038*, 115-124.

Lippincott-Schwartz, J., Erik Snapp, & Anne Kenworthy. (2001). Studying protein dynamics in living cells. *Nature Reviews Molecular Cell Biology, 2*

Loewen, C. J. R., Young, B. P., Tavassoli, S., & Levine, T. P. (2007). Inheritance of cortical ER in yeast is required for normal septin organization. *J.Cell Biol., 179*(3), 467-483.

Lowe, Martin and Francis A. Barr. (2007). Inheritance and biogenesis of organelles in the secretory pathway. *Nature Reviews Molecular Cell Biology, 8*, 429-439.

Mizunaga, T., Katakura, Y., Miura, T., & and Maruyama, T. (1990). Purification and characterization of yeast protein disulfide isomerase. *J. Biochemistry, 108*, 846-851.

Murray, J. (2005). Confocal microscopy, deconvolution, and structured illumination methods. In Robert D. Goldman, & David L. Spector (Eds.), *Live cell imaging A laboratory manual* (pp. 248). 2005: Cold Spring Harbor Laboratory Press.

Oldenburg, K., Vo, K., Michaelis, S., & Paddon, C. (1997). Recombination-mediated PCR-directed plasmid construction in vivo in yeast. *Nucleic Acids Research, 25*(2), 451-452.

Pelham, Hugh R. B, Kevin G. Hardwick, Michael J. Lewis. (1988). Sorting of soluble ER proteins in yeast. *EMBO J., 7*(6), 1757-1762.

Prinz, W. A., Grzyb, L., Veenhuis, M., Kahana, J. A., Silver, P. A., & Rapoport, T. A. (2000). Mutants Affecting the Structure of the Cortical Endoplasmic Reticulum in *Saccharomyces cerevisiae* . *J.Cell Biol., 150*(3), 461-474.

Ravid, T., Kreft, S. G., & Hochstrasser, M. (2006). Membrane and soluble substrates of the Doa10 ubiquitin ligase are degraded by distinct pathways. *EMBO J., 25*, 533-543.

Rines, D. R., Dominik Thomann, Jonas F. Dorn, Paul Goodwin, & and Peter K. Soreger. (2005). Live cell imaging of yeast. In Robert D. Goldman, & David L. Spector (Eds.), *Live cell imaging: A laboratory manual* (pp. 351-369). New York: Cold Spring Harbor Laboratory Press.

Rizzo, M. A., & David W. Piston. (2005). Detection and approaches to live cell imaging: Fluorescent protein tracking and detection. In Robert D. Goldman, & David L. Spector (Eds.), *Live cell imaging: A laboratory manual* (pp. 3-24). Cold Spring Harbor, NY: Cold Spring Harbor Laboratory Press.

Rose, M. D., Leanne M. Misra, & Joseph P. Vogel. (1989). KAR2, a karyogamy gene, is the yeast homolog of the mammalian BiP/GRP78 gene. *Cell, 57*, 1211-1221.

Schlenstedt, G., Sandra Harris, Bernd Risse, Roland Lill, & and Pamela A. Silver. (1995). A yeast DnaJ homolog, Scj1p, can function in the endoplasmic reticulum with BiP/Kar2p via a conserved domain that specifies interactions with Hsp70s. *The Journal of Cell Biology, 129*(4), 979-988.

Schrader, N., Stelter, P., Flemming, D., Kunze, R., Hurt, E., & Vetter, I. R. (2008). Structural basis of the Nic96 subcomplex organization in the nuclear pore channel. *Molecular Cell, 29*(1), 46-55.

Shaner NC, Campbell RE, Steinbach PA, et al. (2004). Improved monomeric red, orange and yellow fluorescent proteins derived from discosoma sp red fluorescent protein *Nature Biotechnology, 22*(12), 1565-1572.

Shaner, N. C., Paul A. Steinbach, & Roger Y Tsien. (2005). A guide to choosing fluorescent proteins. *Nature Methods, 2*(12), 905-909.

Shaner, N. C., Patterson, G. H., & Davidson, M. W. (2007). Advances in fluorescent protein technology. *Journal of Cell Science, 120*(24), 4247-4260.

Simons, J., Ferro-Novick, S., Rose, M., & Helenius, A. (1995). BiP/Kar2p serves as a molecular chaperone during carboxypeptidase Y folding in yeast. *The Journal of Cell Biology, 130*(1), 41-49.

Swanson, R., Martin Locher, & Mark Hochstrasser. (2001). A conserved ubiquitni ligase of the nuclear envelope/endoplasmic reticulum that functions in both ER-associated and Mata2 repressor degradation. *Genes & Development, 15*, 2660-2674.

Tatchell, K. and Robinson, L.C. (2002). Use of green fluorescent protein in living yeast cells. In Christine Guthrie (Ed.), *Methods in enzymology # 351: GUIDE TO YEAST GENETICS AND MOLECULAR AND CELL BIOLOGY, PT C* (351st ed., pp. 661-683). Amsterdam: Academic Press.

Terasaki, M., Jaffe, L. A., Hunnicutt, G. R., & & Hammer, J. A. (1996). Structural Change of the Endoplasmic Reticulum during Fertilization: Evidence for loss of membrane continuity using the Green Fluorescent Protein. *Dev. Biol., 179*, 320-328.

Vitale, A., & Denecke, J. (1999). The endoplasmic Reticulum—Gateway of the secretory pathway. *Plant Cell, 11*(4), 615-628.

Voytas, D. (2000). Section II: Resolution and recovery of large DNA fragments. In Gwen P. Taylor (Ed.), *Current protocols in molecular biology*. John Wiley & Sons.

Wach, A. (1996). PCR-synthesis of marker cassettes with long flanking homology regions for gene disruption in S. cerevisiae. *Yeast, 12*, 259-265.

APPENDIX

A.1 Material and Methods

A.1.1 Primers: Homologous Recombination

Prior to homologous recombination, selected DNA was amplified with polymerase chain reactions with the use of the primers displayed below. Sequences in orange are homologous to the genome; regions depicted in green are homologous to the forward region of the plasmid; sequences in red indicate homology to the reverse region of the plasmid; and black refers to the stop codon within the genome.

PDI Fwd HR
5' TGAATTGGCTGACGAAGAAGATGCCATTCACGATGAATTGGGTCGACGGATCCCCGGG 3'
PDI Rev HR
5' TATATCTCTATTTAATGAAAAACCAAAGTGATCAGAATTAATCGATGAATTCGAGCTCG 3'
BiP(KAR2) Fwd HR
5' TGAAGATGACGATGGTGATTATTTCGAACACGACGAATTGGGTCGACGGATCCCCGGG 3'
BiP(KAR2) Rev HR:
5' TGAAGCTTCCAGCAGCAAAAATTTTTAACTATTTTATCTAATCGATGAATTCGAGCTCG 3'
SEC61 Fwd HR:
5' GTTTACTAAGAACCTCGTTCCAGGATTTTCTGATTTGATGGGTCGACGGATCCCCGGG 3'
SEC61 Rev HR:
5' GCGATTTTTTTTTTCTTTGGATATTATTTTCATTTTATATTCAATCGATGAATTCGAGCTCG 3'
NUP49 Fwd HR:
5' GTTACATCAAAAAACGAAAACACTGGCATCATTGAGCATAGGTCGACGGATCCCCGGG 3'
NUP49 Rev HR:
5' TGTTATACGCACTATATAAACTTTCAGGGCGATTTACTCAATCGATGAATTCGAGCTCG 3'

A.1.2 PCR Clean-up Protocol

The PCR Clean-up System was used to concentrate and purify the amplified DNA. An equal volume of Membrane Binding Solution was added to the 50µL PCR product (amplified DNA). The PCR solution was transferred into an SV Minicolumn and Collection Tube where it is allowed to incubate at room temperature for 1 minute. The contents in the minicolumn were spun down by centrifugation for 60

seconds at 16,000rcf. The flow through was discarded and the membrane of the column was washed with 700 µL of Membrane Washing Solution, followed by centrifugation. The DNA was again washed with 500µL of Membrane Washing solution and the centrifugation was repeated for 5 minutes at 16,000rcf. The flow through in the collection tube was discarded after each washing step. After one minute of incubation at room temperature, the Minicolumn was placed in a 1.5mL microcentrifuge tube and 50µL of Nuclease-Free Water was added. The DNA was eluted from the membrane into the tube by centrifugation for one minute at 16,000rcf.

A.1.3 DNA Extraction from Yeast Cells

After homologous recombination with yeast transformations, plasmid DNA must be extracted to then be inserted into *E. coli* cells for amplification of this newly formed DNA construct. DNA extraction from yeast cells was performed following the QIAprep® Spin Miniprep Kit. Yeast cells are inoculated into 3mL of selective media and grown overnight. The cells are removed by centrifugation for five minutes at 5000rcf and are resuspended in 250µL of Buffer P1 containing 0.1mg/mL RNase A. The cells suspension is transferred to a microcentrifuge tube where 50-100µL of acid-washed glass beads (Sigma) are added. The mixture is vortexed for five minutes. The supernatant is removed and transferred into a clean microcentrifuge tube. 250µL of Lysis Buffer P2 is added to the supernatant and the sample was mixed gently by inverting the tube, followed by incubation at room temperature for five minutes. 350µL of Neutralization Buffer N3 is added to the tube and mixed by inversion. The lysate is spun down by centrifugation at maximum speed (16,000rcf) for ten minutes. The clear lysate is then transferred into the provided QIAprep Spin Column and collection tube and then centrifuged for 60 seconds at 16,000rcf. The

flow through is discarded and the solution is washed with 750µL of Buffer PE followed by a 60 second centrifugation. An additional centrifugation is required to remove excess wash buffer. The QIAprep Spin Column is then placed in a clean microcentrifuge tube. The DNA is eluted by addition of 50µL of distilled water to the column. After one minute of room temperature incubation, the column is centrifuged for one minute. Resulting DNA plasmid is to be used for *E. coli* transformations to produce high copies of this DNA construct.

A.1.4 PCR parameters

The following is a list of parameter settings during the polymerase chain reaction (PRC) which is described above in Chapter 2 (Yeast Resource Center, University of Washington).

1) 94°C for 2 minutes
2) 92°C for 10 seconds
3) 50°C for 30 seconds
4) 68°C for 4 minutes
5) Repeat previous three steps 9 times
6) 92°C for 10 seconds
7) 50°C for 30 seconds
8) 68°C for 4 minutes + 20 seconds per cycle
9) Repeat previous three steps 18 times
10) 68°C for 7 minutes

A.2 Research in Progress

A.2 Current Research Progress

A.2.1 Construction of ERAD Fusion Proteins

Research objectives included examining two ERAD pathways, involving the ERAD proteins Hrd1 and Doa10. In order to construct the fusion proteins for these two ERAD proteins, homologous recombination primers were first designed. The primers included regions of homology with both the chromosomal gene for the ERAD proteins of interest and the regions of homology to the fluorescent marker used to monitor these proteins. The fusion proteins are created with a PCR with these designed primers, and homologous recombination which creates yeast cells which will express the ERAD fusion proteins. Future work includes homologous recombination of the two ERAD proteins for analysis using the confocal microscope.

A.2.2 Construction of PDI-Cerulean and BiP-mCherry Dual Strain

Initial research objectives included the monitoring of PDI-Cerulean (a blue fluorescent protein) and BiP-mCherry expressing simultaneously in the same yeast strain, *S. cerevisiae*. In order to achieve this goal, a new plasmid was constructed of pBS10 with a Cerulean GFP variant tag and a *TRP1* selective marker. Restriction enzymes were used to cut within the original pBS10 selective marker, *hph*.. Polymerase chain reaction (PCR) was performed to amplify *TRP1* portion of the plasmid PRS314 with specific primers that have regions of homology to the *TRP1* selective marker. A yeast transformation was then performed which placed the amplified PCR product of the *TRP1* selective marker (insert) into the pBS10 Cerulean plasmid (vector) and directly into the chromosome of yeast (Oldenburg *et al*., 1997). To obtain the DNA of this newly formed pBS10 with Cerulean GFPv and *TRP1* selective marker, a DNA Yeast Extraction was performed. The resulting DNA was

used to perform an *E. coli* transformation to produce high copies of this newly formed construct. Assays to confirm this structure are in progress.